博士論文

論文題目　Studies on dioecism of hermaphrodite mutants and B-class genes *SlAP3X/Y* deletion mutants in the dioecious plant *Silene latifolia*

（雌雄異株植物ヒロハノマンテマにおける両性花変異体と B クラス遺伝子 *SlAP3X/Y* 欠失変異体の雌雄異株性に関する研究）

氏　名　青沼　航

Studies on dioecism of hermaphrodite mutants and B-class genes *SlAP3X/Y* deletion mutants in the dioecious plant *Silene latifolia*

Wataru Aonuma

2013

Department of Integrated Biosciences

Graduate School of Frontier Sciences

University of Tokyo

ACKNOWLEDGEMENTS

I thank Professor Shigeyuki Kawano at the University of Tokyo for his kind instruction and continuous encouragement throughout this study. I also thank Dr. Yusuke Kazama, Dr. Kotaro Ishii, Dr. Tomoko Abe of RIKEN, and Mr. Yuji Shimizu for their helpful discussions and numerous suggestions. I thank Professor Boris Vyskot of the Academy of Sciences of the Czech Republic (ASCR) for the generous gift of *Silene viscosa* seeds. I acknowledge Professor Hiroshi Mitani and Associate Professor Shoji Oda from the University of Tokyo for their technical help and advice on the gamma irradiation device. I also acknowledge Mr. Sakyo Kaburagi, Mr. Shigeru Sugita, and Mr. Kunio Yasu for their efforts in *Silene latifolia* cultivation. I am also grateful to Ms. Mihoko Ohkami, Dr. Shuhei Ota, Dr. Tomokazu Yamazaki, Dr. Shinsuke Ohnuki, Dr. Wakana Tanaka, Mr. Yuta Imoto, Mr. Youichi Sato, Mr. Masaki Sato, Mr. Ryogo Suzuki, Mr. Tsuyoshi Takeshita, Mr. Kan Ito, Mr. Hiroki Kawamoto, Mr. Tatsuya Suzuki, Ms. Kaori Takita, Ms. Chizuru Hirai, Mr. Zhe Yu, Mr. Kai Ozeki, Ms. Erika Kounosu, Ms. Mai Yoshihara, Mr. Yuichi Yamashita, Ms. Minako Miki, Ms. Rika Shinohara, Ms. Yuko Yoshizawa, and Ms. Kyoko Kudo for their support, kindness, and encouragement throughout this study. Finally, I thank my family for their support and constant encouragement throughout this study.

CONTENTS

ABBREVIATION

AP3	*APETALA3* (gene name)
BAC	bacterial artificial chromosome clone
bp:	base pair(s)
DAA	day(s) after anthesis
EGP	early-stage gynoecium promoted mutant
Em-stamens	early-maturing stamens
ESS	early-stage stamen-suppressed mutant
FDA	fluorescein diacetate
FISH	fluorescence *in situ* hybridization
GPSS	gynoecium promoted and stamen-suppressed mutant
GSF	gynoecium-suppressing factor
HAA	hour(s) after anthesis
ISS	intermediate-stage stamen-suppressed mutant
ITS	internal transcribed genes
kb	kilo base pair(s)
Lm-stamens	late-maturing stamens
LSS	late-stage stamen-suppressed mutant
MFF	male fertility factor

NGS	next-generation sequencing
NRY	non-recombining region on the Y chromosome
PCR	polymerase chain reaction
PI	propidium iodide
RNA-seq	RNA sequencing
RT-PCR	reverse transcription-PCR
SPF	stamen-promoting factor
STS	sequence-tagged site
WT	wild-type

PREFACE

The majority of flowering plants are hermaphroditic, i.e., they have bisexual flowers that contain both male and female organs (Renner and Ricklefs 1995). However, hermaphroditic plants lose genetic diversity through self-pollination due to the effects of inbreeding. Most hermaphroditic plants have various mechanisms to avoid self-pollination by separating their stamens and pistils, such as self-incompatibility (rejection of self-pollen, but acceptance of nonself-pollen for fertilization), dichogamy (having the stamens mature either before or after the period during which the stigmas on the same flower are receptive), and herkogamy (spatial separation of stamens and pistils within flowers of an individual plant) (Barrett 2003; Bertin and Newman 1993; Lloyd and Webb 1986; Webb and Lloyd 1986). In contrast, a minority of angiosperm species (only 6%) are dioecious in that they have separate male and female flowers (Susanne S Renner and Ricklefs 1995). Dioecious plants do not require such mechanisms to avoid self-pollination as all offspring are produced by cross-pollination. However, dioecious plants may not be able to produce offspring when no plants of the opposite sex are present within the reproductive period at nearby sites. To increase the chance of cross-pollination, the dioecious plants mature stamens and pistils simultaneously rather than separately, as seen in hermaphroditic plants.

The genus *Silene* L. contains several hundred species and shows a great variety of ecological and morphological characteristics (Charter and Walters 1964). Three types of reproductive systems exist in this genus: dioecy, gynodioecy (coexistence of females and hermaphrodites), and hermaphroditism. The phylogeny of *Silene* species, constructed using internal transcribed spacer (ITS) sequences of nuclear ribosomal RNA genes (Desfeux et al. 1996) and sequences of multinuclear genes (Marais et al. 2011), shows that dioecy originated at

least twice in this genus. The dioecious plant *Silene latifolia* is the best studied dioecious plant, and its sex is determined by the XY sex chromosomes (XY males, XX females) (Matsunaga and Kawano 2001; Negrutiu et al. 2001; Vyskot and Hobza 2004). *S. latifolia* depends on nectar-seeking insects for pollination and is a nocturnal species (Friedrich 1979; Jürgens, Witt, and Gottsberger 2002). Therefore, pollen grains are released and stigmas are receptive simultaneously at night.

The evolutionary background of dioecy from hermaphroditism has been investigated both experimentally and theoretically since it was first proposed by Darwin (Dawin 1877). Although the evolution of dioecy from hermaphroditism has been well studied, little is known regarding the changes that occur in a self-pollination evasion mechanism during the transition from dioecy to hermaphroditism. The self-pollination evasion mechanisms (dichogamy and delayed selfing) have been reported in some hermaphroditic and gynodioecious plants belonging to the genus *Silene* (Buide 2002; Davis and Delph 2005; Kephart, Brown, and Hall 1999). This raises the question as to whether such ubiquitous mechanisms for avoiding self-pollination in hermaphroditic plants are also used by hermaphroditic mutant dioecious plants. Previous analyses, such as Y-deletion mutant analysis, supported that male sex determination factors are located on the Y chromosome. For example, the gynoecium is suppressed by the gynoecium-suppressing factor (GSF), stamens are promoted by the stamen-promoting factor (SPF), and anther and pollen grain maturation is promoted by the male fertility factor (MFF) (Westergaard 1958). A previous study showed that hermaphroditic mutants can be isolated by deleting GSF on the Y chromosome (Lardon et al. 1999; Lebel-Hardenack et al. 2002).

The hermaphroditic mutants are also suitable to study sex allocation theory, which explains the evolution of

dioecy (Charnov 1982). The dioecious plant *S. latifolia* is thought to have evolved from the hermaphrodite condition via gynodioecy (Delph and Wolf 2005). A model for the evolution of dioecy and gynodioecy suggests that the occurrence of ovule production modifiers reduces ovule production of hermaphrodites and can also increase pollen production through the compensation principle (Charlesworth and Charlesworth 1978). Sex allocation theory predicts that dioecy may be favored over hermaphroditism if the trade-off in investment of resources to males and females results in an increased fitness return on investment in a single sexual function (Charlesworth and Charlesworth 1981; Laguerie et al. 1991).

According to the currently accepted model, X and Y chromosomes evolve from a pair of autosomes via a series of inversions leading to stepwise expansion of a non-recombining region on the Y chromosome (NRY) and the consequential degeneration of genes trapped in the NRY (Charlesworth 2008). In particular, the majority of Y chromosome genes were lost in mammals and *Drosophila* (Bachtrog 2006; Wilson and Makova 2009; Wyckoff, Li, and Wu 2002). Next-generation sequencing (NGS) approaches, such as RNA-seq, have identified over 1700 sex-linked contigs, which increased the number of sex-linked sequences available in *S. latifolia* by over a hundredfold (Muyle et al. 2012). NGS approaches also revealed that Y-linked genes show rapid accumulation of amino-acid replacements and loss of expression compared to X-linked genes (Bergero and Charlesworth 2011; Chibalina and Filatov 2011). However, only two examples of "X-only" genes (*Slcyt*, *SlWUS1*) are known, in which the Y copy has been completely lost during the evolution of dioecy (Bergero et al. 2013; Kaiser, Bergero, and Charlesworth 2009; Kazama et al. 2012). The *S. latifolia* MADS box gene (*SlAP3X/Y*), which is similar to *Arabidopsis thaliana APETALA3* (*AP3*), has been investigated by bacterial

artificial chromosome clone (BAC) sequencing (Cegan et al. 2010; Ishii et al. 2013; Matsunaga et al. 2003; Nishiyama et al. 2010). By isolating the *SlAP3Y* deletion mutant, the presence or absence of specialization between *SlAP3X* and *SlAP3Y* and the affects of specific Y-linked gene deletions can be explored.

In this report, the mechanism for maintaining distinct male and female plants in the dioecious plant *S. latifolia* was explored. I performed the following studies: "Maturation timing of stamens and pistils in the dioecious plant *Silene latifolia*," "Appearance of male/female trade-off and monoecism in hermaphroditic mutants of the dioecious plant *Silene latifolia*," and "Deletion mutations of B class genes *SlAP3X/Y* coded at XY sex chromosomes and their dosage compensation of genes in the dioecious plant *Silene latifolia*"

CHAPTER I

Maturation timing of stamens and pistils in the dioecious plant *Silene latifolia*

SUMMARY

The dioecious plant *Silene latifolia* depends on nocturnal insects for pollination. To increase the chance of cross-pollination, pollen grains seem to be released and stigmas seem to be receptive simultaneously at night. I divided the floral development of *S. latifolia* into 1-20 stages, and determined the timetables of male and female function. The corolla of both male and female flowers opens at sunset (19:00) and closes at sunrise (09:00). To investigate the period of the reproductive phase of male and female function, I measured the germination rate on a pollen mediumand the pollen germination rate on stigma during the period when stamens and stigmas were viable in the timetable. Male flowers had early- and late-maturing stamens that had the highest pollen viability germination rate and pollen tube growth at midnight (00:00) at 1 day after anthesis (DAA) and 00:00 at 2 DAA. In contrast, female flowers maintained a germination rateof nearly 100% from 18:00 at 1 DAA to 12:00 at 3 DAA. These results suggested that *S. latifolia* transferred the matured pollen grains from male flowers to female flowers only at night.

INTRODUCTION

Most flowering plants are hermaphroditic, producing bisexual flowers that contain both male and female organs (Renner and Ricklefs 1995). Therefore, pollen grains are potentially transferred from stamens to pistils. However, a drawback exists in that hermaphroditic plants by self-pollination tend to lose genetic diversity due to the effects of inbreeding. Most hermaphroditic plants have various mechanisms to avoid self-pollination. Especially dichogamy is common in hermaphroditic plants, and stamens and pistils do not mature simultaneously in 76.3% of hermaphroditic plants (Bertin and Newman 1993).

The dioecious plant *Silene latifolia* has stamens and pistils in separate plants preventing self-pollination. However, flowers may not be able to produce offspring when no plants of the opposite sex are present within the reproductive period at a nearby site. Therefore, to increase the chance of cross-pollination, the dioecious plants seem to mature stamens and pistils simultaneously. *S. latifolia* depends on nectar-seeking insects for pollination and is a nocturnal species (Friedrich 1979). To investigate the timing of anthesis of male flowers and female flowers in *S. latifolia*, it is necessary to describe how floral development progresses from bud formation to the falling off of the flower.

Floral development in *S. latifolia* is divided into 12 stages from bud formation to anthesis (Grant, Hunkirchen, and Saedler 1994), and during the period from stages 6 to 11, the development of stamens and pistils is subdivided and explained further (Farbos et al. 1997; Zluvova et al. 2010). In this study, I redefined the floral development stages of *S. latifolia* from anthesis to seed formation parallel to what has been done to *A. thaliana* (Smyth, Bowman, and Meyerowitz 1990).

Furthermore, to investigate the maturation timing of stamens and pistils, I evaluated the pollen germination rates on a pollen medium (*in vitro*) and on the stigmas (*in vivo*) to estimate the degrees of maturity of the stamens and the pistils, respectively, and estimated the timing of maturation.

MATERIALS AND METHODS

Plant materials

S. latifolia seeds were obtained from an inbred line (K-line) in our laboratory (Kazama et al. 2003). The K line was propagated for ten generations of brother-sister mating to obtain genetically homogeneous populations. Plants were grown from seeds in pots in a regulated chamber at 23°C during the vegetative growth phase. Then, plants were transferred outdoors during the generative growth phase. The investigation took place in May and June 2010.

Stereomicroscopic observations

Flowers and anthers were observed under a stereomicroscope (MZ16; Leica Imaging Systems, Cambridge, UK).

Pollen viability and *in vitro* germination determination

To determine the pollen viability double staining with fluorescein diacetate (FDA) and propidium iodide (PI) was performed using the method of Mandaoka and Browse (Mandaokar and Browse 2009). A stock solution of 2 mg/mL FDA was made in acetone and added dropwise to 17% sucrose (Suc) (w/v) until the solution became cloudy. PI was diluted to 1 mg/mL in water and diluted to 100 µL/mL with 17% Suc (w/v). Equal amounts of

FDA and PI solutions were mixed together and added to freshly isolated pollen on glass slides. The pollen was covered with a coverslip and viewed under a fluorescence microscope (BX60; Olympus, Tokyo, Japan). A pollen germination assay was performed according to the method of Jolivet and Bernasconi (Jolivet and Bernasconi 2007a). Pollen was isolated from mature flowers by gently releasing them from the anther locules onto microscope slides containing pollen germination medium.

In vivo pollen germination and tube growth

Stigma staining with aniline blue was performed using the method of Fang (Fang et al. 2010). Previously pollinated pistils were excised from flowers 6 h after pollination and fixed for 24 h in the acetic alcohol (glacial acetic acid:ethanol, 1:3, v/v), then cleared with 8 N NaOH overnight and thoroughly rinsed before staining with decolored 0.1% (w/v) aniline blue in 0.1 M K_3PO_4. The preparation was observed under the fluorescence microscope to measure pollen germination and pollen tube growth down the style. Pollen grains were scored as germinated when the tubes were apparent between the papillate cells of the stigma, and the number of pollen tubes and the number that reached the end of the style, and those which barely elongated, were recorded.

RESULTS

Stages after anthesis of male and female flowers

In *S. latifolia*, female flowers have a gynoecium composed of five fused carpels with five styles, whereas the male flowers have 10 stamens (Fig. 1-1). The 10 stamens are divided into two groups based on their length: the five long stamens mature antecedently, and the five short stamens mature subsequently. Therefore, I call the five long stamens "early-maturing stamens" and five short stamens "late-maturing stamens." The characteristics defining each stage after anthesis are shown in Table 1-1. I divided the floral development after floweing of *S. latifolia* into1–20 stages, similar to the stages of *A. thaliana* (Smyth et al. 1990).

In female flowers, the bud opens in stage 13, stigmas extend above petals in stage 14, the tip of the stigma bends in stage 15, and petals wither in stage 16. When female flowers are pollinated, they move into the seed formation phase. The ovary expands in stage 17, stigmas slough off in stage 18, sepals turn yellow in stage 19, and capsules dehisce and seeds fall in stage 20 (Fig. S1-1a). In male flowers, the bud opens in stage 13, the early-maturing stamens extend above the petals in stage 14, the late-maturing stamens extend above petals in stage 15, and whole flowers wither and fall in stage 16. As male flowers do not have a seed formation period, no stages exist above stage 17 (Fig. S1-1b). However, if pollination has not occurred, whole female flowers fall in the same manner as male flowers in stage 16.

Timetables of male and female flowers

To estimate the duration of each stage and reproductive phase of male and female flowers in, the timetables of male and female flowers were determined, as shown in Fig. 1-2. *S. latifolia* is a nocturnal species (Witt et al. 1999) in which the bud opens at 19:00 and closes at 09:00 in male and female flowers.

In female flowers, stage 13 begins when the bud opens; soon afterward, stage 14 begins when the stigmas extend. Stage 14 continues until 18:00 at 2 days after anthesis (DAA), stage 15 begins when the tips of stigma curled. At 3 DAA, petals hang down vertically, and flower senescence progresses. At 4 DAA, the tips of stigmas and petals wither. At 18:00 on 5 DAA, all petals and stigmas wither, and they move into stage 16. The timetable indicates that the possible pollination period of unpollinated flowers is 96 h. However, if pollination occurs after 18:00 at 2 DAA, at the fastest rate, whole petals and stigmas wither at 18:00 at 3 DAA. Therefore, the pollination period can be shortened to 44 h.

In male flowers, the early-maturing stamens dehisce 6 h before anthesis (stage 12), and pollen grains attach to the outer surfaces of anthers. Stereomicrographs of anthers where no pollinators are present during dehiscence are shown in Fig. S1-2. *S. latifolia* has a longitudinal dehiscence pattern. Dehiscence is completed within 24 min, and almost all pollen grains fall from the anther within 30 h. Pollen grains of the early-maturing stamens gradually fall from 18:00 at 2 DAA (stage 13), and then almost all pollen grains fall until 18:00 at 2 DAA (stage 14). The late-maturing stamens extend from stage 12 to 14 and extend to the same length as early-maturing stamens at 2 DAA at 12:00 (stage 14). Pollen grains of the late-maturing stamens gradually fall from 18:00 at 2 DAA (stage 14), and then almost all pollen grains fall at 18:00 on 3 DAA (stage 15); soon afterward, whole

male flowers fall off, and stage 15 is over. The timetable indicated that male flowers could release pollen grains at later time points by delaying the dehiscence timing of the late-maturing stamens by 1 day from the early-maturing stamens.

Examination of the reproductive phase in male flowers

To investigate the period of the reproductive phase of male flowers, I measured the germination rate on a pollen medium (*in vitro*) during the period when flowers released pollen grains. The viability and pollen germination rate are shown in Table 1-2. The viable pollen grains treated with FDA showed bright green fluorescence, and dead pollen grains treated with PI showed red fluorescence (Fig. 1-3). I stained pollen grains with only FDA at 1 DAA at 12:00 since they were easily stained with PI in this stage (Fig. 1-3a). Blue pollen grains were not viable which were not stained with FDA.

Although the dehiscence of anthers occurs before anthesis, few pollen grains germinate shortly after dehiscence (Fig. 1-3a). As buds opened and night came, the pollen germination rate increased, and it became approximately 70% at midnight (00:00) (Fig. 1-3c). As dawn approached, the pollen germination rate decreased, and it became 0% at 18:00 the following day (Fig. 1-3f). The pollen germination rates of the early- and late-maturing stamens reached the maximum value at midnight (00:00) and decreased rapidly beyond this time. These data indicated that the period of reproductive phase of male flower was 30 h and coincided with the timetable results.

Examination of the reproductive phase in female flowers

To investigate the reproductive phase of female flowers, I measured stigma receptivity the period. I considered the approximate pollen germination rate on stigma as stigma receptivity.

Fluorescence images of aniline blue-stained pollen grains on the stigma in the period between DAA 0 and DAA 5 are shown in Fig. 1-4. Two types of germinated pollen grains were observed: type 1 showed elongation of the pollen tube from the tip of the stigma to the end of the style (arrowhead), while type 2 barely elongated the pollen tube (double arrowhead) (Fig. 1-4a). To estimate the degree of maturity of the stigma in detail, I measured the proportions of type 1+type 2 and type 1 pollen grains in all pollen grains on the stigmas.

The stigma was stained with aniline blue and showed blue-green fluorescence at 0 DAA (Fig. 1-4b). The stigmas at this time point were not fully elongated and exposing the receptive part of the styles; the germination rate of pollen grains on these stigmas was about 70%, and the pollen tube did not elongate far (Fig. 1-4c). At 18:00 at 1 DAA, and almost all pollen grains germinated on these stigmas until midnight at 2 DAA (Fig. 1-4d). Female flowers had high stigma receptivity after anthesis regardless of day or night. The period in which pollen germination rate was nearly 100% continued from 18:00 at 1 DAA to 06:00 at 3 DAA. After 12:00 at 3 DAA, the pollen germination rate began to decrease, and stigma senescence began. The proportions of type 1 and type 2 pollen grains became 0 at 18:00 at 5 DAA. These data indicated that the reproductive phase of female flowers was 96 h and coincided with the timetable results.

Maturation timing of stamens and pistils

To estimate the maturation timing of stamens and pistils, I combined the *in vitro* and *in vivo* data in Fig. 1-5. Male flowers with early- and late-maturing stamens had highest pollen viability and germination rate at midnight at 1 DAA and midnight at 2 DAA, respectively. In female flowers pollen germination rate on stigmas was nearly 100% from 18:00 at 1 DAA to 12:00 at 3 DAA. After 12:00 at 3 DAA, the stigma receptivity began to decrease, the corolla opened, and the petals of female flowers hung down vertically.

These results suggested that only pollen grains transferred at night are successful in *S. latifolia*.

DISCUSSION

Timing of anthesis in *S. latifolia*

In *S. latifolia*, the corolla of both male and female flowers opens at sunset (19:00 in Fig. 1-2) and closes at sunrise (09:00 in Fig. 1-2). Male flowers cannot deliver pollen and female flowers cannot receive pollen during the period when the corolla is closed. *S. latifolia* depends on nocturnal pollinators for pollination, and its amount of nectar increases in the evening until midnight (Comba 1999; Witt et al. 1999). Furthermore, nocturnal pollinators carried pollen over longer distances than diurnal pollinators (Young 2002). *S. latifolia* seems to flower only at the time when nocturnal pollinators are active and limits the period of pollen delivery to nighttime.

Longevity of flowers and stamens and pistils

Male flowers fall at 18:00 at 3 DAA, while female flowers fall at 18:00 at 5 DAA when pollination fails (Fig. 1-2). With regard to the longevity of stamens and pistils, the pollen germination rate (*in vitro*) of late-maturing stamens decreases to 0% at 18:00 at 3 DAA, while the pollen germination rate on the stigma (*in vivo*) decreases to 0% at 18:00 at 5 DAA (Fig. 1-5). These data indicated that the timing of flower shedding coincided with the timing of the end of the stamen and pistil maturation period. In many plants, the cost related to maintenance of a petal is greater than those associated with stamens and pistils (Galen 2000). Therefore, the whole flower may

fall soon after the end of the stamen and pistil maturation period.

The reproductive period of male flowers and the maturation timing of stamens

In vitro experiments indicated that the reproductive periods of early- and late-maturing stamens was 30 h. Furthermore, the pollen germination rates showed a transient elevation and reached the highest level at midnight. The amount of nectar in *S. latifolia* increases in the evening until midnight (Comba 1999; Witt et al. 1999). These results related to the nectar were in agreement with the increase in pollen germination rate at night. Male flowers divided the 10 stamens into five early- and five late-maturing stamens, and delayed the timing of maturation of the late-maturing stamens by 1 day from that of early-maturing stamens. In female flowers, not all ovules are fertilized unless a pollinator carries the pollen grains several times (Young and Gravitz 2002). Therefore, male flowers are thought to increase the opportunity for pollination by dividing the 10 stamens into early- and late-maturing stamens and thereby increasing the pollen presentation period.

The reproductive period of female flowers and the maturation timing of pistils

The stigmas of female flowers survive for as long as 96 h when put in an environment that prevents pollination by bagging with netting (Fig. 1-5). This life span of stigmas can be shortened to 44 h when female flowers are pollinated artificially until 2 DAA. In many plants, when pollination has failed, stigma receptivity last longer

time (Steinacher and Wagner 2010). The pollinated female flowers are thought to reduce the cost of maintaining a flower by promptly withering the floral organ after it has fulfilled its role in reproduction.

The maturation level of pistils remained high from 0 h after anthesis (HAA) to 36 HAA rather than showing a transient elevation as seen for the stamens (Fig. 1-5). The pistil was thought to be able to be pollinated regardless of day/night. However, as the corolla closed in the period of 12-24 HAA, the female flowers appeared to be substantially pollinated only in the period of 0-12 HAA and24-36 HAA. After 36 HAA, the maturation level of pistils decreased gradually, petals hung down vertically, and female flowers maintained the open corolla. Although female flowers could still be pollinated under these conditions, pollinator visit frequency decreases to flowers in which the petals have wilted (Galloway, Cirigliano, and Gremski 2002). The pollination frequency may decrease after 36 HAA. Therefore, the dioecious plant, *S.latifolia* could transfer pollen grains from the male flower to the female flower only for synchronous 24h at two nights.

Table 1-1. Summary of the floral developmental stages of *Silene latifolia* after anthesis

Stage	Description	
	Female and male plants	
1	Apical meristem begins to elongate at 90° to last leaf primordia.	
2	Elongated meristem divides into five parts. Center forms first flower, flanked by two lateral inflorescence and two bracts.	
3	Sepal primordia appear.	
4	Sepal primordia well-established.	
5	Petal and stamen primordia arise. First differences between male and female.	
	Female plants	Male plants
6	Height of undifferentiated fourth whorl is 60%of width.	Height of undifferentiated fourth whorl is 20%of width.
7	Five carpel primordia first visible.	Single gynoecium primordium is first visible.
8	Gynoecium continues to elongate; first appearance of block to stamen development.	Stamens become stalked at base; theca form; tapetum initiated.
9	Gynoecium becomes constricted at tip.	Pollen mother cells clearly visible.
10	Gynoecium tube closes and styles grow from carpel tips; meiosis; ovule become stalked.	meiotic tetrads visible in anthers.
11	Stigmas form along inside ridges of styles.	Microspores separate from one another in upper anthers and lie freely in pollen sac; tapetum degenerates.
12	Integuments surround ovules.	Stamen filaments elongate and pollen matures.
13	Bud opens.	Bud opens.
14	Stigmas extend above petals.	Early-maturing stamens extend above petals.
15	Tips of stigmas curl.	Late-maturing stamens extend above petals.
16	Petals wither.	Petals wither and whole flower falls.
17	Ovary expands.	
18	Stigmas slough off.	
19	Sepals turn yellow.	
20	Capsule dehisces, and seeds fall.	

The description of stage 1-12 is from Grant et al. (1994).

Table 1-2. Germination and viable ratio of pollen of the early- and late-maturing stamens (*in vitro*)

Time	Early-maturing stamens		Late-maturing stamens	
	Viable pollen (%)	Germination (%)	Viable pollen (%)	Germination (%)
1 DAA at 12:00	91	0	-	-
1 DAA at 18:00	91	38	-	-
2 DAA at 00:00	92	71	-	-
2 DAA at 06:00	89	37	-	-
2 DAA at 12:00	82	23	82	0
2 DAA at 18:00	33	1	80	33
3 DAA at 00:00	-	-	78	61
3 DAA at 06:00	-	-	82	38
3 DAA at 12:00	-	-	63	11
3 DAA at 18:00	-	-	15	0

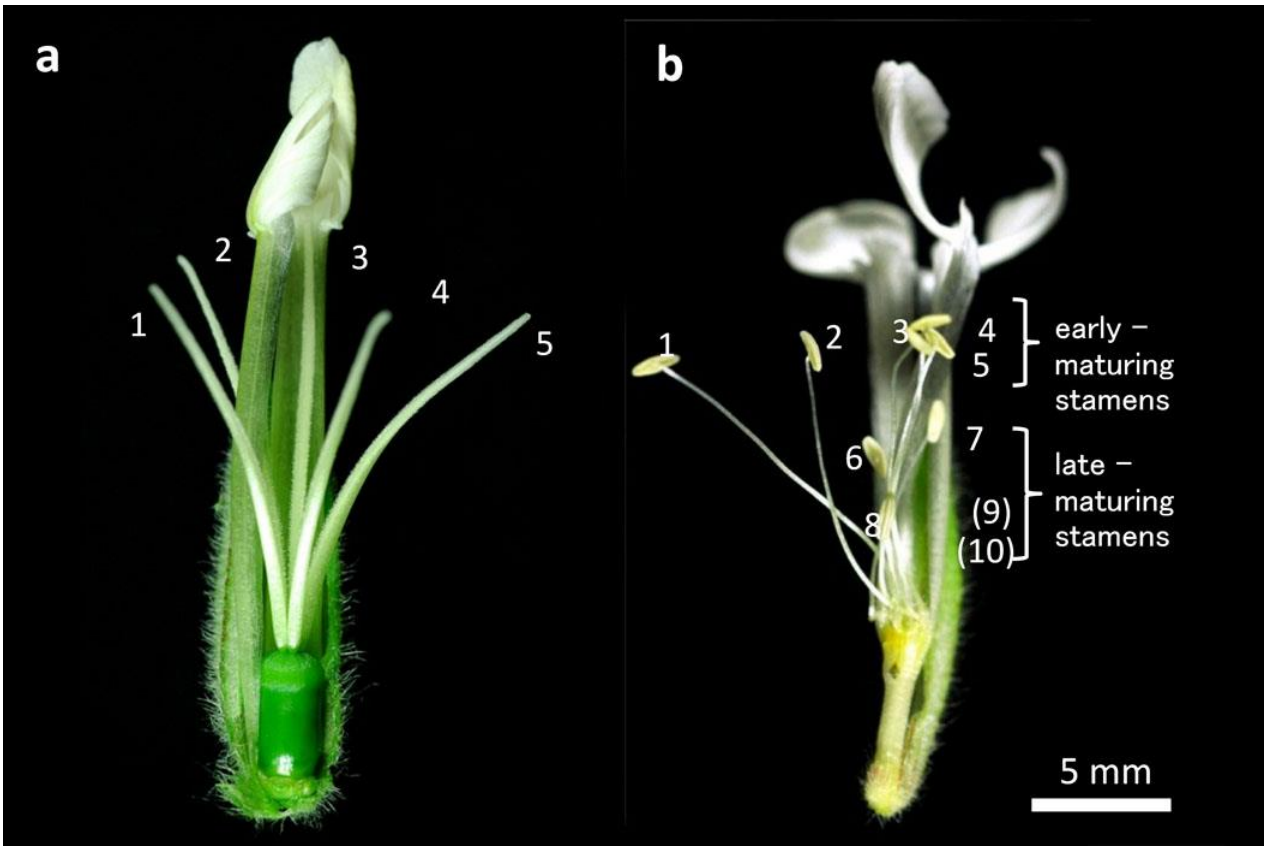

Fig. 1-1. Photographs of wild-type male and female flowers of *Silene latifolia*. A half part of petals and sepals were removed. (**a**) Side view of a female flower. The female flower has five stigmas. (**b**) Side view of a male flower. The male flower has 10 stamens. As the long stamens mature earlier than the short stamens.

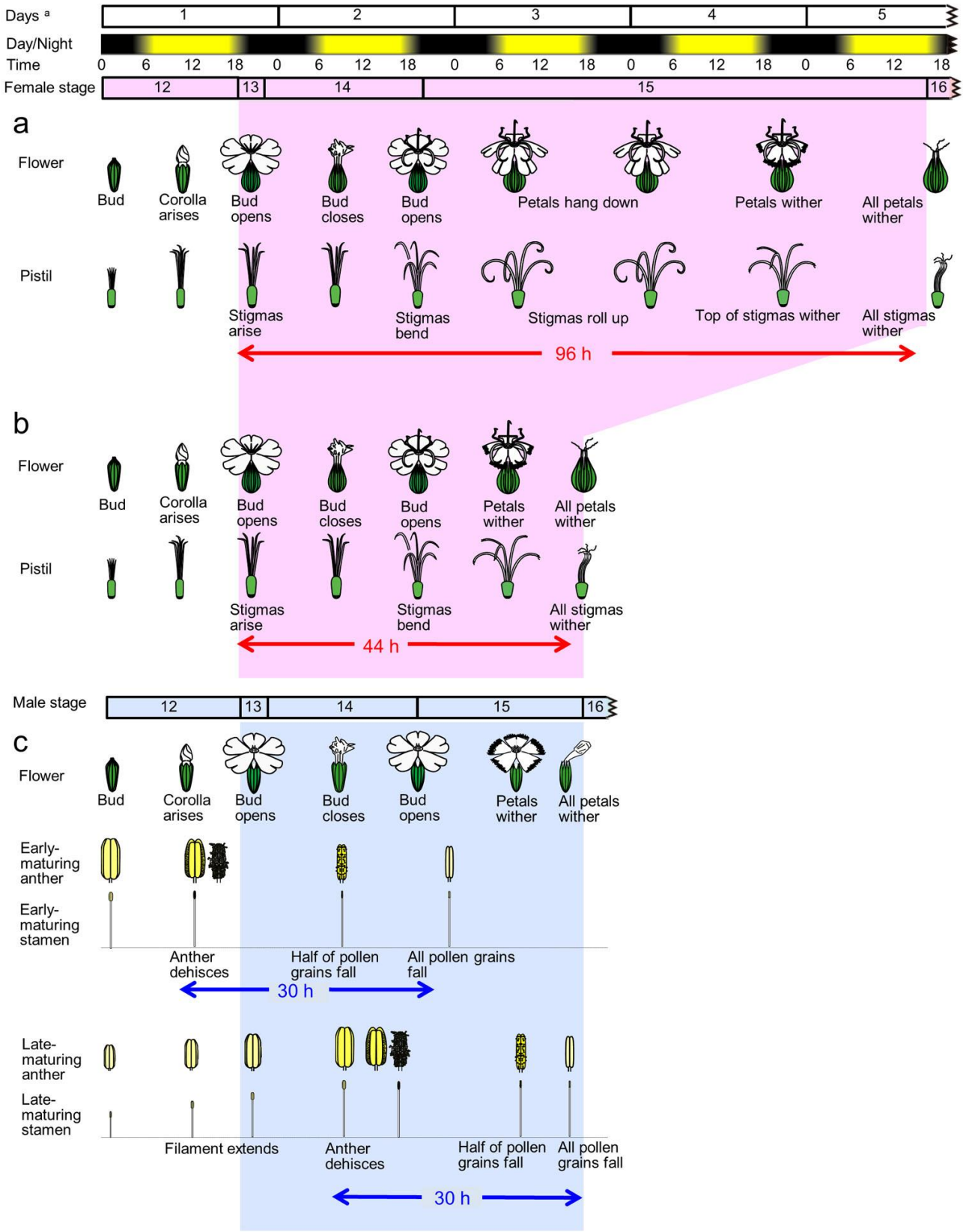
Days a
1
2
3
4
5
Day/Night
Time
0 6 12 18 0 6 12 18 0 6 12 18 0 6 12 18 0 6 12 18
Female stage
12
13
14
15
16
a
Flower
Bud
Corolla arises
Bud opens
Bud closes
Bud opens
Petals hang down
Petals wither
All petals wither
Pistil
Stigmas arise
Stigmas bend
Stigmas roll up
Top of stigmas wither
All stigmas wither
96 h
b
Flower
Bud
Corolla arises
Bud opens
Bud closes
Bud opens
Petals wither
All petals wither
Pistil
Stigmas arise
Stigmas bend
All stigmas wither
44 h
Male stage
12
13
14
15
16
c
Flower
Bud
Corolla arises
Bud opens
Bud closes
Bud opens
Petals wither
All petals wither
Early-maturing anther
Early-maturing stamen
Anther dehisces
Half of pollen grains fall
All pollen grains fall
30 h
Late-maturing anther
Late-maturing stamen
Filament extends
Anther dehisces
Half of pollen grains fall
All pollen grains fall
30 h

Fig. 1-2. Timetables of male and female flower development after anthesis in *Silene latifolia*. Schemes of the flower and pistil and the stamen during stages 12–16 are indicated. (**a**) Scheme of the female flower and the pistil when pollination does not occur. (**b**) Scheme of the female flower and the pistil when pollination occurs until stage 15. (**c**) Scheme of the male flower, the filament, and anther. Days from anthesis, day/night, and stages are indicated above the scheme. The red arrow indicates the longevity of the stigma (the period during which the stigma can be pollinated). The longevity of the stigma can be shortened when pollination occurs until stage 15. The blue arrow indicates the period during which the anthers hold pollen grains.

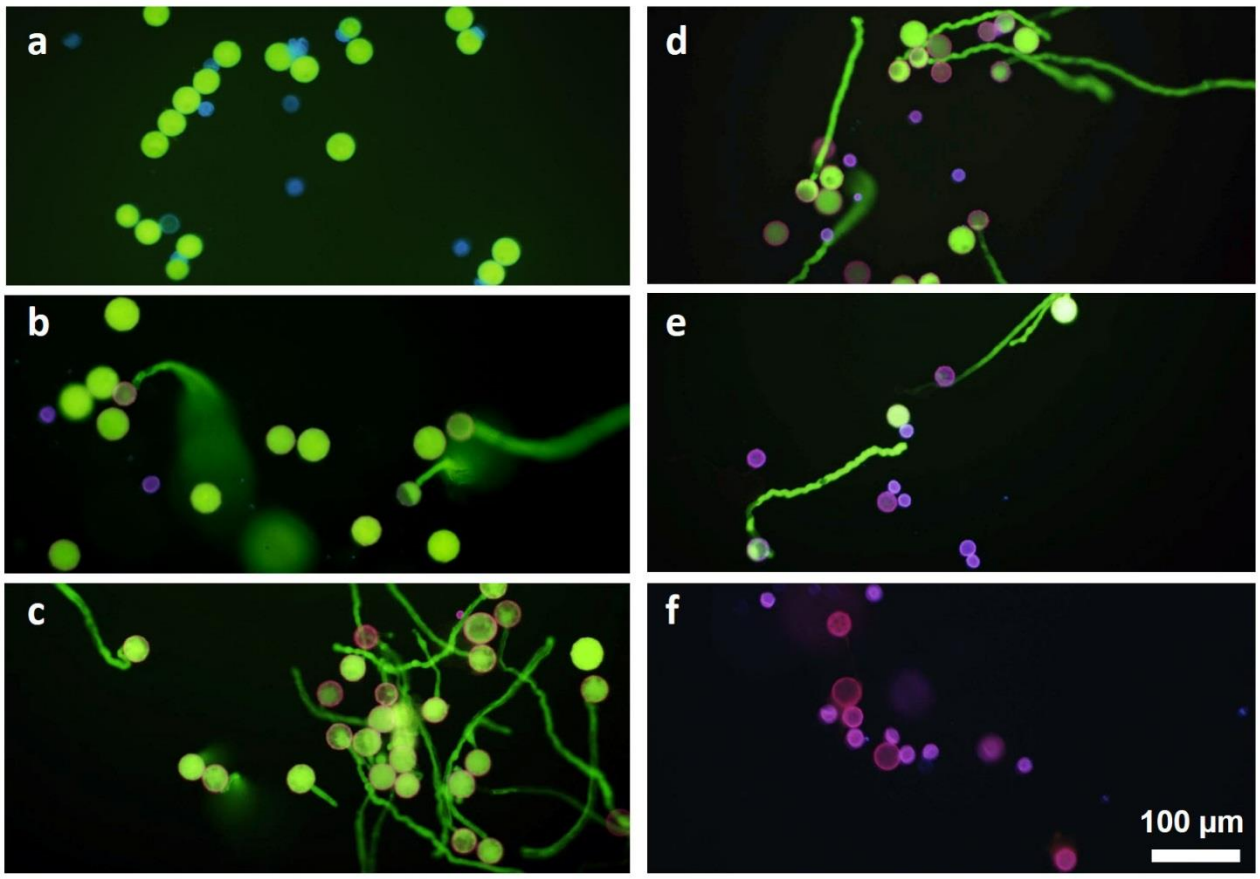

Fig. 1-3. *In vitro* pollen viability on the pollen medium. Fluorescence images of FDA/PI double-stained pollen grains. Viable pollens were stained with FDA (yellow to green), and nonviable pollen grains were stained with PI (purple to red). (**a**) The pollen grains were collected and stained on 1 DAA at 12:00, (**b**) 1 DAA at 18:00, (**c**) 2 DAA at 00:00, (**d**) 2 DAA at 06:00, (**e**) 2 DAA at 12:00, and (**f**) 2 DAA at 18:00.

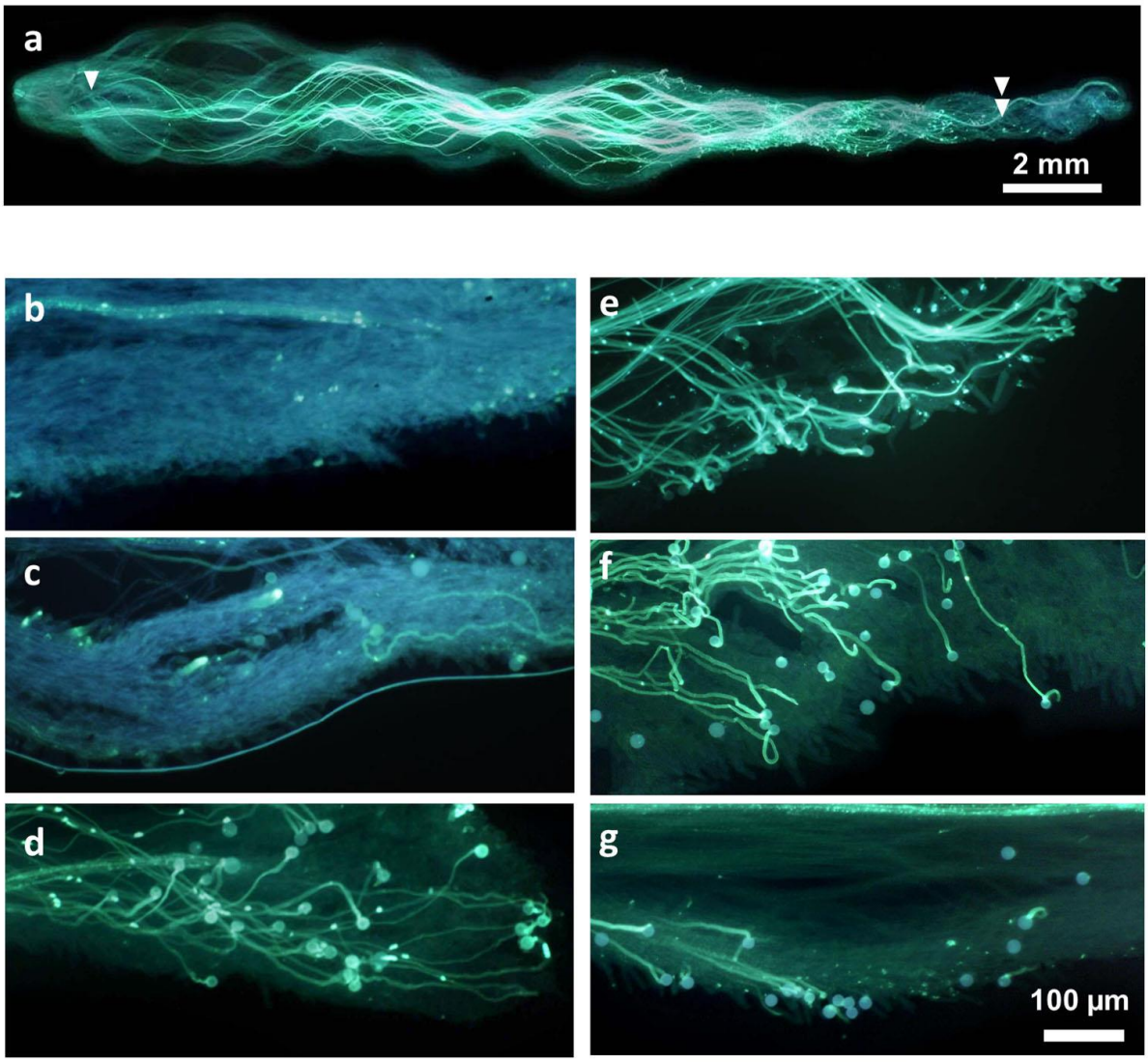

Fig. 1-4. *In vivo* pollen viability on the stigma. Fluorescent images of aniline blue-stained pollen grains on the stigma. Aniline blue stained the immature stigma blue, and stained the mature stigma green. (**a**) The whole stigma. The mature Type 1 pollen tubes extend from right to left and arrive at the ovary (arrowhead). However, immature Type 2 pollen tubes did not arrive at the ovary (double arrowhead). (**b**) The stigma at 0 DAA. (**c**) The stigma with pollen grains at 1 DAA, (**d**) 2 DAA, (**e**) 3 DAA, (**f**) 4 DAA, and (**g**) 5 DAA.

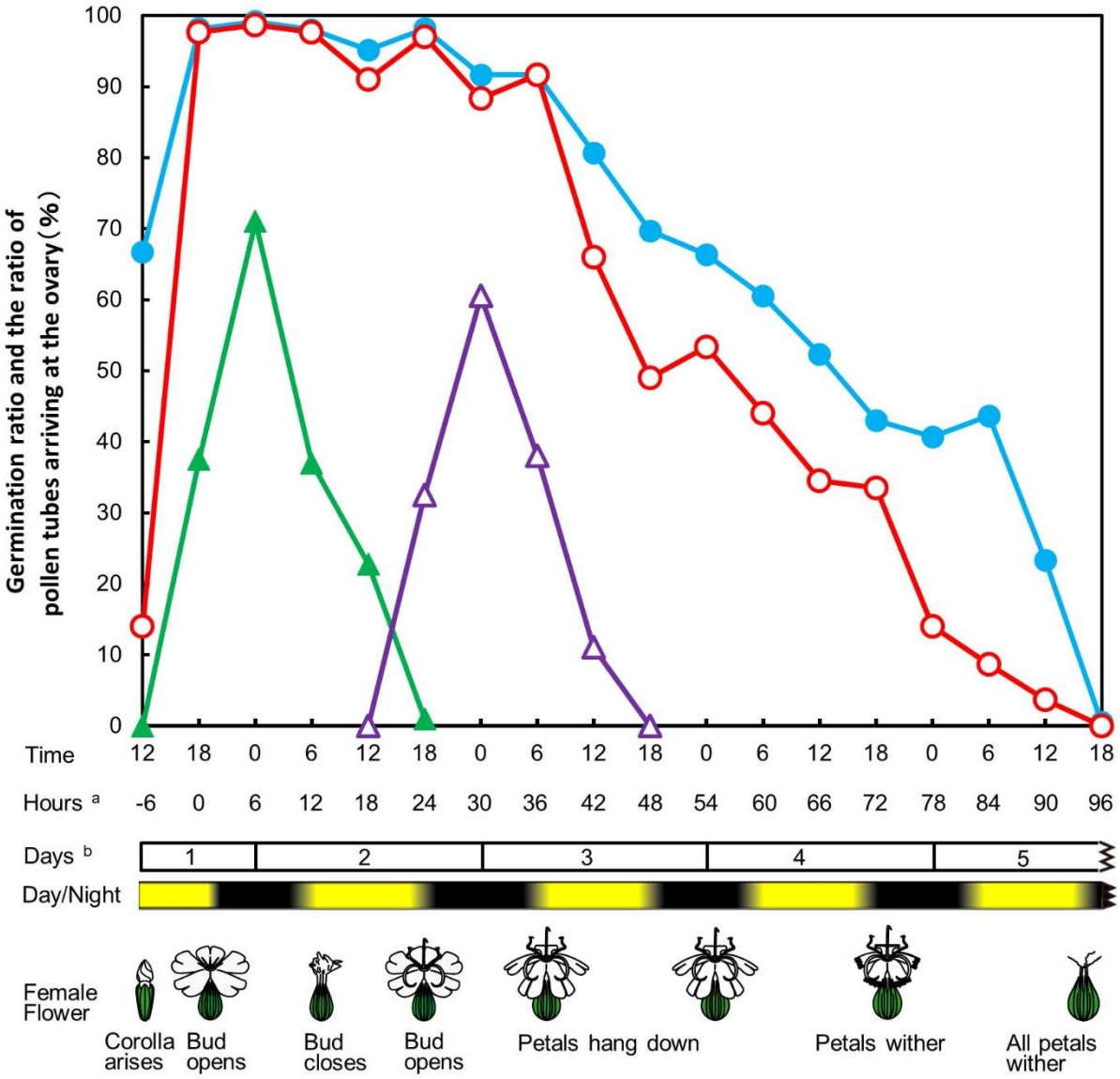

Fig. 1-5. Stamen and pistil maturation timing based on *in vitro* and *in vivo* experiments. The filled circle indicates the *in vivo* germination ratio of pollen grains. The open circle shows the ratio of pollen tubes arriving at the ovary. The filled triangle indicates the *in vitro* germination ratio of pollen grains from early-maturing stamens. The open triangle represents the *in vitro* germination ratio of pollen grains from late-maturing stamens.

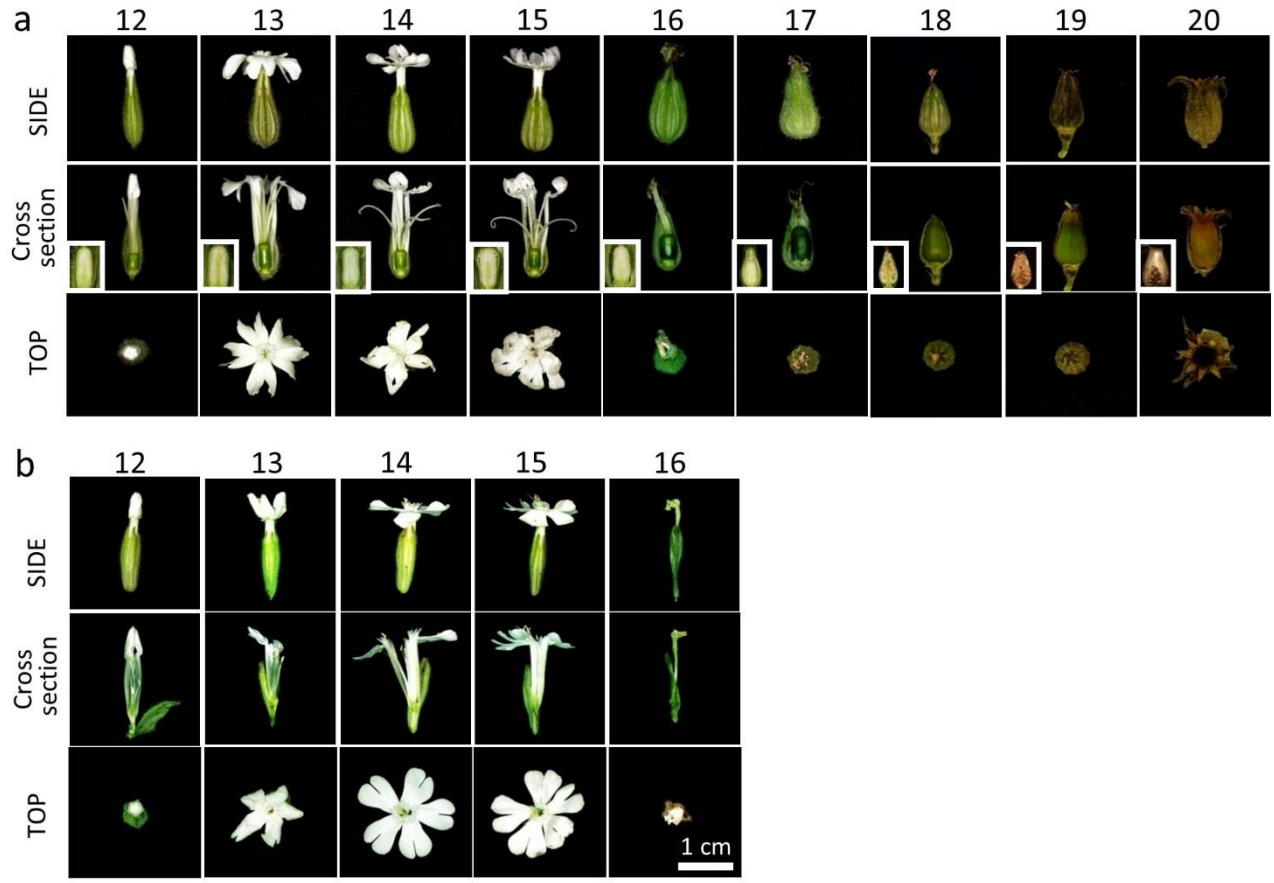

Fig. S1-1. Photographs of floral developmental stages after anthesis represent the visual appearance of flowers at each designated stage. (**a**) Stages of development of a female flower. Insets in cross sections are the inside the ovary and show ovules or seeds. (**b**) Stages of development of a male flower. The numbers above the photographs indicate the stages of flower development.

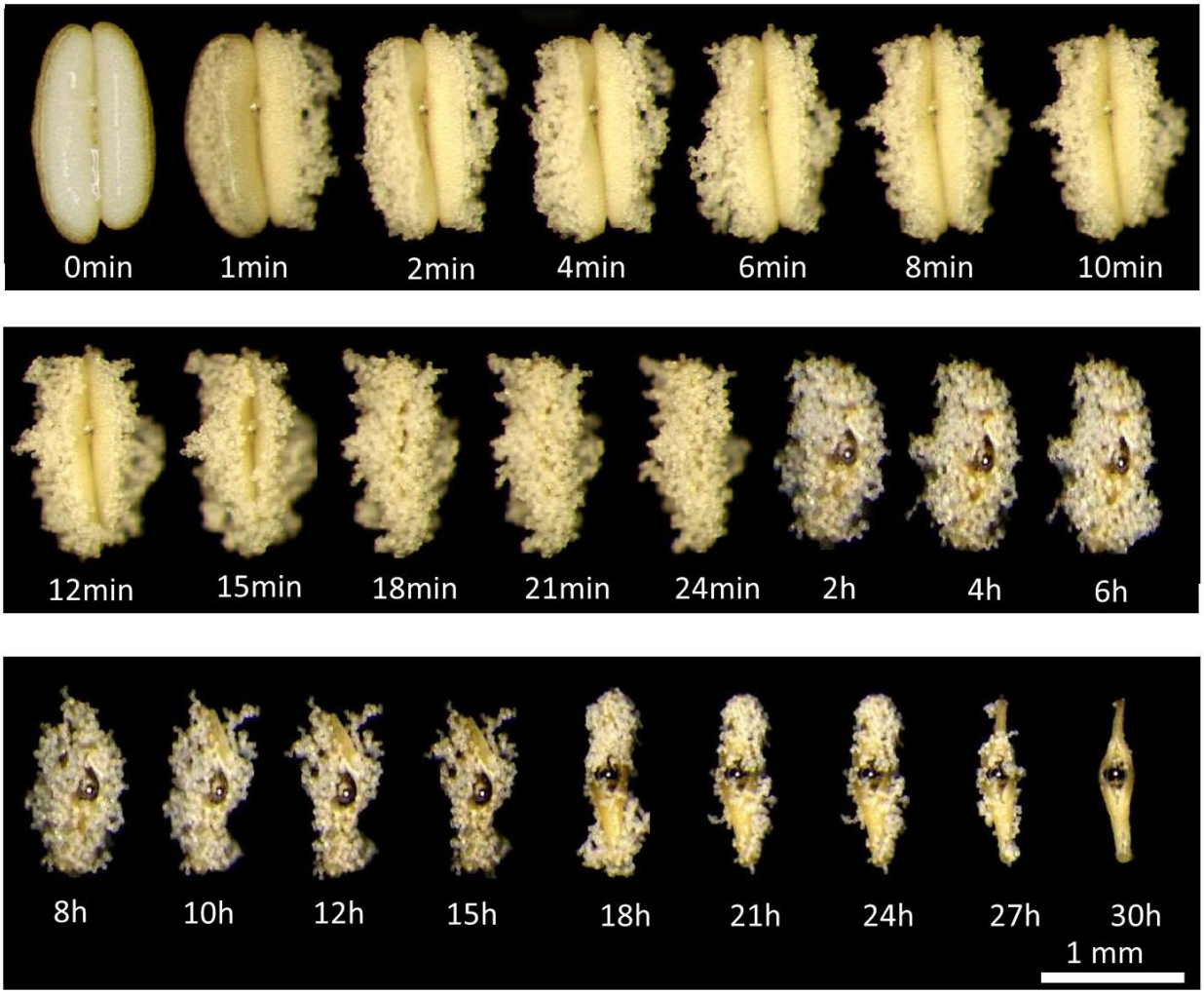

Fig. S1-2. Structure of an anther during dehiscence. Dehiscence was completed in 24 min. Then, the mature pollen grains gradually fell from the anther, followed by almost all pollen grains.

CHAPTER II

Appearance of male/female trade-off and monoecism in hermaphroditic mutants of the dioecious plant *Silene latifolia*

SUMMARY

The evolution of dioecy from hermaphroditism is also a measure for avoiding self-pollination, and its evolutionary background has been investigated both experimentally and theoretically since it was first proposed by Darwin. Here, I isolated nine hermaphroditic mutants of the dioecious plant *Silene latifolia* by mutagenesis and showed that a trade-off between stamens and pistils, and monoecism appeared in these mutants. Approach herkogamy appeared in five of them as pistils lengths were constantly longer than stamens. Although the maturation period of stamens coincided with that of pistils, the pistils terminated 6–30 h earlier than in wild-type females. Two of them showed signs of protogyny (dichogamy) as the pistils matured 12 h earlier than in wild-type females. These results suggest that both male/female trade-off, which is considered to be the condition of evolution of dioecy from hermaphroditism, and an avoidance mechanism for self-pollination, appeared in the hermaphroditic state in *S. latifolia*.

INTRODUCTION

The first explanation for the evolution of dioecious plants from hermaphrodite forms was provided by Darwin (Dawin 1877), and it has since been studied both theoretically and experimentally. Most hermaphroditic plants have various mechanisms to avoid self-pollination, such as herkogamy, dichogamy, and self-incompatibility (Barrett 2003; Bertin and Newman 1993; Lloyd and Webb 1986; Webb and Lloyd 1986). This raises the question as to whether such nearly ubiquitous mechanisms for avoiding self-pollination in hermaphroditic plants will also appear in hermaphroditic mutant dioecious plants. The dioecious plant *Silene latifolia* is assumed to have evolved from the hermaphrodite condition via gynodioecy, and males with loss of female sterility (hermaphrodites carrying a Y chromosome) occasionally arise in this species (Charlesworth 2006; Desfeux et al. 1996; Marais et al. 2011). Dichogamy has been reported in some hermaphrodite and gynodioecious plants belonging to the genus *Silene* (Buide 2002; Davis and Delph 2005; Kephart et al. 1999). *Silene viscosa*, which is a hermaphroditic plant most closely related to *S. latifolia*, shows both spatial separation of stamens/pistils within the flower and temporal separation of stamen/pistil maturation. Determining whether these mechanisms for avoiding self-pollination in hermaphroditic plants of the *Silene* genus will appear in hermaphrodite *S. latifolia* mutants is a topic of interest.

Investigation on characteristics of the hermaphroditic condition in *S. latifolia* requires the production of many hermaphroditic mutants. Sex in the dioecious plant *S. latifolia* is determined by XY sex

chromosomes, and the male flower (XY) has three characteristics controlled by sex-determining factors on the Y chromosome (Westergaard 1958); the gynoecium is suppressed by the GSF, the stamens are promoted by the SPF, and anther and pollen grain maturation is promoted by the MFF. A previous study showed that hermaphroditic mutants can be isolated by deleting GSF on the Y chromosome (Lardon et al. 1999; Lebel-Hardenack et al. 2002). The Y chromosome sequence-tagged site (STS) markers MK17 and ScQ14 were isolated as the most proximal markers to GSF and SPF, respectively (Hobza et al. 2006; Zhang et al. 1998). Hermaphroditic mutants in *S. latifolia* are not self-incompatible; they have both fertile stamens and fertile pistils and can form seeds by self-pollination (Lardon et al. 1999; Miller and Kesseli 2011). Dichogamy and herkogamy can be investigated using these hermaphroditic mutants, as has been broadly examined in many hermaphroditic species. I subjected pollen grains to either heavy ion beam or γ-ray irradiation. The irradiated pollen grains were then used to pollinate wild-type (WT) female flowers, and M_1 seeds were obtained. I cultured 2772 M_1 plants and searched for hermaphroditic mutants by screening for (1) three STS markers and (2) flower phenotype (Fig. S2-1). I also mapped all mutants obtained from M_1 plants using 25 Y chromosome STS markers.

Models for sex allocation and the evolution of plant breeding systems generally assume that sex allocation patterns exhibit genetic variation, and that trade-offs will occur between allocation to male and female functions (Campbell 2000; Charnov 1982). In *S. latifolia*, the trade-off between male and female functions has been suggested based on the sizes of stamens and pistils in hermaphroditic mutants (Fujita et

al. 2012). In the present study, I attempted to quantify the trade-off between male and female functions by counting the numbers of pollen grains and ovules in hermaphroditic mutants. I also investigated whether ubiquitous hermaphrodite characters of herkogamy or dichogamy appeared in dioecious plants by measuring both the lengths and maturation periods of stamens and pistils in hermaphroditic mutants. Both dichogamy and herkogamy were observed in *S. viscosa*, which is the hermaphroditic plant most closely related to *S. latifolia*. By comparing the isolated hermaphroditic mutants and *S. viscosa*, the modification of floral characters that occurred in connection with evolution of the breeding system from hermaphroditic to dioecious plant can be demonstrated.

MATERIALS AND METHODS

Plant material and growth conditions.

S. latifolia seeds were obtained from an inbred line (K-line) in our laboratory (Kazama et al. 2003). The K-line was propagated for 16 generations of brother–sister matings to obtain genetically homogeneous populations. Plants were grown from seeds in pots in a regulated chamber at 23°C with a 16-h light/8-h dark cycle.

Screening for hermaphroditic mutants with partial Y chromosome deletion

The Y deletion mutants were obtained by either heavy-ion beam irradiation or γ irradiation of pollen, and 2722 M_1 generation plants were grown in a field. To obtain both hermaphroditic mutants and other phenotype mutants in M_1 generation plants, I performed (1) polymerase chain reaction (PCR) screening using four STS markers (MK17, ScQ14, MS4, SlAP3Y) (Table S2-2) and (2) flower phenotype screening (Fig. S2-1). Genomic DNA was extracted from fresh leaves using a Nucleon Phytopure Genomic DNA Extraction Kit (GE Healthcare, Milwaukee, WI) according to the manufacturer's instructions. PCR amplification was performed using Blend Taq polymerase (Toyobo, Tokyo, Japan) in a Thermal Cycler (Dice TP600; Takara Bio, Otsu, Japan). The conditions were 5 min at 94°C, followed by 30 cycles of 30 s at 94°C, 30 s at 60°C, and 1 min at 72°C, with a final extension of 5 min at 72°C. Each 20-μL reaction mixture contained 50 ng of template DNA, 2 μL of 10 dNTPs, 10× Blend Taq Buffer, 0.2 μL of Blend Taq,

and 1 μL of each primer at 5 mM. The reaction products (5 μL) were electrophoresed on 1.5% agarose gels. After staining with ethidium bromide, fragments were visualized on a UV illuminator (Atto, Tokyo, Japan). WT male and female genomic DNAs were used as controls.

Y chromosome deletion mapping

In total, 38 Y deletion mutants and 25 STS markers were used for Y chromosome deletion mapping in this study (Tables 2-1 and S2-2) (Fujita et al. 2012). The PCR procedure was the same as described above. PCR detection was repeated three times for each STS marker.

Pollen grain, ovule, and seed numbers

For determination of pollen grain and ovule numbers, mature buds just before flower opening were used. To determine the pollen grain number, anthers were opened under a stereomicroscope and half of the pollen grains contained in the anther were spread onto agar-covered microscope slides. The numbers of pollen grain were counted under a fluorescence microscope (BX60; Olympus, Tokyo, Japan). To determine the ovule number, the ovary was opened, and ovules were counted at 40× magnification under a stereomicroscope. Each hermaphroditic mutant was emasculated and pollinated with WT male pollen. Then, the numbers of seeds in the resulting capsules were counted.

Stereomicroscopic observations

Flowers, anthers, ovaries, and capsules were observed under a stereomicroscope (MZ16; Leica Imaging Systems, Cambridge, UK).

Measurement of floral organ length

To determine the length of the floral organ, the calyx was partially dissected, and the inner floral organs were measured without nipping off the flower. The lengths of the pistil, Em-stamen, Lm-stamen, petal, calyx, ovary (longitudinal), and ovary (horizontal), and gynophore in each hermaphroditic mutant were measured every 6 h using a ruler.

Pollen viability and *in vitro* germination determination

To determine the pollen viability double staining with FDA and PI was performed (Mandaokar and Browse 2009). A stock solution of 2 mg/mL FDA was made in acetone and added dropwise to 17% sucrose (Suc; w/v) until the solution became cloudy. PI was diluted to 1 mg/mL in water and diluted to 100 µL/mL with 17% Suc (w/v). Equal amounts of FDA and PI solutions were mixed together and added to freshly isolated pollen on glass slides. The pollen was covered with a coverslip and viewed under a fluorescence microscope. A pollen germination assay was performed (Jolivet and Bernasconi 2007b). Pollen was isolated from mature flowers by gently releasing them from the anther locules onto microscope slides containing pollen germination medium.

***In vivo* pollen germination and tube growth**

Stigma staining was performed with aniline blue (Fang et al. 2010). Previously pollinated pistils were excised from flowers 6 h after pollination and fixed for 24 h in acetic alcohol (glacial acetic acid:ethanol, 1:3, v/v), then cleared with 8 N NaOH overnight and rinsed thoroughly before staining with decolored 0.1% (w/v) aniline blue in 0.1 M K_3PO_4. The preparation was observed under a fluorescence microscope to measure pollen germination and pollen tube growth down the style. Pollen grains were scored as germinated when the tubes were apparent between the papillate cells of the stigma, and the number of pollen tubes, the number that reached the end of the style, and the number of those that barely elongated were recorded.

RESULTS

The dioecious plant *S. latifolia* and the hermaphroditic plant *S. viscosa*

The dioecious plant *S. latifolia* has male and female flowers in which the stamens and pistils are present in separate plants, whereas the hermaphroditic plant *S. viscosa* has hermaphrodite flowers in which both stamens and pistils are present in the same plant (Fig. 2-1a–c). In *S. viscosa*, the pistils extend straight, while the stamens hang down vertically (Fig. 2-1c). In the previous chapter, I divided the 10 stamens into two groups based on their lengths: the five long stamens as "Early-maturing stamens (Em-stamens)" and the five short stamens as "Late-maturing stamens (Lm-stamens)" (Aonuma et al. 2013). The lengths of eight floral organs were measured every 6 h (Fig. 2-1d–f). Fig. S2-2 shows the lengths of each floral organ. In *S. latifolia*, Em-stamens and pistils extended above the petals at 6 HAA (Fig. 2-1d,e). In *S. viscosa*, Em-stamens extended above the petals at –6 HAA, while pistils extended above the petals at 30 HAA (Fig. 2-1f). Although the stamen and pistil lengths of *S. latifolia* synchronously arrived at the petal length after anthesis, the pistil length of *S. viscosa* arrived at petal length more than 1 day late compared to its stamen length. In *S. viscosa*, both the Em-stamen and Lm-stamen lengths were consistently longer than the pistils, and the pistil length never caught up throughout the anthesis period. In addition, the stamens hang down vertically from the petals, thus maintaining physical distance from the pistils (Fig. 2-1c). Therefore, herkogamy existed in *S. viscosa*. Herkogamy has been divided into two types: approach herkogamy in

which the pistils are located above the stamens and contacts pollinators first upon entry into flowers, and reverse herkogamy in which stamens are located above the pistils (Barrett 2003). *S. viscosa* was classified as showing reverse herkogamy.

The degrees of maturation of the stamens and the pistils were measured every 6 and 12 h, respectively, based on the pollen germination rates on pollen medium (*in vitro*) and on the stigmas (*in vivo*) (Fig. 2-1g–i). The maturation periods of the Em-stamens and the Lm-stamens in *S. latifolia* male flowers were –6 to 24 HAF and 18 to 48 HAA, respectively (Fig. 2-1g). The maturation period of pistils in *S. latifolia* female flowers was –6 to 96 HAA (Fig. 2-1h). On the other hand, although the maturation periods of Em-stamens and Lm-stamens in *S. viscosa* were –6 to 24 HAA and 18 to 48 HAA, respectively, as in *S. latifolia* male flowers, the maturation period of pistils in *S. viscosa* was 42 to 138 HAA, and was markedly delayed compared to *S. latifolia* female flowers (Fig. 2-1i). The maturation period of the pistils in *S. viscosa* was markedly delayed compared to that of its stamens, and *S. viscosa* showed a distinct temporal separation of stamen/pistil maturation. Thus, *S. viscosa* possessed dichogamy, with the stamens maturing prior to pistils, which is an example of protandry.

As *S. viscosa* possessed both dichogamy and herkogamy, this raised a question whether the hermaphroditic mutant *S. latifolia*, which is thought to be the ancestral state, also possessed these functions. The results of our investigations regarding *S. latifolia* WT male and female flowers indicated that both stamens and pistils of *S. latifolia* matured synchronously shortly after anthesis. However, investigating whether herkogamy or dichogamy appeared in hermaphroditic mutants of *S. latifolia* by delaying extension

and maturation of pistils as in *S. viscosa* is a topic of interest.

Partial deletion Y chromosome mutants including hermaphroditic mutants obtained from M_1 generation and Y chromosome deletion mapping

Thirty mutants with partial deletions in the Y chromosome were isolated by screening of M_1 generation plants generated by C-ion beam, Fe-ion beam, or γ-ray irradiation. Thirty-eight mutants, including eight previously isolated mutants, are shown in Table 2-1 and Fig. 2-2 (Fujita et al. 2012; Koizumi et al. 2007, 2010). The sex segregation and appearance ratios in the M_1 generation are shown in Table S2-1. The hermaphroditic mutants (EGP: early-stage gynoecium promoted mutant) formed both 10 complete stamens and gynoecium composed of 5 fused carpels with 5 styles. EGP5, EGP6, and EGP7 had such small petals that the corolla did not open fully (Fig. 2-2a). Asexual mutants (ESS: early-stage stamen-suppressed mutant) formed neither the gynoecium nor the stamens. The corolla of ESS3 did not open fully (Fig. 2-2b). The asexual flowers are arranged in order according to the development degree of the petals from left to right. The anther defect mutants (ISS: intermediate-stage stamen-suppressed mutant) had stamens that did not elongate fully. The ISS mutants are arranged in order according to the degree of development the stamens from left to right. ISS9 had stamens in which the filaments were very short, and a gynoecium composed of two fused carpels with two styles (Fig. 2-2c). The pollen defect mutants (LSS: late-stage stamen-suppressed mutant) had sterile stamens. The LSS mutants are arranged in order according to the

degree of development of the gynophore from left to right (Fig. 2-2d). The XY female mutant (GPSS: gynoecium promoted and stamen-suppressed mutant) did not form stamens, but formed the gynoecium composed of five fused carpels with five styles. Although the XY female mutant had a Y chromosome, the phenotype was the same as the WT female flower (Fig. 2-2e). WT male and female flowers in *S. latifolia* are shown in Fig. 2-2f.

In total, 38 Y deletion mutants were used for Y chromosome deletion mapping in this study (Table 2-1). The Y chromosome deletion regions were determined using 25 STS markers (Fujita et al. 2012) (Fig. 2-3). Most of the EGP mutants had deletions near GSF, whereas most of the ESS mutants had deletions near SPF. Most of the EGP mutants had deletions of MK17. No deletions were found in R025 or EGP14 with any of these 25 STS markers. All of the ESS mutants had deletions in ScQ14 and STS609. EGP12 formed complete stamens, while it carried deletions in ScQ14 and STS609. GPSS1 had deletions in MK17, ScQ14, and STS609. Although the phenotype of GPSS1 was thought to be a WT male, it seemed to change to a female flower with deletion of both SPF and GSF in the Y chromosome. Further investigations of the Y chromosome deletion regions of R025, EGP14, and EGP12 may lead to isolation of the male sex determination regions. A common deletion was not found in ISS and LSS mutants. In addition, no deletions were found in 10 mutants with 25 STS markers (ISS1, ISS3, ISS5, ISS6, ISS8, ISS11, LSS1, LSS2, LSS3, and LSS4).

Trade-off: resource–fitness allocation to stamens versus pistils in hermaphroditic mutants

As the hermaphroditic mutants isolated in this study had both complete stamens and pistils, this enabled us to quantitatively investigate whether a trade-off between stamens and pistils occurred in the hermaphroditic state of *S. latifolia*. The numbers of pollen grains and ovules in 9 hermaphroditic mutants (R025, EGP4, EGP9, EGP10, EGP11, EGP12, EGP13, EGP14, and EGP15) and XY female mutant (GPSS1) were counted. The hermaphroditic mutants are arranged in order of increasing number of ovules from left to right in Fig. 2-4a. The numbers of pollen grains and seeds in hermaphroditic mutants are shown in Table 2-2. Ovule numbers in hermaphroditic mutants ranged from 129 in EGP9 to 334 in EGP13. Ovule number in the WT female was 367, which was greater than in any of the hermaphroditic mutants. The hermaphroditic mutants did not produce as many seeds as the WT female, and EGP11 produced a maximum of only 69 seeds. EGP14 did not produce any seeds because its whole flower withered and fell after pollination (Fig. 2-4c). The pollen numbers in hermaphroditic mutants ranged from 910 in EGP13 to 2193 in EGP9 (Fig. 2-4d). Pollen number in WT males was 1735, which was less than in EGP9, EGP10, EGP12, and EGP15.

A pollen–ovule scatterplot was drawn to investigate resource allocation to male versus female functions in hermaphroditic mutants (Fig. 2-5a). With the exception of GPSS1, all of the mutants generally produced many pollen grains and ovules, and were located on the upper right of a straight line connecting the WT male and WT female in the pollen–ovule scatterplot (Fig. 2-5a). A trade-off relationship was revealed between pollen and ovules in the scatterplot.

Although the hermaphroditic mutants seemed to show greater resource investment in male and female functions compared to WT males and WT females, determining whether these pollen grains and ovules

were indeed fertile and thus whether the fitness of hermaphroditic mutants was high is important.

A scatterplot of germinated pollen seeds was drawn to investigate the fitness allocation to male versus female functions in hermaphroditic mutants (Fig. 2-5b). The pollen germination rates in the hermaphroditic mutants were all lower than in WT male flowers (70%) (Fig. S2-3) (Aonuma et al. 2013). The number of germinated pollen grains was determined as the number of pollen grains multiplied by the pollen germination rate (Table 2-2). A scatterplot of germinated pollen seeds was drawn to investigate the fitness allocation to male versus female functions in hermaphroditic mutants (Fig. 2-5b). All of the hermaphroditic mutants were located on the lower left of a straight line connecting WT males and WT females in the germinated pollen seed scatterplot (Fig. 2-5b). The hermaphroditic mutants have poor ability to produce germinated pollen grains and seeds, and therefore, the fitness of WT male and WT female seemed to be higher than for any of the hermaphroditic mutants. In addition, a trade-off relationship was revealed between germinated pollen and seeds in the scatterplot.

Herkogamy: spatial separation of stamens and pistils within the flowers of hermaphroditic mutants

To investigate whether herkogamy appears during anthesis among the hermaphroditic mutants in *S. latifolia* as well as in *S. viscosa*, the lengths of eight floral organs were measured every 6 h during the period from –18 to 96 HAA (Fig. 2-6). The lengths of each floral organ are shown in Fig. S2-2.

After anthesis, the pistil length, the Em-stamen length, and finally the Lm-stamen length exceeded the

petal length. The pistils were longer than stamens in most of the hermaphroditic mutants, with differences of 2–10 mm between the two. In five hermaphroditic mutants (EGP12, R025, EGP15, EGP11, and EGP13), the pistil lengths constantly exceeded those of the stamens, and the stamens did not catch up throughout the anthesis period (Fig. 2-6b,e,f,h,i). Outline arrows indicate the time points when the stamen length came closest to the pistil length after anthesis. In four hermaphroditic mutants (EGP9, EGP14, EGP4, and EGP10), however, the stamen lengths caught up with the pistil lengths during the anthesis period (Fig. 2-6a,c,d,g). Black arrows indicate the time points when the stamen lengths caught up with the pistil lengths. Although the stamen lengths temporarily caught up with the pistil lengths in these four hermaphroditic mutants, they exceeded the stamen lengths during the later anthesis period (Fig. 2-6a,d,g). The Lm-stamen lengths did not catch up with the pistil lengths in any of the hermaphroditic mutants throughout the anthesis period.

In contrast to *S. viscosa*, the pistils grew in advance of the stamen in the hermaphroditic mutants of *S. latifolia* rather than delayed pistil growth. In five hermaphroditic mutants (EGP12, R025, EGP15, EGP11, and EGP13), the pistils were longer than the stamens, and approach herkogamy appeared. This pattern was the opposite of that in *S. viscosa*, which showed reverse herkogamy.

Dichogamy: temporal separation of stamen and pistil maturation in hermaphroditic mutants

During the anthesis period in these hermaphroditic mutants, to investigate whether the pistil maturation

period coincided with that of the stamen as in WT *S. latifolia* or was delayed for more than 1 day compared to that of the stamen as in *S. viscosa*, the degrees of maturity of the stamens and pistils were estimated by the same method as shown in Fig. 2-1g–i (Fig. 2-7).

In all of these hermaphroditic mutants, the maturation timings of the Em-stamen and Lm-stamen were 6 HAA and 30 HAA, respectively, and coincided with those in WT *S. latifolia*. The maturation period of stamens coincided with that of pistils during the anthesis period in these hermaphroditic mutants. Pistil maturation commenced in both R025 and EGP15 at –18 HAA, which was 12 h earlier than in the other hermaphroditic mutants and WT females (Fig. 2-7e,f).

The hermaphroditic mutants of *S. latifolia* showed synchronous maturation of their pistils during the maturation period of the Em-stamen and Lm-stamen, rather than delayed pistil maturation until the stamens withered as seen in *S. viscosa* (Fig. 2-1i). In addition, because the commencement of pistil maturation in R025 and EGP15 (–18 HAA) occurred 12 h earlier than in WT *S. latifolia* females (–6 HAA), the hermaphroditic mutants of *S. latifolia* tended to show accelerated pistil maturation ahead of the stamen, rather than delayed maturation as seen in *S. viscosa*.

DISCUSSION

To compare the floral characters of hermaphroditic mutants and WT *S. latifolia* and WT *S. viscosa*, the stamen/pistil maturation periods and timing of when the stamen length caught up with the pistil length are compiled in Fig. 2-8. Approach herkogamy in which the pistil length exceeds the stamen length appeared in five of nine hermaphroditic mutants, as indicated by outline stars in Fig. 2-8. The stamen length caught up with the pistil length in only four hermaphroditic mutants, as indicated by black stars in Fig. 2-8. Herkogamy is nearly ubiquitous in hermaphroditic plants (Barrett 2003; Webb and Lloyd 1986). As herkogamy appeared not only in *S. viscosa* but also in five of nine hermaphroditic mutants of *S. latifolia* in this study, it seemed to appear frequently in the hermaphroditic state of dioecious plants.

Stamen length caught up with pistil length during the period of 0–12 HAA in four hermaphroditic mutants. In all hermaphroditic mutants, as the Em-stamen began to mature at –6 HAA, the timing of when the stamen length caught up with the pistil length was later than the beginning of stamen maturation (Fig. 2-8). In most of the hermaphroditic plants, stamen–pistil contact occurred during the later period of anthesis (Duan et al. 2010; Jia and Tan 2012; Kephart et al. 1999; Luo and Widmer 2013; Vos et al. 2012). Delaying stamen–pistil contact has the advantage of enhanced possibility of both cross-pollination and reproductive assurance (Fenster and Marten-Rodriguez 2007; Lloyd and Schoen 1992; Ruan and Silva 2012). The character of delayed autonomous selfing has also been reported in *Silene* (*S. acutifolia*, *S. noctiflora*, and *S.* douglasii) (Buide 2002; Davis and Delph 2005; Kephart et al. 1999). In *S. latifolia*, the timing of pollen

arrival significantly affects the siring success of competing pollen donors, and the paternity success of the second-arriving pollen was significantly lower than 50% after a 2-h delay (Burkhardt, Internicola, and Bernasconi 2009). The hermaphroditic mutants of *S. latifolia* seem to have ample chance of outcrossing due to a delay of stamen–pistil contact.

The hermaphroditic mutants of *S. latifolia* showed synchronous maturation of both stamens and pistils shortly after anthesis as in WT *S. latifolia*, rather than delayed maturation of the pistils compared to the stamens by more than 40 h as in *S. viscosa* (Fig. 2-8). Furthermore, the hermaphroditic mutants tended to show accelerated maturation of pistils as seen in R025 and EGP15. To increase the chance of cross-pollination between separate male and female plants, WT *S. latifolia* flowers and matures stamens and pistils simultaneously with circadian rhythm (Aonuma et al. 2013). However, to avoid self-pollination, stamens and pistils do not mature simultaneously in most hermaphroditic plants (Bertin and Newman 1993; Lloyd and Webb 1986). The tendency to show accelerated pistil maturation suggests the appearance of protogyny in the hermaphroditic state of *S. latifolia*. Both herkogamy and dichogamy avoid interference between pollen dispatch and pollen receipt, and maintain a degree of pollination precision. Herkogamy and/or dichogamy are almost universally present in outcrossing angiosperms and play a vital role in the successful functioning of blossoms, and should be investigated in greater detail.

Dioecy may be favored over hermaphroditism if the trade-off in investment of resources to male and female functions results in increased fitness return on investment in a single sexual function (Charlesworth and Charlesworth 1981; Laguerie et al. 1991). The dioecious plant *S. latifolia* has been assumed to have

evolved from the hermaphrodite condition via gynodioecy (Delph and Wolf 2005). A model for the evolution of dioecy and gynodioecy suggested that the occurrence of ovule production modifiers reduces ovule production of hermaphrodites, and can also increase pollen production, by the compensation principle (Charlesworth and Charlesworth 1978). Our scatterplots of both the pollen–ovule predicting investment set and germinated pollen seed predicting fitness set showed that a trade-off relationship exists between male and female functions in hermaphroditic mutants (Fig. 2-5a,b). These results were consistent with the model based on the premise that reducing investment in one reproductive function can be compensated for by allocating additional resources for the other sexual function. Several fieldwork-based studies have attempted to quantify the allocation of resources to male and female fitness, and showed a phenotypic trade-off relationship between stamens and pistils in hermaphrodites of some species (Ashman 2003; Davis 2002; Rosas and Domínguez 2009).

Sex allocation theory is a robust branch of evolutionary biology, and aims to understand the allocation of optimal amounts of resources to male and female functions in simultaneous hermaphrodites (hereafter referred to as “hermaphrodites”) (Charnov 1982; Klinkhamer, de Jong, and Metz 1997; Schärer 2009). Sex allocation theory proposes that the shape of the fitness set could be decisive in determining the advantage of hermaphroditism (cosexuality) over dioecy (unisexuality). If the shape of the fitness set is concave, dioecy will be favored in angiosperms because the rate of increase in male fitness increases with investment in the stamen. Conversely, if the shape of the fitness set is convex, hermaphroditism will be favored in angiosperms because the rate of increase in male fitness decreases with increasing resource allocation to

the stamen, allowing a temporal separation of the resource costs of each sexual organ (Campbell 2000; Charnov 1982). The shape of the investment set predicted by the pollen–ovule scatterplot in the hermaphroditic mutants was nearly convex because these mutants were located in the upper right of a straight line connecting WT males and WT females (Fig. 2-5a). However, the shape of the fitness set predicted by the scatterplot of germinated pollen seeds in hermaphroditic mutants was nearly concave because these mutants were located on the lower left of a straight line connecting WT males and WT females (Fig. 2-5b). As indicated by sex allocation theory, our results suggested that dioecy will be favored in populations consisting of dioecious and hermaphroditic *S. latifolia*. The results of the present study, based on the numbers of pollen grains, ovules, and seeds in the hermaphroditic mutants of a dioecious plant, provide some guidance for setting up these manipulative experiments, and also contribute to the emerging consensus that floral traits may influence several aspects of plant mating, extending the traditional focus on patterns of self- and cross-fertilization.

Table 2-1. List of mutants induced by heavy-ion beam irradiation and γ irradiation.

Genotype	Phenotype	Mutagen Source	Reference
R025	Hermaphroditic	C-ion 100-120 Gy	(Koizumi et al. 2010)
EGP4	Hermaphroditic	C-ion 20 Gy	This study
EGP5	Hermaphroditic	γ 40 Gy	This study
EGP6	Hermaphroditic	C-ion 20 Gy	This study
EGP7	Hermaphroditic	γ 40 Gy	This study
EGP8	Hermaphroditic	C-ion 20 Gy	This study
EGP9	Hermaphroditic	C-ion 20 Gy	This study
EGP10	Hermaphroditic	C-ion 10 Gy	This study
EGP11	Hermaphroditic	C-ion 20 Gy	This study
EGP12	Hermaphroditic	C-ion 20 Gy	This study
EGP13	Hermaphroditic	C-ion 20 Gy	This study
EGP14	Hermaphroditic	C-ion 20 Gy	This study
EGP15	Hermaphroditic	γ 20 Gy	This study
K034	Asexual	n/a	(Koizumi et al. 2007)
ESS1	Asexual	C-ion 20 Gy	(Fujita et al. 2012)
ESS2	Asexual	C-ion 20 Gy	This study
ESS3	Asexual	C-ion 40 Gy	(Fujita et al. 2012)
ESS4	Asexual	C-ion 20 Gy	This study
ESS5	Asexual	C-ion 20 Gy	This study
ESS6	Asexual	C-ion 100 Gy	This study
ESS7	Asexual	C-ion 20 Gy	This study
ESS8	Asexual	C-ion 20 Gy	This study
ESS9	Asexual	C-ion 20 Gy	This study
ISS1	Anther development	C-ion 100 Gy	(Fujita et al. 2012)
ISS3	Anther development	C-ion 100 Gy	(Fujita et al. 2012)
ISS5	Anther development	C-ion 20 Gy	(Fujita et al. 2012)
ISS6	Anther development	C-ion 20 Gy	This study
ISS7	Anther development	C-ion 20 Gy	This study
ISS8	Anther development	C-ion 20 Gy	This study
ISS9	Anther development	C-ion 20 Gy	This study
ISS10	Anther development	C-ion 20 Gy	This study
ISS11	Anther development	C-ion 120 Gy	This study
LSS1	Pollen fertility	γ 40 Gy	(Fujita et al. 2012)
LSS2	Pollen fertility	C-ion 20 Gy	This study
LSS3	Pollen fertility	C-ion 100 Gy	This study
LSS4	Pollen fertility	C-ion 20 Gy	This study
LSS5	Pollen fertility	Fe-ion 4 Gy	This study
GPSS1	XY Female	γ 20 Gy	This study

Table 2-2. Number of germinated pollen and ovule in hermaphroditic mutants.

	EGP9	EGP12	EGP14	EGP4	R025	EGP15	EGP10	EGP11	EGP13	GPSS1	WT♂	WT♀
Pollen	2193	1803	1271	1534	1654	2149	1944	1366	910	0	1735	0
Pollen germination rate	0.4	0.16	0.6	0.48	0.2	0.47	0.17	0.03	0	0	0.7	0
Germinated pollen	877	288	763	736	331	1010	330	41	0	0	1215	0
Ovule	129	144	150	155	210	248	270	290	334	277	0	367

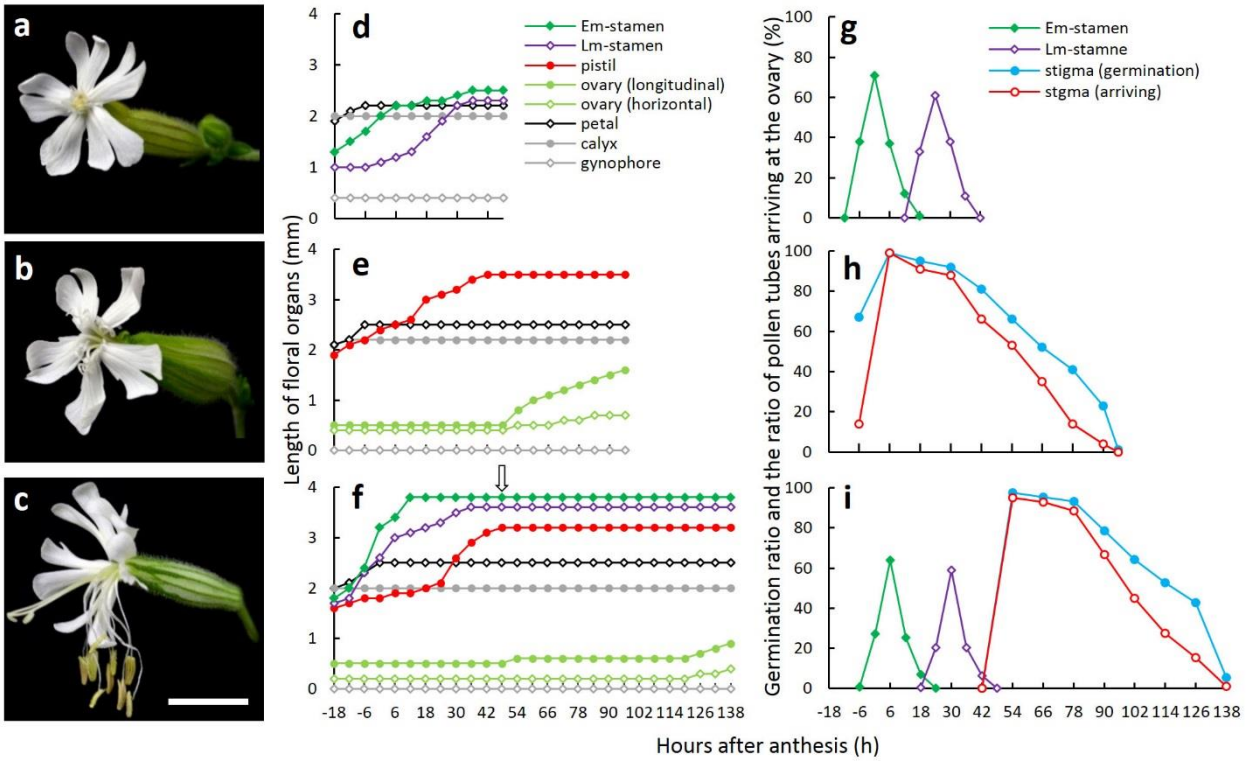

Fig. 2-1. Comparison of dichogamy and herkogamy in *S. latifolia* and *S. viscosa*. The dioecious plant *S. latifolia* has stamens and pistils in separate plants, and mature stamens and pistils simultaneously at night. In the hermaphroditic plant *S. viscosa*, stamens mature earlier than pistils. In addition, the stamens and pistils are separated, and dichogamy and herkogamy were observed in *S. viscosa*. The outline arrow indicates the time point when the stamen length came closest to the pistil length after anthesis. (**a**) Appearance of the *S. latifolia* WT male. (**b**) *S. latifolia* WT female. (**c**) *S. viscosa* WT. (**d**) Patterns of floral organ elongation in the *S. latifolia* WT male. (**e**) *S. latifolia* WT female. (**f**) *S. viscosa* WT. (**g**) Maturation timing of stamens in the *S. latifolia* WT male. (**h**) Maturation timing of pistils in *S. latifolia* WT female. (**i**) Maturing timing of stamens and pistils in the *S. viscosa* WT. Scale bar = 1 cm.

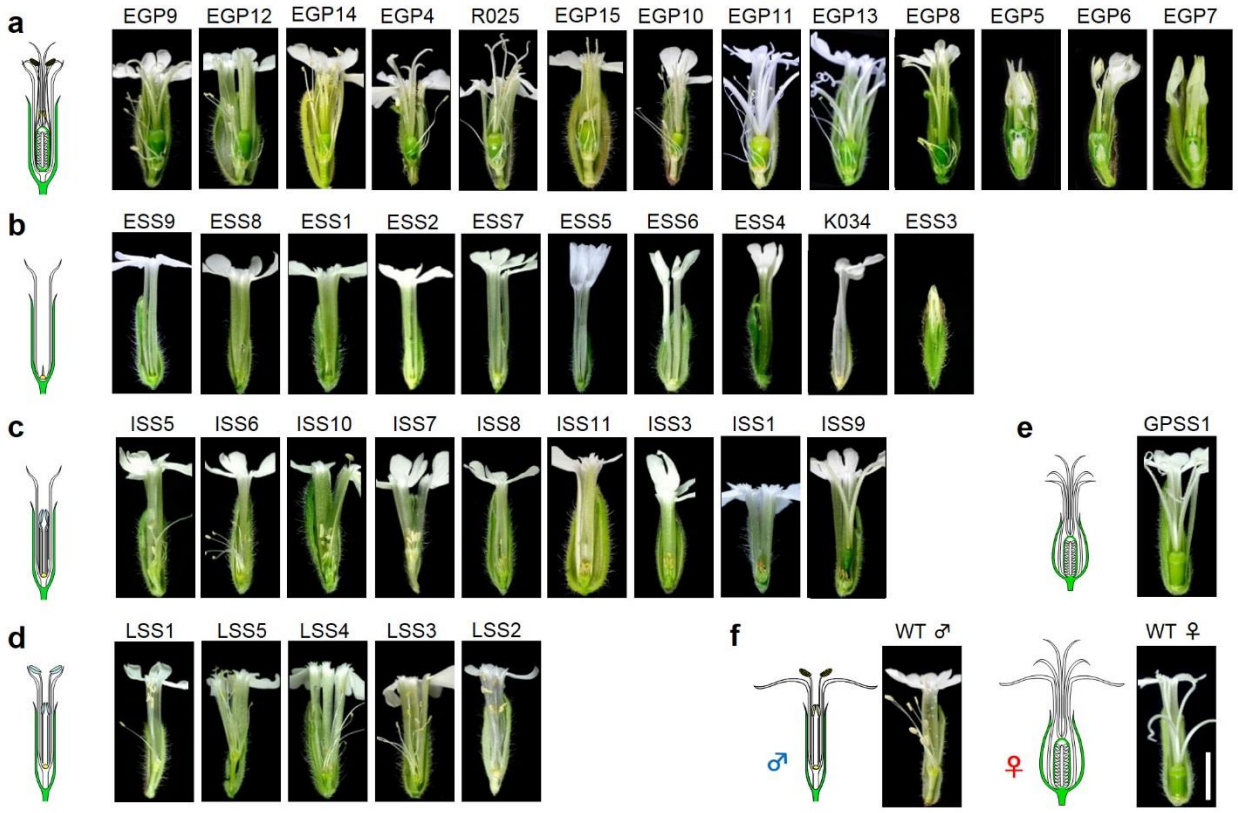

Fig. 2-2. Photographs of the mutants produced by heavy-ion beam irradiation and γ irradiation. Half of the petals and sepals were removed. All mutants are arranged in developmental order of stamen from left to right. (**a**) The hermaphroditic mutants (EGP: Early-stage Gynoecium Promoted mutant). (**b**) Asexual mutants (ESS: Early-Stage Stamen-suppressed mutant). (**c**) Anther defect mutants (ISS: Intermediate-stage Stamen-Suppressed mutant). (**d**) Pollen defect mutants (LSS: Late-stage Stamen-Suppressed mutant). (**e**) XY female (GPSS: Gynoecium Promoted and Stamen-Suppressed mutant). (**f**) WT male and female. Scale bar = 1 cm.

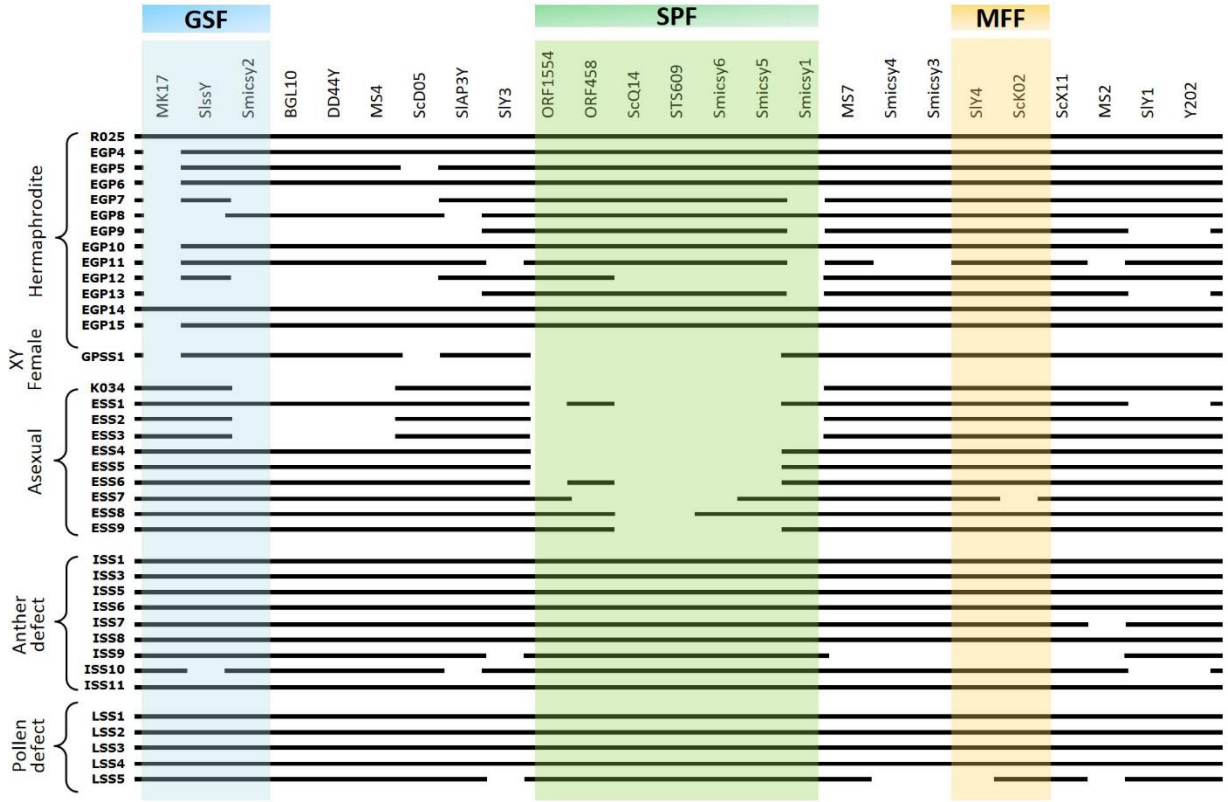

Fig. 2-3. Deletion map of the Y chromosome. The STS markers are shown at the top, ordered according to the Y map (Fujita et al. 2012). The mutant names and phenotypes are indicated on the left. Full lines denote markers present in each deletion mutant. The deletions are indicated by a blank without scale

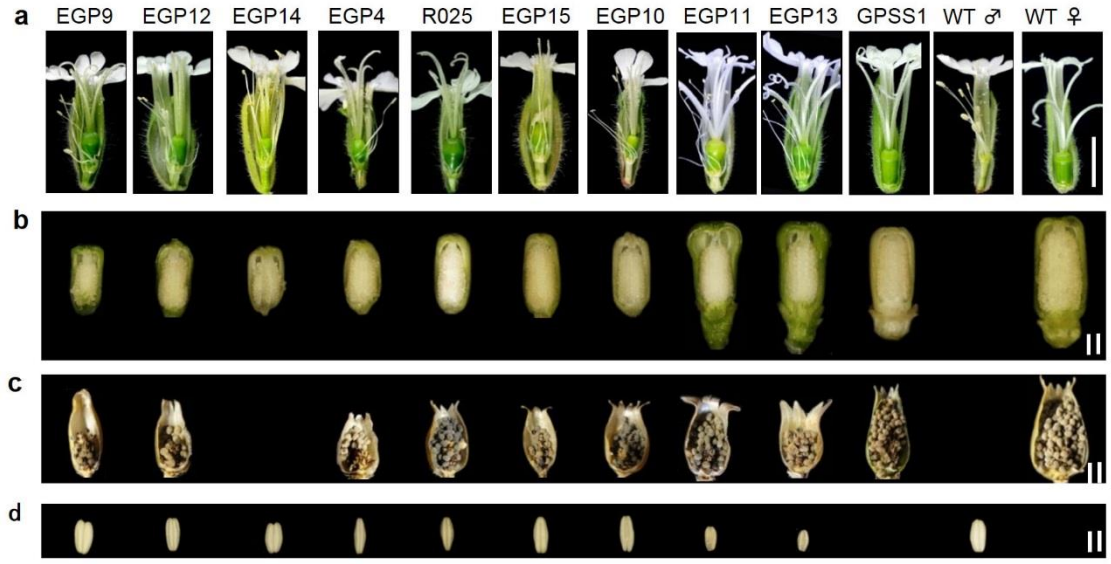

Fig. 2-4. Photographs of carpels and anthers in hermaphroditic mutants. (**a**) Cross sections of the hermaphroditic mutants. (**b**) Cross sections of the carpels are shown with ovules. (**c**) Cross sections of the capsules are shown with seeds. (**d**) Side views of the anthers. The hermaphroditic mutants are arranged in order of increasing number of ovules from left to right. Scale bar = 1 cm. Double scale bar = 1 mm.

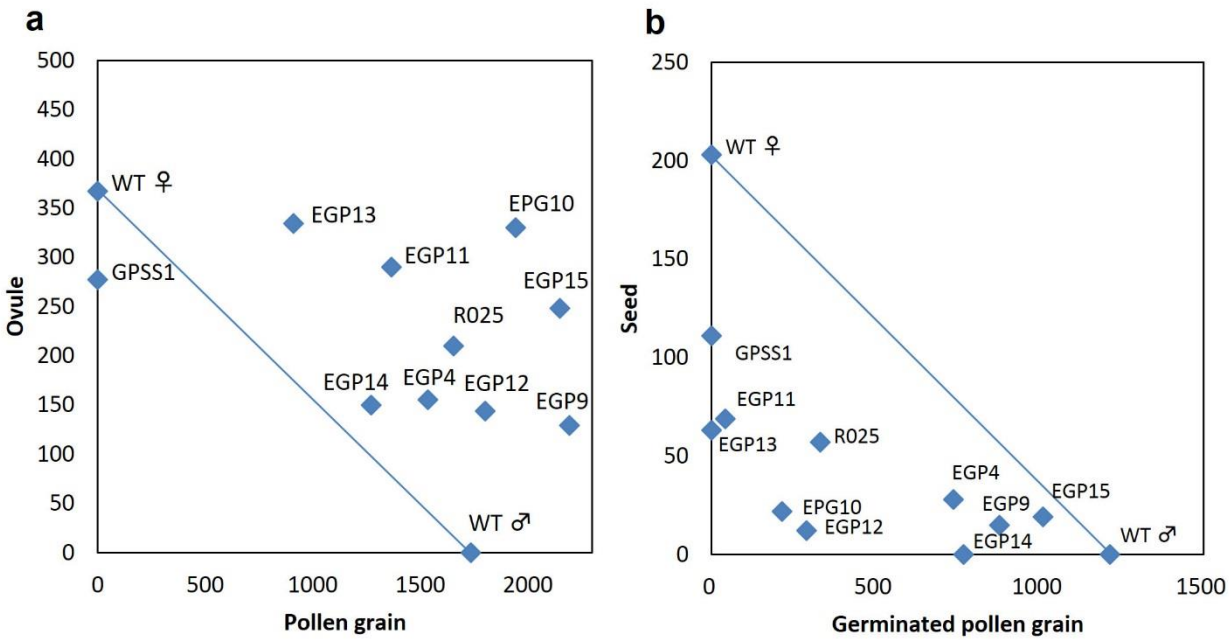

Fig. 2-5. Relationship between male and female functions in *S. latifolia*. (**a**) Scatterplot of the number of pollen grains and the number of ovules. (**b**) Numbers of the germinated pollen grains and seeds.

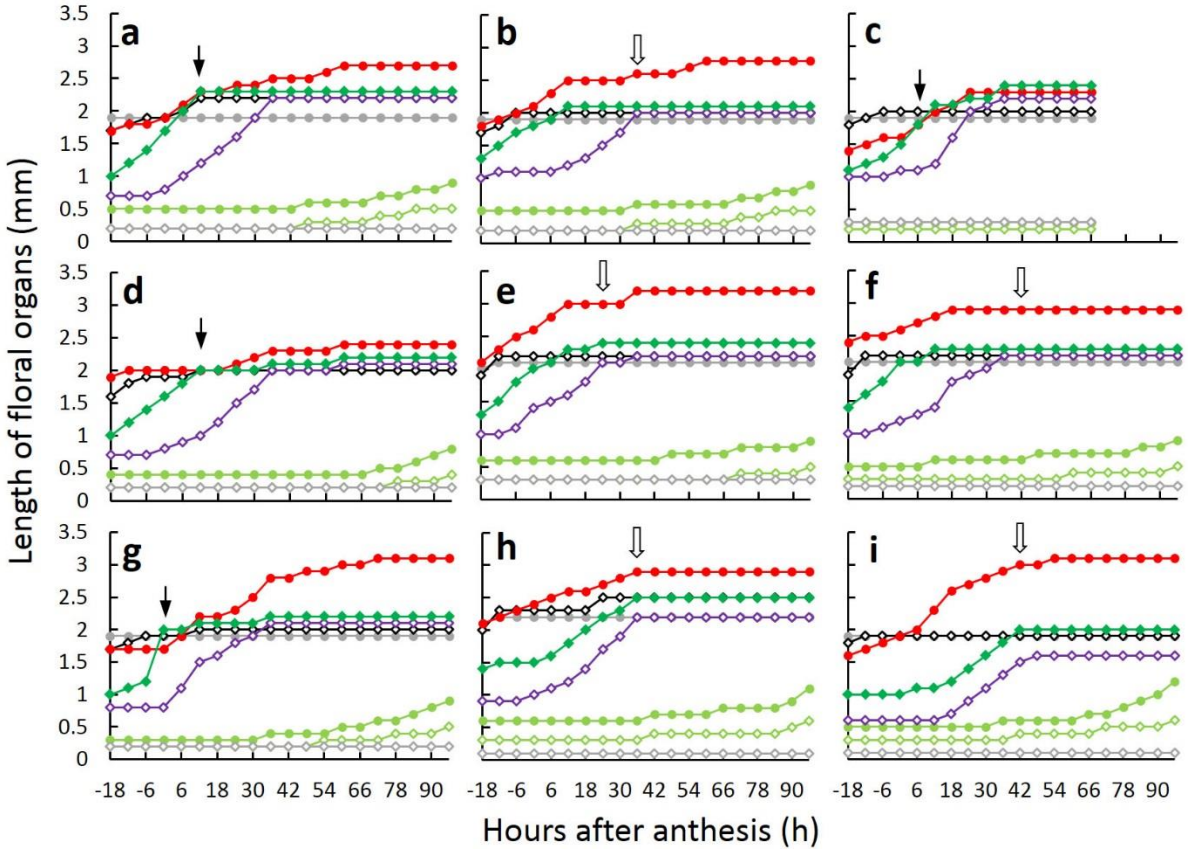

Fig. 2-6. Patterns of floral organ elongation in hermaphrodite flowers. Black arrows indicate the time points when the stamen length caught up with the pistil length. Outline arrows indicate the time points when the stamen length came closest to the pistil length after anthesis. The description of each color line is shown in Fig. S2-2. (**a**) EGP9. (**b**) EGP12. (**c**) EGP14. (**d**) EGP4. (**e**) R025. (**f**) EGP15. (**g**) EGP10. (**h**) EGP11. (**i**) EGP13.

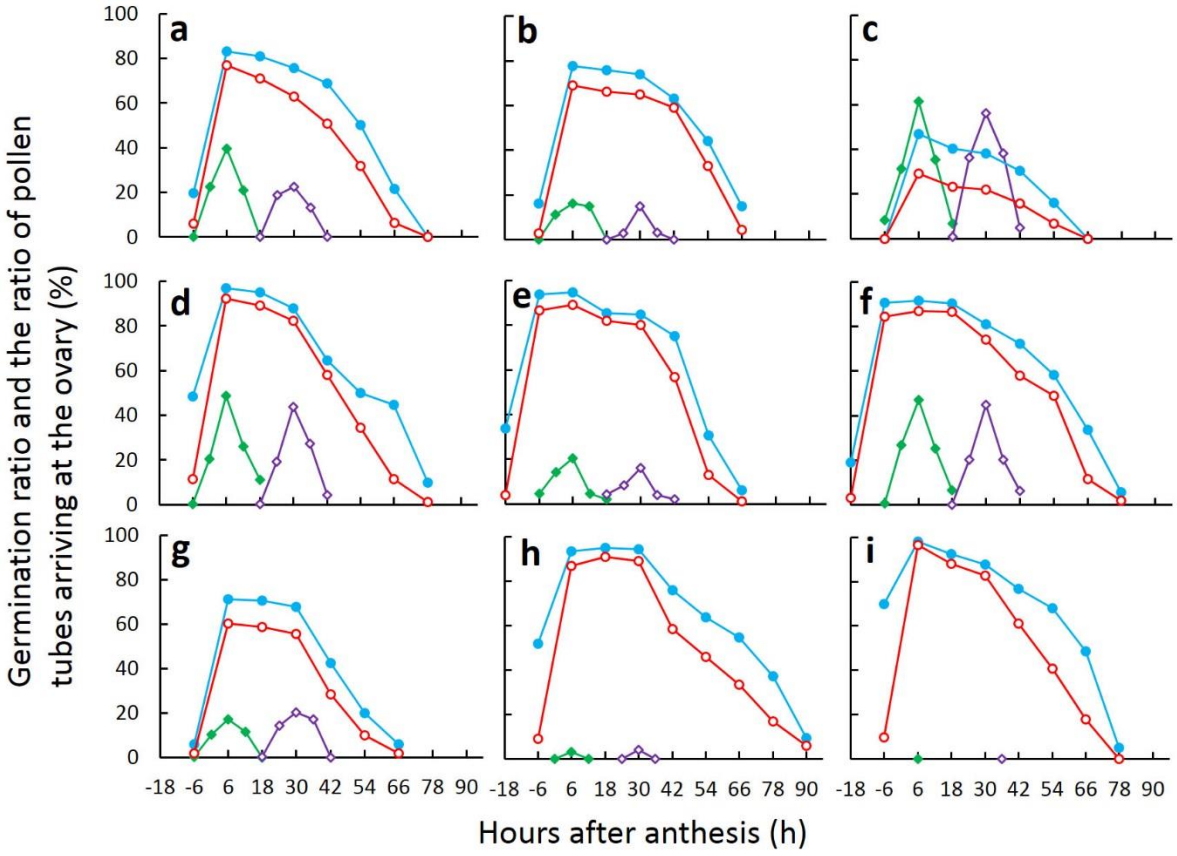

Fig. 2-7. Stamen and pistil maturation period based on *in vitro* and *in vivo* experiments. The filled circle indicates the *in vivo* germination ratio of pollen grains. The open circle shows the ratio of pollen tubes arriving at the ovary. The filled rhombus indicates the *in vitro* germination ratio of pollen grains from Em-stamens. The open rhombus represents the *in vitro* germination ratio of pollen grains from Lm-stamens. (**a**) EGP9. (**b**) EGP12. (**c**) EGP14. (**d**) EGP4. (**e**) R025. (**f**) EGP15. (**g**) EGP10. (**h**) EGP11. (**i**) EGP13.

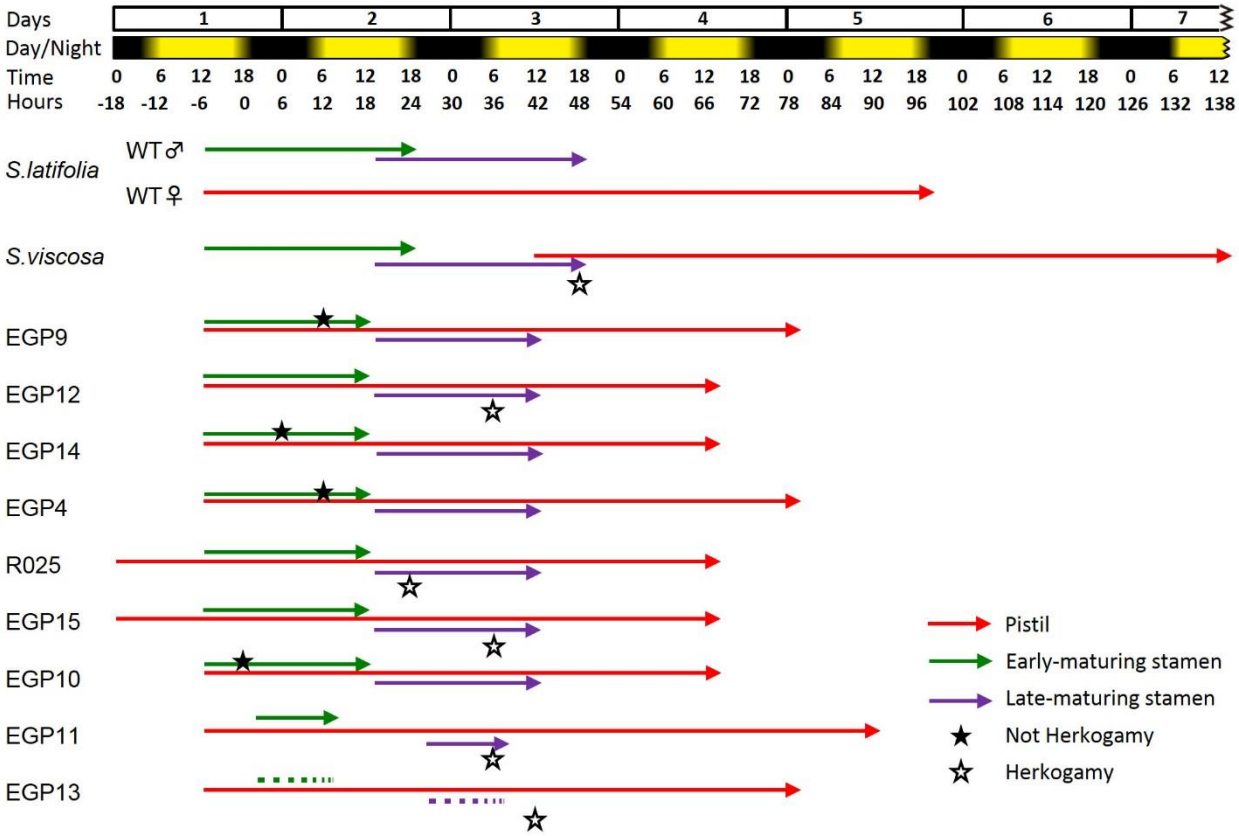

Fig. 2-8. Timetables of the *S. viscosa* WT flower and *S. latifolia* WT male and female flower, and hermaphroditic mutant development. Horizontal arrows indicate longevity of the stigma, and early-maturing stamen and late-maturing stamen. Black stars indicate the time points when the stamen length caught up with the pistil length. Outline stars indicate the time points when the stamen length came closest to the pistil length after anthesis.

Table S2-1. List of mutants induced by heavy-ion beam irradiation and γ irradiation.

Mutagen Source	Screening	WT female	WT male	Mutant	Appearance ratio
γ10 Gy	60	33	27	0	0.0
γ20 Gy	297	173	122	2	0.7
γ40 Gy	155	87	65	3	1.9
γ80 Gy	26	18	8	0	0.0
C-ion 5 Gy	56	32	24	0	0.0
C-ion 10 Gy	283	167	115	1	0.4
C-ion 20 Gy	1086	481	582	23	2.1
C-ion 40 Gy	188	104	83	1	0.5
C-ion 80 Gy	122	61	61	0	0.0
C-ion 100 Gy	167	89	74	4	2.4
C-ion 120 Gy	102	51	50	1	1.0
Fe-ion 1 Gy	29	15	14	0	0.0
Fe-ion 2 Gy	35	22	13	0	0.0
Fe-ion 4 Gy	52	16	35	1	1.9
Fe-ion 8 Gy	15	9	6	0	0.0
Fe-ion 16 Gy	49	23	26	0	0.0
Total	2722	1381	1305	36	1.3

Table S2-2. List of STS primers and conditions.

No.	Name	Forward	Reverse	Tm	Accession	reference
1	MK17	GGCAGATGTGGGTAATTGCT	GGACTAGAAGGTAACACGGGAAG	56	DQ376008	(Hobza et al. 2006)
2	SlssY	GGTCCCCTCTCTCTAGCTTCCTTG	GCAAAAGATGAATATTTAGTCTCTCCA	58	AY705439	(Filatov 2005)
3	BGL10	ATCACCTTCCACCTTCACGC	AAATGCGGCCAGGCTAACAG	55	-	(Matsunaga et al. 1999)
4	DD44Y	CACAGGCGGAGTTACCTCAT	CCCAATGGCTCACTCTTGAT	60	JN394464	(Donnison et al. 1996)
5	MS4	GGACACGATGACACCAAC	AGGCGTTGACCAGTTCAG	58	AB072492	(Obara et al. 2002)
6	ScD05	TGAGCGGACACGGGTGGGGC	TGAGCGGACATTGTGAGGTTACCTCC	65	-	(Zhang et al. 1998)
7	SlAP3Y	GGCATGGAGATCTCCTCATGGATC	TATATTCGAGACAACATGGCCTGG	60	AB090864	(Matsunaga et al. 2003)
8	SlY3	GGAAGTATTAAAACGGAAATCTGGACCAG	ATGCCTGAGCAGCAGTAAGGC	60	AJ631223	(Nicolas et al. 2005)
9	ORF1554	TAGGGATAGCAAGGGAATGGGTGA	GAACTTTGGCGGATGGTAGCCTAGGT	68	-	(Fujita et al. 2012)
10	ORF458	TAGCCAAGGCTAGTGGTCAAGGAG	ACCAGAAAACCTGATGAGAGCATTCCAG	62	-	(Fujita et al. 2012)
11	ScQ14	GGACGCTTCATGACCCATTTACTC	GGACGCTTCAGCGGGCGGGATT	67	-	(Zhang et al. 1998)
12	STS609	ACAGCAAATGAAGCTAAGCAAGTCC	CCTTGTCTCTCTGTGGTTCGACC	62	-	(Fujita et al. 2012)
13	MS7	GATGACGGACCATATGAG	CGCTGACTTCCCCTTACA	58	-	(Lebel-Hardenack et al. 2002)
14	SlY4	CAACCTGACTTCTCCGCTCCTTCTGG	CAACATGAGCTCCTCGTGAGCACGGCG	65	AJ310659	(Atanassov et al. 2001)
15	Sck02	GCAAATGGGTTTAGTGTAGTGGTT	GTCTCCGCAATTATCACACTAAGT	60	-	(Zhang et al. 1998)
16	ScX11	GGAGCCTCAGGGATTAGAAAGCCT	GGAGCCTCAGTACTAATAACATCA	58	-	(Zhang et al. 1998)
17	MS2	ATGACGGACCCTACATTTGG	AGGCGTTGACAAGGAGTATT	58	AB257588	(Ishii et al. 2008)
18	SlY1	ATGTAGATTCTGGAAGATCCCCTTG	GGCCAGGCTCATTTTCAAGTAAATG	65	Y18517	(Delichère et al. 1999)
19	Y202	GACCTTCCGAACGGTTGAAA	GGCATACACAAACAAGCTAC	58	-	(Fujita, Ishii, and Kawano 2008)
20	Smicsy1	CTCACCGTAGCCGAGAAGAAGGAGAAAGG	AACAACAACAACAACAACAATAATAAT	58	-	(Fujita et al. 2012)
21	Smicsy2	TGTCGATCGTTCAAAGCAACTACAGG	AACAACAACAACAACAACAATAATAAT	55	-	(Fujita et al. 2012)
22	Smicsy3	GCTCCCAACACTACGCCTTA	AACAACAACAACAACAACAATAATAAT	60	-	(Fujita et al. 2012)
23	Smicsy4	GCAAATGAAATCATCTCGACTG	AACAACAACAACAACAACAAGAAGAAG	60	-	(Fujita et al. 2012)
24	Smicsy5	AGTCGAGAGGCACGAAAATG	AACAACAACAACAACAACAAGAAGAAG	56	-	(Fujita et al. 2012)
25	Smicsy6	CCATTTCAATTTGGGGTTTG	AACAACAACAACAACAACAAGAAGAAG	55	-	(Fujita et al. 2012)

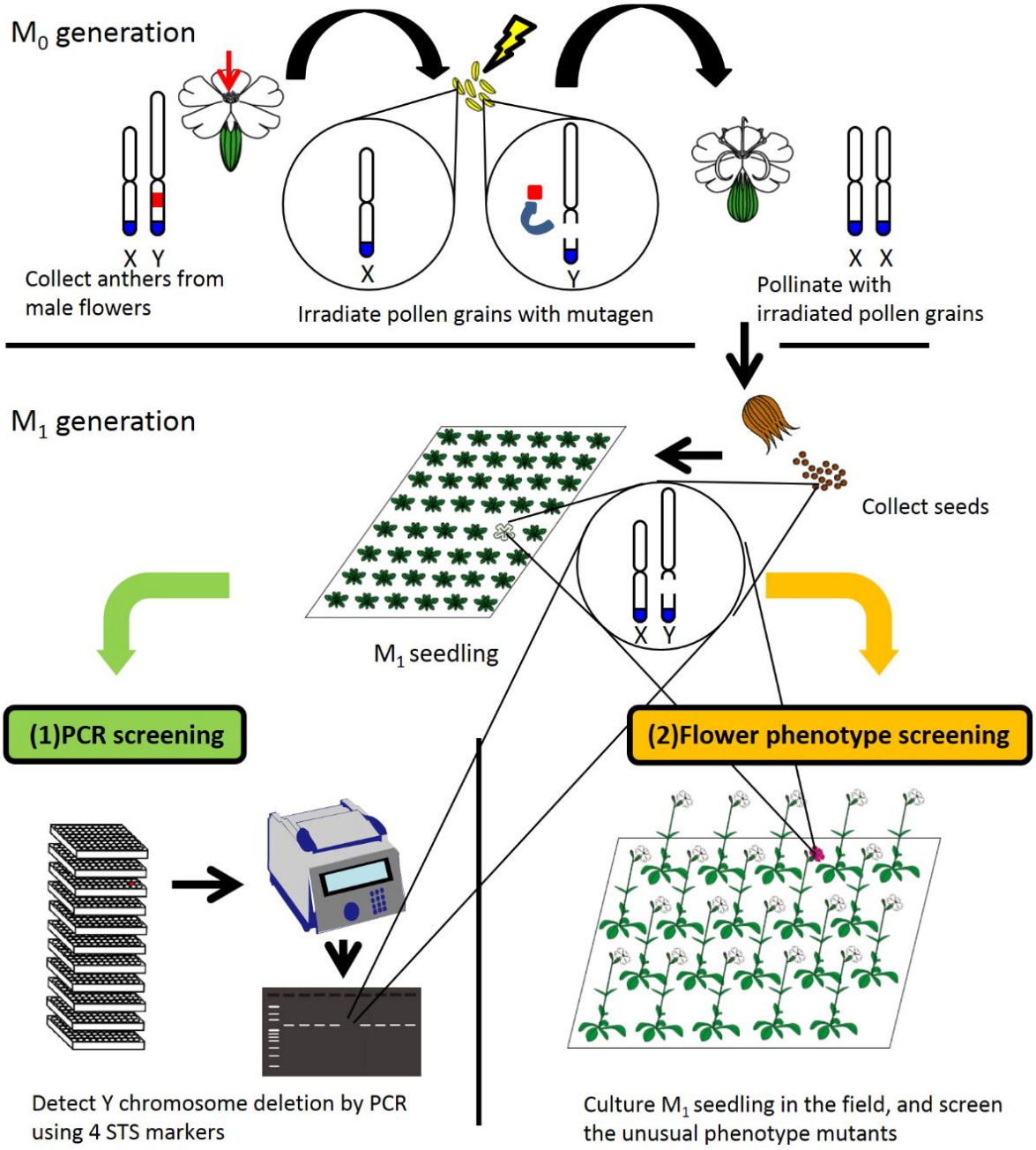

Fig. S2-1. Screening for the hermaphroditic mutants with partial Y chromosome deletion. The anthers were collected from male flowers and irradiated with either heavy-ion beams or γ-rays. Female flowers were pollinated with irradiated pollen grains, and then the resultant seeds were sown to obtain M_1 seedlings. Both partial Y chromosome deletion mutants and unusual phenotype mutants were screened by both (1) PCR screening and (2) flower phenotype screening.

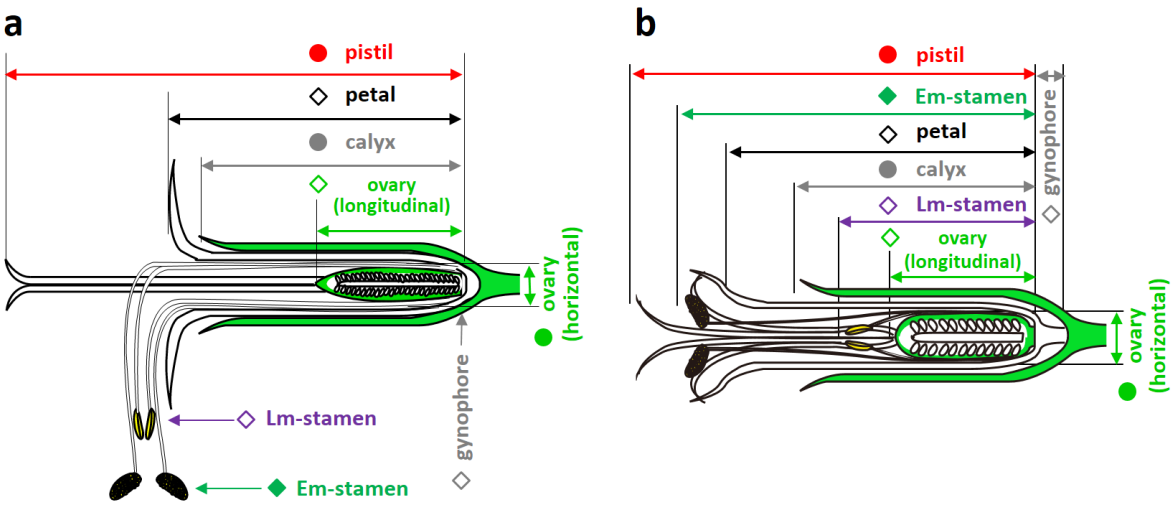

Fig. S2-2. Schematic diagram of *S. viscosa* and hermaphroditic mutant in *S. latifolia*. (**a**) *S. viscosa* WT, (**b**) *S. latifolia* hermaphroditic mutant.

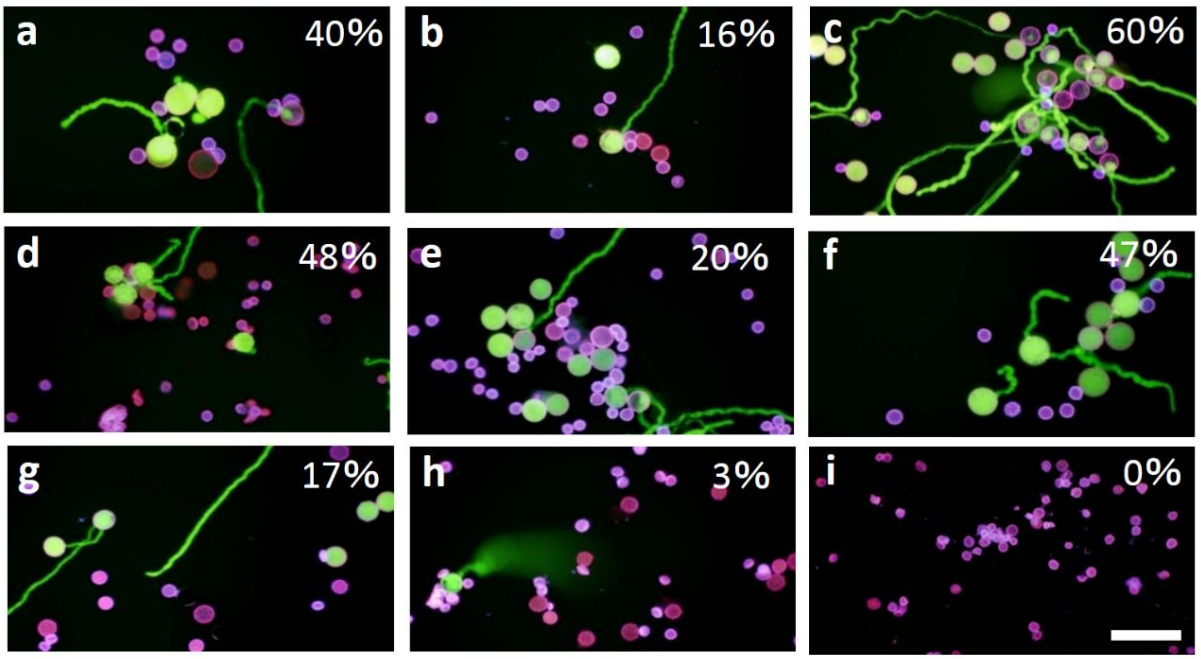

Fig. S2-3. ***In vitro*** **pollen viability on the pollen medium.** Fluorescence images of FDA/PI double-stained pollen grains. Viable pollen were stained with FDA (yellow to green), and nonviable pollen grains were stained with PI (purple to red). (**a**) EGP9. (**b**) EGP12. (**c**) EGP14. (**d**) EGP4. (**e**) R025. (**f**) EGP15. (**g**) EGP10. (**h**) EGP11. (**i**) EGP13. Scale bar = 100 μm.

CHAPTER III

Deletion mutations of B class genes *SlAP3X/Y* coded at XY sex chromosomes and their dosage compensation of genes in the dioecious plant *Silene latifolia*

SUMMARY

In most diploid sexual species with morphologically distinct sex chromosomes, the heterogametic sex chromosome pair was originally a recombining pair of autosomes that progressively stopped recombining. The suppression of X–Y chromosome recombination in the dioecious plant *Silene latifolia* is thought to have initiated 5–10 million years ago, relatively recently compared with animals. Evaluating the stages along a continuum of degeneration in *S. latifolia* requires the isolation of Y-linked gene deletion mutants and the comparison of floral phenotypes between the deletion mutant and wild-type (WT) males. Here, I targeted *SlAP3X/Y*, which is located on both X and Y chromosomes and isolated gene deletion mutants by irradiation mutagenesis. Four *SlAP3Y* deletion mutants (*SlAP3X, ⊿SlAP3Y*) were isolated from 1787 M_1 seedlings. One of the four *SlAP3Y* deletion mutants showed exactly the same phenotype as WT males. The normal development of stamens and petals in this mutant indicated that neo-functionalization has not occurred between *SlAP3X* and *SlAP3Y*. I cultured 1240 cross progeny of *slap3y-4* mutant × WT♀ to obtain *SlAP3X* hetero deletion mutants (*SlAP3X, ⊿SlAP3X*). RT-PCR analysis of B-class genes indicated that the expression level of *SlAP3X* increased in both *SlAP3Y* deletion mutants and *SlAP3X* hetero mutants. The complementary gene-expression pattern in these mutants suggested that the *SlAP3X/Y* functions were

compensated by increasing the expression level of the surviving *SlAP3X* not only when *SlAP3Y* was deleted but also when *SlAP3X* was deleted in *S. latifolia.*

INTRODUCTION

In most diploid sexual species with morphologically distinct sex chromosomes, the heterogametic sex chromosome pair was originally a recombining pair of autosomes that progressively stopped recombining (Bachtrog 2006; Lemaitre et al. 2009). In most animals with XY chromosomes, the Y chromosome seems to have been more degraded and gene specialization more advanced than X chromosome since the proto-Y chromosome stopped recombination, most likely because of a series of inversions and insertions on the Y chromosome (Graves 2006). In particular, most of Y chromosome genes were lost in mammals and *Drosophila* (Bachtrog 2006; Wilson and Makova 2009; Wyckoff et al. 2002).

In the dioecious plant *Silene latifolia* (Caryophyllaceae), sex is determined by heteromorphic XY chromosomes as in animals. The initiation of recombination suppression of the XY orthologs in *S. latifolia* is thought to have occurred 5–10 million years ago, which is recent compared with animals (Bergero et al. 2007; Nicolas et al. 2005). Fluorescence *in situ* hybridization (FISH) analysis with microsatellites as probes indicated that both X and Y chromosomes include a high percentage of microsatellites in *S. latifolia* (Kejnovsky et al. 2009; Kubat et al. 2008). Recently, NGS approaches such as RNA sequencing (RNA-seq) have revealed that Y-linked genes accumulate amino-acid replacements and loss of expression faster than X-linked genes (Bergero and Charlesworth 2011; Chibalina and Filatov 2011). NGS approaches also identified >1,700 sex-linked contigs, increasing by almost 100-fold the number of sex-linked sequences previously available in *S. latifolia* (Muyle et al. 2012). However, there are only two examples of "X-only" genes (*Slcyt*, *SlWUS1*) for which the Y-chromosome copy has been completely lost during the evolution of

dioecy (Bergero et al. 2013; Kaiser et al. 2009; Kazama et al. 2012).

Y-linked genes in the non-recombining region (the male-specific region on the Y chromosome) may be found of every stage of degeneration, from fully active to inactive. A few Y-linked genes may have or acquire a sex-specific function (specialization) (Graves 2006). Investigation of these continuous stages of degeneration in *S. latifolia* requires the isolation of Y-linked gene deletion mutants and the comparison of their floral phenotypes with those of wild-type (WT) males. However, no study has estimated the function of Y-linked genes with known full sequences by isolating the deletion mutant, partly because of a lack of detailed genomic information on X/Y chromosomes in *S. latifolia*.

Here, I targeted the gene *SlAP3X/Y*, which is located on both X and Y chromosomes, and isolated gene deletion mutants of *S. latifolia* by mutagenesis. The *S. latifolia* MADS box gene, *SlAP3*, which exhibits significant similarity to *Arabidopsis thaliana APETALA3*, was first isolated in 2003 and reported as having originated by duplication from autosomes to the Y chromosome (Matsunaga et al. 2003). Subsequently, X chromosome microdissection and analysis of *SlAP3* segregation in different lines of *S. latifolia* revealed that *SlAP3* are located on both X and Y chromosomes (Cegan et al. 2010; Nishiyama et al. 2010). Bacterial artificial chromosome clones containing the *SlAP3X* and *SlAP3Y* genes and 115- and 73- kilo base pairs (kb) of flanking sequences, respectively, have been sequenced (Ishii et al. 2013). Comparisons between the flanking sequences revealed that recombination stopped about 3.4 million years ago, and most noncoding DNA regions rapidly lost their counterparts because of the introduction of transposable elements and indels.

Both its long generation time (> 6 months from seed germination to next-generation seed maturation) and tall plant height (> 80 cm) pose challenges to isolating specific gene deletion mutants in *S. latifolia*. I

subjected pollen grains to either C-ion beam or γ-ray irradiation. The irradiated pollen grains were then used to pollinate WT female flowers, and M_1 seeds were obtained. DNA was isolated both easily and quickly from leaves of M_1 seedlings at the first true leaf stage, then PCR screening for *SlAP3Y* deletion mutants was conducted. By isolating the *SlAP3Y* deletion mutants, the presence or absence of specialization between *SlAP3X* and *SlAP3Y* and the effects of deleting the specific Y-linked gene can be demonstrated.

MATERIALS AND METHODS

Plant material and growth conditions

Silene latifolia seeds were obtained from an inbred line (K-line) in our laboratory (Aonuma et al. 2013). The K-line was propagated for 16 generations of brother–sister mating to obtain genetically homogeneous populations. Plants were grown from seeds in pots in a regulated chamber at 23 °C with a 16-h light/8-h dark cycle.

Stereomicroscopic observations

Flowers, anthers, ovaries, and capsules were observed under a stereomicroscope (MZ16; Leica Imaging Systems, Cambridge, UK).

Isolation of SlAP3Y deletion mutants and *SlAP3X* hetero deletion mutants

Screening of *SlAP3Y* deletion mutants and SlAP3X hetero deletion mutants was done by genomic PCR using four STS markers (MK17, ScQ14, MS4, and *SlAP3X/Y*). *SlAP3Y* deletion mutants were obtained by either C-ion beam irradiation ($^{12}C^{6+}$; energy: 135 MeV/nucleon, LET: 23 keV/μm) or γ irradiation (Gammacell 3000 Elan, Nordion, Ontario, Canada) of pollen, and 1781 of those seedlings were grown on soil. *SlAP3X* hetero deletion mutants were obtained by either C-ion beam irradiation or γ irradiation of seeds which from the cross between WT females and *slap3y-4* mutants, and 1240 of those seedlings were grown on soil. Genomic DNA was extracted from fresh leaves using the REDExtract-N-Amp Plant PCR

kit (Sigma-Aldrich, St. Louis, MO, USA) according to the manufacturer's instructions. PCR amplification was performed using the Kapa Taq PCR Kit (Kapa Biosystems, Woburn, MA, USA) in a thermal cycler (Dice TP600; Takara Bio, Otsu, Japan). The thermocycling profile was 5 min at 94°, followed by 30 cycles of 30 s at 94°, 30 s at the appropriate annealing temperature, and 1 min at 72°, with a final extension for 5 min at 72°. Each 20-μL reaction mixture contained 1 μL of template DNA, 0.6 μL of 10 dNTPs, 4 μL of 5× buffer, 2 μL of 25 mM $MgCl_2$, 0.1 μL of KAPA Taq, and 1 μL of each primer at 5 mM. The reaction products (5 μL) were electrophoresed on 1.5% agarose gels, stained with ethidium bromide, and visualized on a UV illuminator (Atto, Tokyo, Japan).

Y chromosome deletion mapping

In total, four *SlAP3Y* deletion mutants and 25 STS markers were used for Y chromosome deletion mapping (Tables S3-1). Genomic DNA was extracted from fresh leaves using a Nucleon Phytopure Genomic DNA Extraction Kit (GE Healthcare, Little Chalfont, UK) according to the manufacturer's instructions. PCR amplification was performed using Blend Taq polymerase (Toyobo, Tokyo, Japan) in a Dice TP600 thermal cycler. PCR cycling was as described above. Each 20-μL reaction mixture contained 50 ng of template DNA, 2 μL of 10 dNTPs, 10× Blend Taq Buffer, 0.2 μL of Blend Taq, and 1 μL of each primer at 5 mM. The reaction products (5 μL) were electrophoresed on 1.5% agarose gels. After staining with ethidium bromide, fragments were visualized on a UV illuminator (Atto). WT male and female genomic DNAs were used as controls. PCR detection was repeated three times for each STS marker.

Reverse transcription-PCR (RT-PCR) analysis

Total RNA was extracted from WT male, WT female, *slap3y-4*, and *slap3x-1* flower buds using an RNeasy Plant Mini Kit (QIAGEN, Hilden, Germany). cDNA was synthesized from 3 mg of total RNA using Superscript III reverse transcriptase (Invitrogen, Carlsbad, CA, USA). Specific primers for *SlAP3X*, *SlAP3Y*, *SLM2*, and *SLM3* (Table S3-1) were used to amplify a fragment. Primers specific for the *S. latifolia* eukaryotic translation initiation factor 4A gene *SleIF4A* (Table S3-1) were also used as a control. PCR cycling was the same as described above. The resulting 508-base pairs (bp) fragments of the *SlAP3X* and *SlAP3Y* genes were purified with Illustra ExoStar (GE Healthcare) and subjected to direct sequencing performed by Eurofins MWG Operon (Ebersberg, Germany) to verify the amplified products.

RESULTS

Screening for *SlAP3Y* deletion mutants (*SlAP3X, ⊿SlAP3Y*) in M_1 seedlings

I subjected pollen grains to either C-ion beam or γ-ray irradiation. The irradiated pollen grains were then used to pollinate wild-type (WT) female flowers, and M_1 seeds were obtained. I cultured 1787 M_1 seedlings and screened for *SlAP3Y* deletion mutants using four sequence-tagged sit (STS) markers (MK17, ScQ14, MS4, and *SlAP3X/Y*) (Table S3-1). Although Y chromosome-specific bands of either MS4, MK17, or ScQ14 were amplified in *SlAP3Y* deletion mutants (*SlAP3X, ⊿SlAP3Y*), the *SlAP3Y* band (Fig. S3-1) was not. Genetic segregation from the M_1 seedlings was XX:XY = 992:789. Four *SlAP3Y* deletion mutants (*SlAP3X, ⊿SlAP3Y*) were isolated from among the 789 XY seedlings (Table S3-2) and named *slap3y-1*, *slap3y-2*, *slap3y-3*, and *slap3y-4* (Table 3-1).

I mapped the four *SlAP3Y* deletion mutants using 25 Y-chromosome STS markers (Fig. 3-1A). The *slap3y-1*, *slap3-2*, and *slap3y-3* mutants had multiple deletions on the Y chromosome other than *SlAP3Y*. WT male flowers had five petals and 10 stamens (Fig. 3-1B). In contrast, the *slap3y-1* mutant formed both complete stamens and pistils, with eight petals and 16 stamens. The *slap3y-2* mutant also formed complete stamens and pistils and had five petals and 10 stamens. The eight stamens of the *slap3y-3* mutant did not elongate fully, and this mutant had four petals. The phenotypes of both the *slap3y-1* and *slap3y-2* mutants were thought to be hermaphroditic, as they had deletions in the gynoecium-suppressing factor gene (Fig. 3-1A). Although the *slap3y-3* mutant did not have a deletion in the male fertility factor gene, its phenotype

was considered to be stamen defective because of the other deletion in the Y chromosome. The abnormal numbers of both petals and stamens in the *slap3y-1* and *slap3y-3* mutants was expected because they had deletions in the B-class gene *SlAP3Y*, which is involved in forming both petals and stamens. However, the *slap3y-4* mutant showed exactly the same phenotype as the WT male, with five petals and 10 stamens (Fig. 3-1B). The normal development of stamens and petals in this mutant indicated that neo-functionalization did not occur between *SlAP3X* and *SlAP3Y*.

Screening for *SlAP3X/Y* deletion mutants (*Δ SlAP3X, Δ SlAP3Y*) in progeny of the *slap3y-4* mutant × WT♀ cross

The pollen grains of the *slap3y-4* mutant (*SlAP3X, Δ SlAP3Y*) were used to pollinate WT females. The resulting seeds were subjected to either C-ion beam or γ-ray irradiation. I cultured 1240 *slap3y-4* mutant × WT♀ progeny and searched for *SlAP3X/Y* deletion mutants by screening for two STS markers (MS4 and *SlAP3X/Y*) (Fig. S3-2). Although these progeny showed the Y-specific MS4 band, the *SlAP3Y* band was not amplified in any of them because they had deletions of *SlAP3Y* (Fig. 3-2, § symbol). Genetic segregation in the progeny was XX:XY = 249:991, and the Y chromosome in the *slap3y-4* mutant did not transmit well to the progeny (Table S3-3). The *SlAP3X/Y* deletion mutant (*Δ SlAP3X, Δ SlAP3Y*) was not obtained partly because of a shortage of XY seedlings. However, there were seedlings in which the *SlAP3X* band was weak compared with the control MS4 band in the *slap3y-4* mutant × WT♀ progeny (Fig. 3-3, white arrow). The seedlings showing this PCR pattern were thought to be candidate *SlAP3X* hetero deletion mutants (*SlAP3X,*

Δ SlAP3X); 16 such candidates were isolated from the 991 XX seedlings.

Screening of *SlAP3X* hetero deletion mutants (*SlAP3X, ΔSlAP3X*)

To verify the *SlAP3X* hetero deletion in the 16 candidate mutants, DNA was extracted and subjected to PCR analysis again (Fig. S3-3). Three primer sets for *SlAP3X* (*SlAP3X-1*, *SlAP3X-2*, and *SlAP3X-3*) were used in PCR (Table S3-1). In addition, primers for the autosomal single-gene *SlSUP* were used as a control (Kazama et al. 2009). The *SlAP3X-1*, *2*, and *3* bands in WT males were all almost half as bright as those in WT females, because these plants had one and two copies of *SlAP3X*, respectively (Fig. S3-3, solid arrows). Similarly, the brightnesses of the *SlAP3X-1*, *2*, and *3* bands in six of the 16 candidate mutants were almost half of those in the WT females, confirming these six seedlings as *SlAP3X* hetero deletion mutants (Fig. S3-3, open arrows; Table 3-2). Four of these mutants were named *slap3x-1*, *slap3x-2*, *slap3x-3*, and *slap3x-4* (Fig. 3-1C). All of these mutants showed exactly the same phenotype as the WT female, with no abnormal development (Fig. 3-1C, Table 3-1).

I tried separation of the *SlAP3X/Y* deletion mutant (*Δ SlAP3X, Δ SlAP3Y*) by crossing *slap3x-1*, *2*, *3*, and *4* mutants (*SlAP3X, Δ SlAP3X*) with the *slap3y-4* mutant (*SlAP3X, Δ SlAP3Y*) (Fig. S3-4). Genetic segregation in progeny from the four combinations is shown in Table 3-2. The inheritance of the X chromosome in *slap3x-1*, *2*, and *4* mutants was verified because the (*SlAP3X, ΔSlAP3X*) genotype was obtained in the progeny of these mutants crossed with *slap3y-4* mutants (Table 3-2). However, the (*ΔSlAP3X, ΔSlAP3X*) genotype was obtained in progeny of all four combinations, partly because of the

difficulties of inheriting the X chromosome from *SlAP3X* hetero deletion mutants and the Y chromosome from the *slap3x-4* mutant (Table S3-2).

B-class gene expression in *SlAP3Y* deletion mutants and *SlAP3X* hetero deletion mutants

The expression of B-class genes, including *SlAP3X*, *SlAP3Y*, *SLM2*, and *SLM3* (Hardenack et al. 1994), in WT males (*SlAP3X*, *SlAP3Y*), WT females (*SlAP3X*, *SlAP3X*), *slap3y-4* (*SlAP3X*, *ΔSlAP3Y*), and *slap3x-1* (*SlAP3X*, Δ*SlAP3X*) was investigated by RT-PCR (Fig. 3-3, Table 3-3). The *S. latifolia* eukaryotic translation initiation factor 4A gene *SleIF4A* was amplified as a control (Zluvova et al. 2005) (Table S3-3). Total RNA was isolated from leaves. In addition, buds (divided into sepal & petal and stamen & pistil) were sampled at stages 1–8 (<1 mm, small flower buds) and at stages 9–11 (2–5 mm, large flower buds) (Grant et al. 1994). The expression levels of all genes were nearly same in small and large flower buds in all plants. Both *SlAP3X* and *SlAP3Y* were expressed in sepal & petal and stamen & (pistil) from WT males. Although *SlAP3Y* was not expressed in all regions from WT female, the expression of *SlAP3X* was stronger in sepal & petal and (stamen) & pistil from WT females than in the same regions from WT male. In WT females, the expression of *SlAP3X* in sepal & petal was stronger than in (stamen) & pistil from WT female. Although *SlAP3Y* was not expressed in all regions from *slap3y-4*, the expression of *SlAP3X* was stronger in sepal & petal and stamen & (pistil) from *slap3y-4* than in the same regions from WT males. *SlAP3X* expression levels in sepal & petal and (stamen) & pistil from *slap3x-1* was nearly identical to that in the same regions from WT females.

Both *SLM2* and *SLM3* were expressed in both sepal & petal and stamen & (pistil) from WT males and *slap3y-4*. *SLM2* was expressed in sepal & petal, not in (stamen) & pistil from WT females and *slap3x-1*. In contrast, *SLM3* was expressed in both sepal & petal and (stamen) & pistil from WT females and *slap3x-1*. There was little difference in the expression patterns of *SLM2* and *SLM3* between WT (male and female) and mutant plants (*slap3y-4* and *slap3x-1*).

The results of RT-PCR are summarized in Table 3-3. The gene expression patterns from small and large flower buds are shown separately. The expression levels of *SlAP3X* in both sepals & petal and stamen & (pistil) from WT male were weak, because the WT males had only one *SlAP3X*. In contrast, although the *slap3y-4* mutants also had only one *SlAP3X*, the expression levels of *SlAP3X* in both sepal & petal and stamen & (pistil) were strong. The expression level of *SlAP3X* in sepal & petal from WT females was strong, because these plants had two *SlAP3X*. The expression level of *SlAP3X* in (stamen) & pistil from WT females was weak. I assumed that *SlAP3X* is a B-class gene that functions in forming stamens and that stamen development was suppressed in (stamen) & pistil from WT females. On the other hand, although the *slap3x-1* mutant had only one *SlAP3X*, its expression level in sepal & petal was strong, while it was weakly expressed in (stamen) & pistil.

These RT-PCR results indicated that the expression level of *SlAP3X* was high in both the *SlAP3Y* deletion and *SlAP3X* hetero mutants. The complementary gene-expression pattern in these mutants suggested that the *SlAP3X/Y* functions were compensated by increasing the expression level of the surviving *SlAP3X* both when *SlAP3Y* was deleted and when *SlAP3X* was deleted.

DISCUSSION

The damage to the *slap3y-4* Y chromosome and isolation of *slap3x-1, 2, 3,* and *4*

I subjected 1240 seeds that were obtained from crossing WT♀× *slap3y-4* to either C-ion beam or γ-ray irradiation and tried to isolate *SlAP3X/Y* deletion mutants (*Δ SlAP3X, Δ SlAP3Y*) from among the resulting seedlings. Genetic segregation in the progeny was XX:XY = 991: 249, and there were fewer XY than XX genotypes (Table S3-3). The phenomenon of fewer XY genotypes than XX genotypes in progeny when the male parent has a partial deletion in the Y chromosome has been seen previously in *S. latifolia* (Koizumi et al. 2007, 2010; Lardon et al. 1999). The *SlAP3X/Y* deletion mutant (*Δ SlAP3X, Δ SlAP3Y*) was not found among the 249 XY genotype seedlings. However, the *SlAP3X* hetero deletion mutant (*SlAP3X, Δ SlAP3X*) was obtained from 991 XX genotype seedlings.

I also investigated genetic segregation in the progeny of crosses between *slap3x-1, 2, 3,* and *4* mutants (*SlAP3X, Δ SlAP3X*) and the *slap3y-4* mutant (*SlAP3X, Δ SlAP3Y*) (Table 3-2, Fig. S3-4). Both a *SlAP3Y* deletion mutant (*SlAP3X, Δ SlAP3Y*) and a *SlAP3X* hetero deletion mutant (*SlAP3X, Δ SlAP3X*), which had the same genotype as the parents, were obtained from these crosses; however, the *SlAP3X/Y* deletion mutant (*Δ SlAP3X, Δ SlAP3Y*) was not produced. More than 1700 functional genes, including haploid-specific genes, have been found on both the X and Y chromosomes in *S. latifolia* (Chibalina and Filatov 2011; Muyle et al. 2012). A gametophyte that lacks haploid-specific genes is less likely to transmit them to the next generation because of haploid selection (Bull 1983; Chibalina and Filatov 2011). In addition, essential genes located near *SlAP3X* and *SlAP3Y* may have been lost from the X chromosome in the *slap3x-1, 2, 3,*

and *4* mutants or from the Y chromosome in the *slap3y-4* mutant as a consequence of the mutagenesis. These genetic segregation results indicated that mutations involving partial deletions on both X and Y chromosomes are inevitably lethal.

The phenotype of *SlAP3Y* deletion mutants (*SlAP3X*, *⊿ SlAP3Y*)

SlAP3X/Y belongs to the TM6 group of MADS-box genes; TM6 controls stamen specification in petunia and tomato (Airoldi and Davies 2012; de Martino et al. 2006; Matsunaga et al. 2003; Rijpkema et al. 2006). *SlAP3Y* was thought to function in the maturation of anthers and pollen grains when it was first isolated (Matsunaga et al. 2003). Even after it became clear that *SlAP3X* was located not on an autosome but on the X chromosome, subsequent studies showed that the full-length genes including introns were quite different between *SlAP3X* and *SlAP3Y* (Fig. S3-1) (Cegan et al. 2010; Nishiyama et al. 2010). The synonymous and nonsynonymous substitution rates between *SlAP3X* and *SlAP3Y* were 0.135 and 0.055, respectively (Cegan et al. 2010). Although the coding regions are well conserved, these are some nonsynonymous substitutions between *SlAP3X* and *SlAP3Y*.

The shared phenotype among the *SlAP3Y* deletion mutant, *slap3y-4*, and the WT male (Fig. 3-1B) indicated that *SlAP3Y* is not essential for stamen specification. In addition, *SlAP3Y* was expressed in WT males and the expression level of *SlAP3X* increased in *slap3y-4*, as if it compensated for the lack of *SlAP3Y* in that mutant. These results suggested that *SlAP3Y* has not degenerated fully and has the same function as *SlAP3X*.

Increased expression levels of *SlAP3X* in the *SlAP3Y* deletion mutants and *SlAP3X* hetero deletion mutants

RT-PCR analysis indicated that the expression levels of *SlAP3X* increased in both sepal & petal and stamen & (pistil) from the *SlAP3Y* deletion mutant *slap3y-4* (Table 3-3). The expression level of the X-linked *SlWUS1* was investigated in both WT males and females as an example of an "X-only" gene whose Y-linked counterpart has been lost (Kazama et al. 2012). Female flower buds expressed *SlWUS1* at twice the level in male buds in stages 1–8. The increase of expression level of *SlWUS1* was not detected in male buds. Because *SlWUS1* is thought to be required for the fourth floral whorl (gynoecium) and benefits female function (Deyhle et al. 2007; Koizumi et al. 2010; Laux et al. 1996), its expression level might be low in male flowers in which gynoecium development is suppressed.

SlAP3X belongs to the TM6 MADS-box group and may control stamen development (de Martino et al. 2006; Rijpkema et al. 2006). In contrast to *SlWUS1*, *SlAP3X* is thought to benefit male function. Therefore, the higher expression level of *SlAP3X* in stamen & (pistil) from *slap3y-4* was assumed to promote stamen development. Stronger expression of *SlAP3X* was detected not only in sepal & petal from *slap3y-4*, but also in sepal & petal from *slap3x-1*. *SlAP3X* may also control sepal and petal development.

RNA-seq has revealed that 75% of sex-linked genes show similar expression levels between XX females and XY males, meaning that the expression of X-chromosome genes increases in males to compensate for the lack of Y-chromosome expression (Muyle et al. 2012). Our results showing elevated expression levels of *SlAP3X* in *slap3y-4* were consistent with the results of NGS approaches.

The mechanism controlling the expression levels of X-linked genes in *S. latifolia*

Myule et al. (Muyle et al. 2012) described that the mechanisms of dosage compensation have previously been documented in male heterogametic organisms (XY) such as *Drosophila*, *Caenorhabditis elegans*, and mammals (Deng et al. 2011; Mank 2013; Vicoso and Bachtrog 2009). Vicoso and Bachtrog (Vicoso and Bachtrog 2009) have described that these mechanisms have been classified into the following three categories. First, dosage compensation is achieved by doubling the expression of X-linked genes in males in *Drosophila* (up-regulation of X in males). Second, in mammals, it is accomplished by inactivating the expression of one X-linked allele in females (in-activation of one X in females). Third, the expression of both X-linked alleles is halved in females in *C. elegans* (down-regulation of both Xs in females).

Although sex chromosomes in *S. latifolia* are evolutionarily young compared with those of animals, NGS approaches have revealed that their dosage compensation has evolved *de novo* in probably less than 10 million years (Muyle et al. 2012). Our RT-PCR analysis showing enhanced expression of *SlAP3X* in *slap3y-4* (XY genotype) suggested that a mechanism similar to that in *Drosophila* (up-regulation of X-chromosome genes in males). In addition, the high expression level of *SlAP3X* in *slap3x-1* (XX genotype) suggested the existence of mechanisms of controlling the expression levels of X-linked genes in XX females as well as in XY males. Our results support the view that the degeneration of Y-linked genes in *S. latifolia* is compensated by increasing the expression levels of X-linked genes and that this species offers fertile ground for further research on sex-chromosome evolution.

Table 3-1. Phenotypes and genotypes of the *SlAP3Y* deletion and *SlAP3X* hetero deletion mutants.

Strain		Phenotype description	Genotype	Parents (♀ × ♂)	Mutagen	Target
slap3y-1	abnormal	hermaphrodite (8 petals, 16 stamens)	*SlAP3X, ΔSlAP3Y*	WT♀× WT♂*	C-ion 20 Gy	Pollen
slap3y-2	abnormal	hermaphrodite (5 petals, 10 stamens)	*SlAP3X, ΔSlAP3Y*	WT♀× WT♂*	C-ion 20 Gy	Pollen
slap3y-3	abnormal	stamen defective (4 petals, 8 stamens)	*SlAP3X, ΔSlAP3Y*	WT♀× WT♂*	C-ion 20 Gy	Pollen
slap3y-4	normal	-	*SlAP3X, ΔSlAP3Y*	WT♀× WT♂*	C-ion 20 Gy	Pollen
slap3x-1	normal	-	*SlAP3X, ΔSlAP3X*	WT♀ × *slap3y-4***	γ-ray 80 Gy	Seed
slap3x-2	normal	-	*SlAP3X, ΔSlAP3X*	WT♀ × *slap3y-4***	C-ion 120 Gy	Seed
slap3x-3	normal	-	*SlAP3X, ΔSlAP3X*	WT♀ × *slap3y-4***	C-ion 80 Gy	Seed
slap3x-4	normal	-	*SlAP3X, ΔSlAP3X*	WT♀ × *slap3y-4***	C-ion 80 Gy	Seed

*Pollen grains of a wild-type male flower were subjected to irradiation mutagenesis, and then used to pollinate a wild-type female flower.

** Seeds from the cross WT female × *slap3y-4* were subjected to mutagenesis.

Table 3-2. Genetic outcomes from crosses between *slap3x-1, 2, 3,* and *4* mutants (*SlAP3X, Δ SlAP3X*) and the *slap3y-4* mutant (*SlAP3X, Δ SlAP3Y*).

Parents (♀ × ♂)	*SlAP3X, SlAP3X*	*SlAP3X, ΔSlAP3X*	*SlAP3X, ΔSlAP3Y*	*ΔSlAP3X, ΔSlAP3Y*
slap3x-1 × slap3y-4	38 (76.0)*	4 (8.0)	8 (16.0)	0 (0.0)
slap3x-2 × slap3y-4	18 (78.3)	2 (8.7)	3 (13.0)	0 (0.0)
slap3x-3 × slap3y-4	5 (71.4)	0 (0.0)	2 (28.6)	0 (0.0)
slap3x-4 × slap3y-4	2 (28.6)	4 (57.1)	1 (14.3)	0 (0.0)
Total	63 (72.4)	10 (11.5)	14 (16.1)	0 (0.0)

*The numbers in parentheses represent the appearance rate of each genotype.

Table 3-3. Expression of B-class genes in flower buds of wild-type (WT) males, WT females, *slap3y-4* mutants, and *slap3x-1* mutants.

		WT male (*SlAP3X, SlAP3Y*)		WT female (*SlAP3X, SlAP3X*)		*slap3y-4* (*SlAP3X, ΔSlAP3Y*)		*slap3x-1 (SlAP3X, ΔSlAP3Y)*	
	Gene	petal & stamen	stamen & (pistil)	petal & stamen	(stamen) & pistil	petal & stamen	stamen & (pistil)	petal & stamen	(stamen) & pistil
SB	*SlAP3X*	+	+	++	+	++	++	++	+
	SlAP3Y	+	+	-	-	-	-	-	-
	SLM2	++	++	++	-	++	++	++	-
	SLM3	++	++	++	++	++	++	++	++
LB	*SlAP3X*	+	+	++	+	++	++	++	+
	SlAP3Y	+	+	-	-	-	-	-	-
	SLM2	++	++	++	-	++	++	++	-
	SLM3	++	++	++	++	++	++	++	++


A
GSF
SPF
MFF
MK17
SlssY
Smicsy2
BGL10
DD44Y
MS4
ScD05
SlAP3Y
SlY3
ORF1554
ORF458
ScQ14
STS609
Smicsy6
Smicsy5
Smicsy1
MS7
Smicsy4
Smicsy3
SlY4
ScK02
ScX11
MS2
SlY1
Y202
slap3y-1
slap3y-2
slap3y-3
slap3y-4
B
WT ♂
slap3y-1
slap3y-2
slap3y-3
slap3y-4
TOP
cross-section
C
WT ♀
slap3x-1
slap3x-2
slap3x-3
slap3x-4
TOP
cross-section

Fig. 3-1. Deletion map of the Y chromosome and floral phenotypes of eight deletion mutants. A. Deletion map of the Y chromosome of four *SlAP3Y* deletion mutants. The STS markers are shown at the top, ordered according to the Y map (Fujita et al. 2012). The mutant names are indicated on the left. Full lines denote markers present in each deletion mutant. The deletions are indicated by a blank (without scale). **B.** Floral phenotypes of wild-type (WT) males and four *SlAP3Y* deletion mutants. Both *slap3y-1* and *slap3y-2* mutants had complete stamens and pistils. The *slap3y-3* mutants had stamens that did not elongate fully. The *slap3y-4* mutants shared the phenotype of the WT males. **C.** Floral phenotypes of WT females and four *SlAP3X* deletion mutants. All four mutants showed the same phenotype as the WT females.

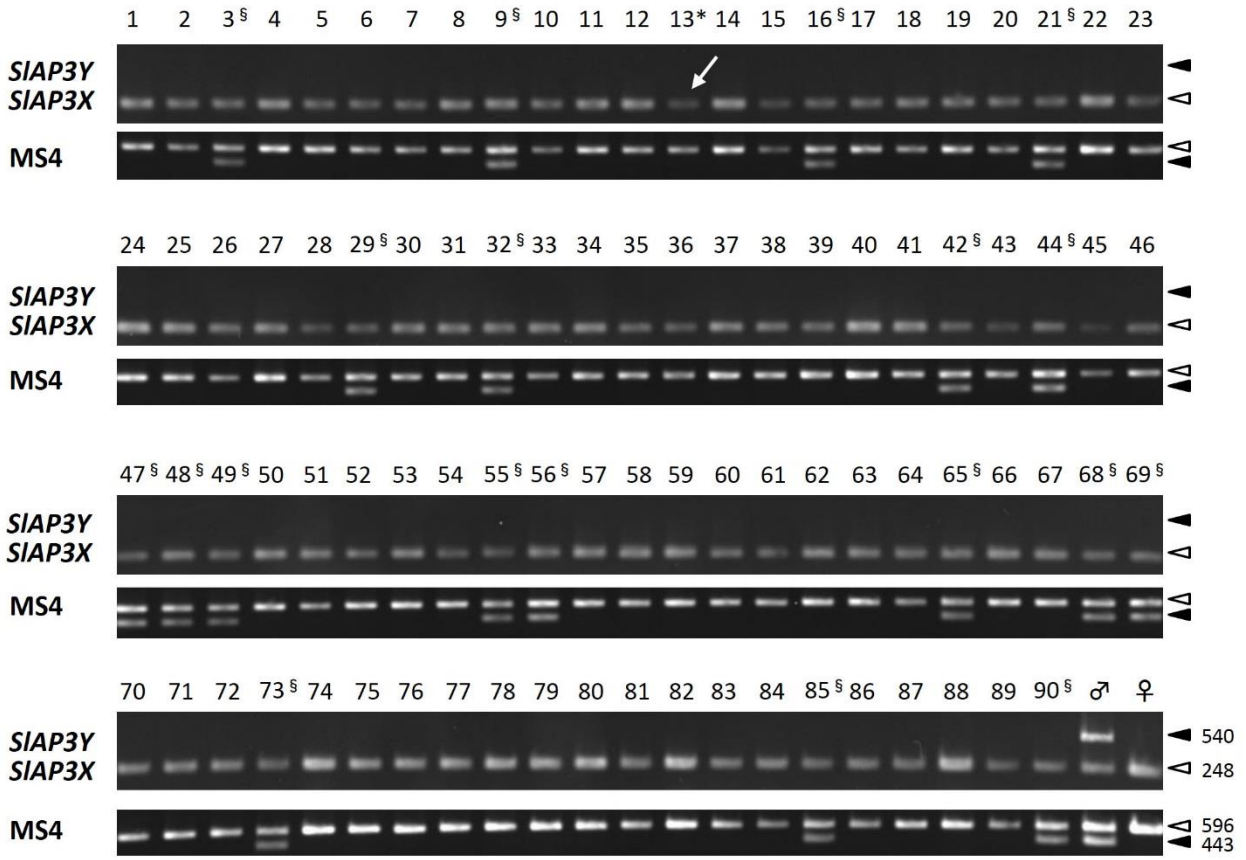

Fig. 3-2. PCR screening for *SlAP3X* hetero deletion mutants (*SlAP3X*, *ΔSlAP3X*). DNA was isolated from 90 progeny from the cross WT female × *slap3y-4*, and from WT males and WT females. The open and solid arrowheads indicate bands specific to the X- and Y-chromosomes, respectively. The 540 bp band of *SlAP3Y* was not amplified in these progeny, although the Y-specific band of MS4 (§) was. The white arrow indicates the prospective *SlAP3X* hetero deletion mutant in which the *SlAP3X* band was weak compared with the control MS4 band (*).

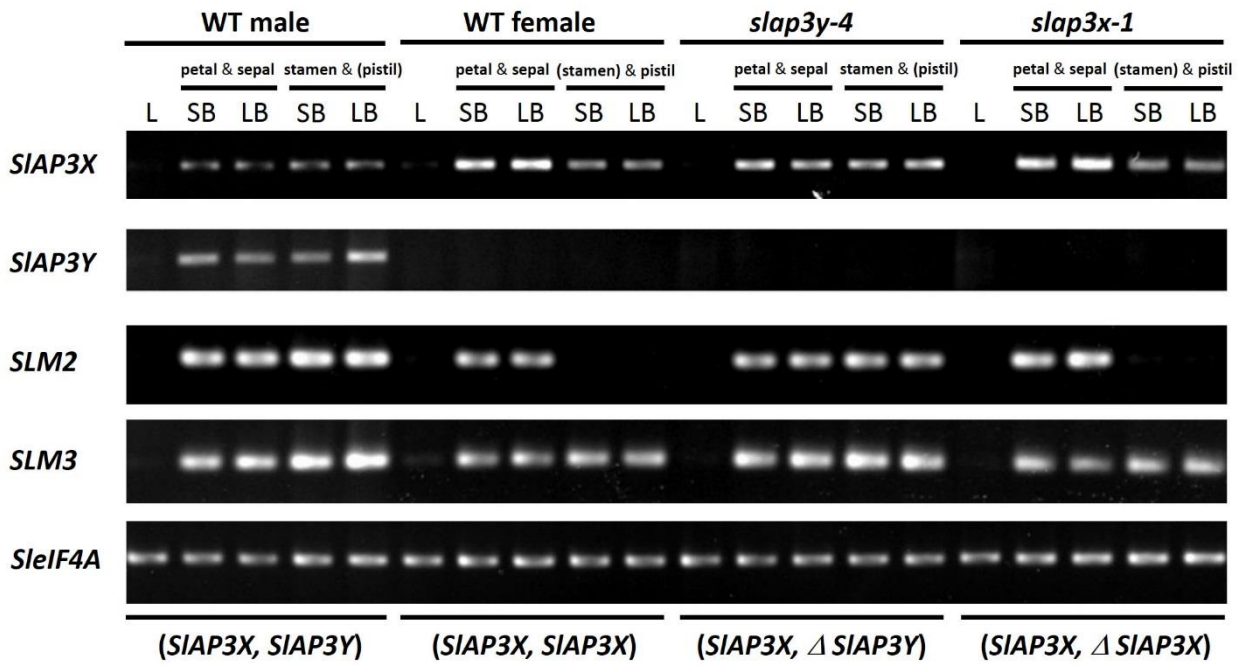

Fig. 3-3. RT-PCR analysis of B-class gene expression in WT males, WT females, *slap3y-4*, and *slap3x-1*. Total RNA was isolated from leaves and buds at stages 1–8 (<1 mm, SB: small flower buds) and from buds at stages 9–11 (2–5 mm, LB: large flower buds) as defined by (Grant et al. 1994). *SlAP3Y* was expressed only in petal & sepal and stamen & (pistil) of WT males. *SlAP3X* expression was stronger in petal & sepal of *slap3y-4* than in those of WT males. *SlAP3X* expression was also stronger in both petal & sepal and stamen & (pistil) of *slap3y-4* than in those of WT males. Although *slap3x-1* had hetero deletion in *SlAP3X*, its *SlAP3X* expression level was nearly the same as in WT females. The *S. latifolia* eukaryotic translation initiation factor 4A gene *SleIF4A* was amplified as a control as described previously (Zluvova et al. 2005).

Table S3-1. List of oligonucleotide primers used for Y deletion mapping

name	forward	reverse	Tm
MK17	GGCAGATGTGGGTAATTGCT	GGACTAGAAGGTAACACGGGAAG	56
SlssY	GGTCCCCTCTCTCTAGCTTCCTTG	GCAAAAGATGAATATTTAGTCTCTCCA	58
BGL10	ATCACCTTCCACCTTCACGC	AAATGCGGCCAGGCTAACAG	55
DD44Y	CACAGGCGGAGTTACCTCAT	CCCAATGGCTCACTCTTGAT	60
MS4	GGACACGATGACACCAAC	AGGCGTTGACCAGTTCAG	58
ScD05	TGAGCGGACACGGGTGGGGC	TGAGCGGACATTGTGAGGTTACCTCC	65
SlAP3Y	GGCATGGAGATCTCCTCATGGATC	TATATTCGAGACAACATGGCCTGG	60
SlY3	GGAAGTATTAAAACGGAAATCTGGACCAG	ATGCCTGAGCAGCAGTAAGGC	60
ORF1554	TAGGGATAGCAAGGGAATGGGTGA	GAACTTTGGCGGATGGTAGCCTAGGT	68
ORF458	TAGCCAAGGCTAGTGGTCAAGGAG	ACCAGAAAACCTGATGAGAGCATTCCAG	62
ScQ14	GGACGCTTCATGACCCATTTACTC	GGACGCTTCAGCGGGCGGGATT	67
STS609	ACAGCAAATGAAGCTAAGCAAGTCC	CCTTGTCTCTCTGTGGTTCGACC	62
MS7	GATGACGGACCATATGAG	CGCTGACTTCCCCTTACA	58
SlY4	CAACCTGACTTCTCCGCTCCTTCTGG	CAACATGAGCTCCTCGTGAGCACGGCG	65
Sck02	GCAAATGGGTTTAGTGTAGTGGTT	GTCTCCGCAATTATCACACTAAGT	60
ScX11	GGAGCCTCAGGGATTAGAAAGCCT	GGAGCCTCAGTACTAATAACATCA	58
MS2	ATGACGGACCCTACATTTGG	AGGCGTTGACAAGGAGTATT	58
SlY1	ATGTAGATTCTGGAAGATCCCCTTG	GGCCAGGCTCATTTTCAAGTAAATG	65
Y202	GACCTTCCGAACGGTTGAAA	GGCATACACAAACAAGCTAC	58
Smicsy1	CTCACCGTAGCCGAGAAGAAGGAGAAAGG	AACAACAACAACAACAACAATAATAAT	58
Smicsy2	TGTCGATCGTTCAAAGCAACTACAGG	AACAACAACAACAACAACAATAATAAT	55
Smicsy3	GCTCCCAACACTACGCCTTA	AACAACAACAACAACAACAATAATAAT	60
Smicsy4	GCAAATGAAATCATCTCGACTG	AACAACAACAACAACAACAAGAAGAAG	60
Smicsy5	AGTCGAGAGGCACGAAAATG	AACAACAACAACAACAACAAGAAGAAG	56
Smicsy6	CCATTTCAATTTGGGGTTTG	AACAACAACAACAACAACAAGAAGAAG	55

Table S3-2. List of *SlAP3Y* deletion mutants induced by either heavy-ion beam or γ irradiation

Mutagen	PCR	XY	XX	*slap3y*
γ-ray 10 Gy	60	27	33	0
γ-ray 20 Gy	103	50	53	0
C-ion 10 Gy	169	62	107	0
C-ion 20 Gy	1018	436	582	4
C-ion 40 Gy	65	28	37	0
C-ion 80 Gy	104	61	43	0
C-ion 100 Gy	166	74	92	0
C-ion 120 Gy	96	51	45	0
Total	1781	789	992	4

Table S3-3. List of *SlAP3X* hetero deletion mutants from cross progeny of wild-type female × *slap3y-4* mutant

Mutagen	PCR	XY	XX	*slap3xy*	*slap3x*
γ-ray 10 Gy	90	16	74	0	0
γ-ray 20 Gy	270	73	197	0	0
γ-ray 40 Gy	233	44	189	0	0
γ-ray 80 Gy	180	26	154	0	1(3)
C-ion 80 Gy	250	48	202	0	3(8)
C-ion 120 Gy	180	37	143	0	2(5)
C-ion 140 Gy	37	5	32	0	0
Total	1240	249	991	0	6

Table S3-4. List of oligonucleotide primers used in RT-PCR

name	forward	reverse	Tm	Accession	reference
SlAP3X	CTCAAAGAGAAGAAATGGGATCATG	TGCACTCTCGTAATTCCCCT	56	AB090863	(Matsunaga et al. 2003)
SlAP3Y	CTCAAAAAGAAGAAATGGGATTCTG	TGCACCGCCGTAGTTCCTCA	56	AB090864	(Matsunaga et al. 2003)
SLM2	TGAGGCTTGAGGATGCTCTT	CACCTGCCTCCATCTCTCTC	56	X80489	(Hardenack et al. 1994)
SLM3	ATTGCTTTGAGTTCCCATCG	AGTTGTTGCGTTGCATTCAC	56	X80490	(Hardenack et al. 1994)
SleIFaA	AAGGTTATGCGAGCTCTTGG	TTCTTCCTTGTCCACGTTCA	56	AJ697652	(Hardenack et al. 1994)

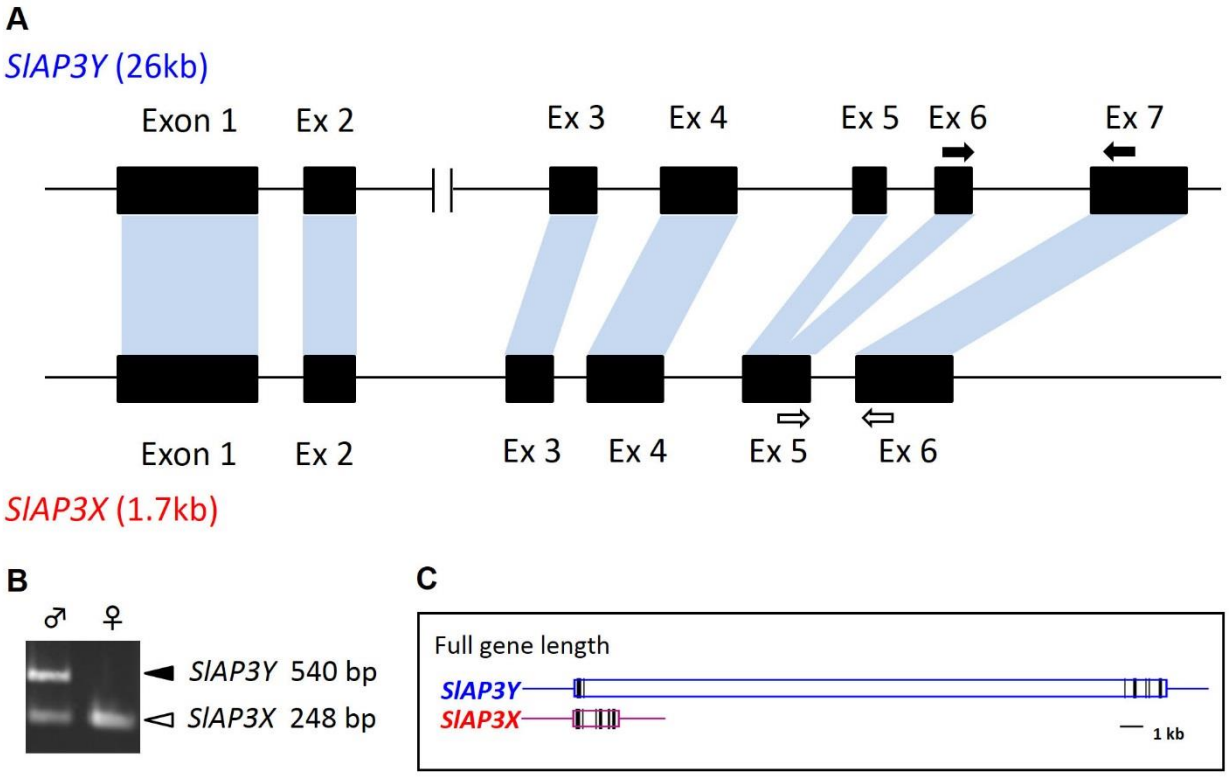

Fig. S3-1. Genomic structure of *SlAP3Y* and *SlAP3X*. A. Alignment of the coding regions of *SlAP3Y* and *SlAP3X*. Exons are shown with black boxes and numbered. Regions possessing similarity between *SlAP3Y* and *SlAP3X* are indicated by aqua parallelograms. The locations of *SlAP3X/Y* primers are shown by open and solid arrows. **B.** PCR amplification of *SlAP3X/Y* using genomic DNA isolated from WT males (♂) and WT females (♀). Both the 540-bp band of *SlAP3Y* and the 248-bp band of *SlAP3X*, which differed in intron lengths, were amplified in WT males, whereas, only the 248-bp band of *SlAP3X* was amplified in WT females. **C.** Schematic diagram of full-length *SlAP3Y* (1.7 kb) and *SlAP3X* (26 kb). Full-length genes and exons are indicated by open and solid boxes, respectively.

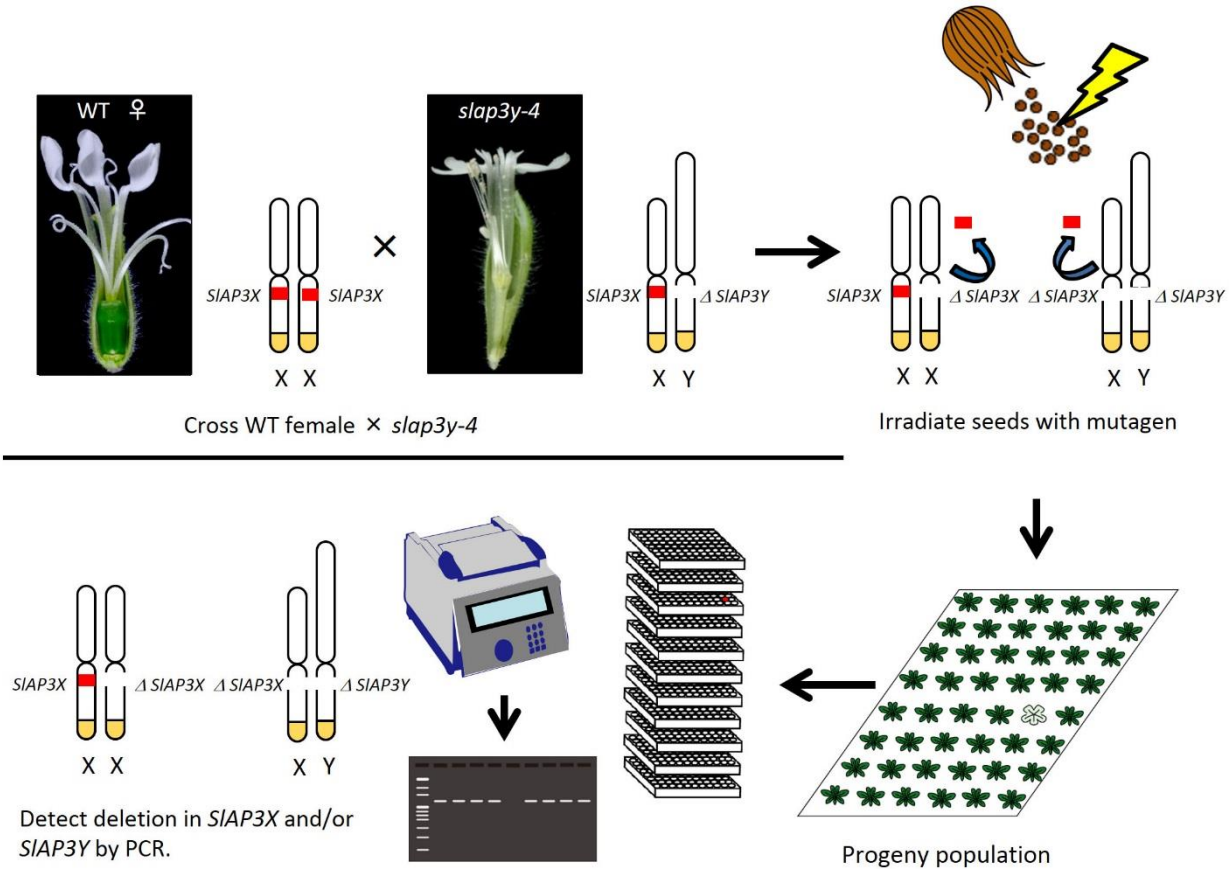

Fig. S3-2. Screening for either *SlAP3X/Y* deletion or *SlAP3X* hetero deletion mutants. Seeds were obtained from the cross WT female × *slap3y-4* and were subjected to either heavy ion beam or γ-ray irradiation. The irradiated seeds were sown to obtain the progeny population. Both *SlAP3X/Y* deletion and *SlAP3X* hetero deletion were screened by PCR.

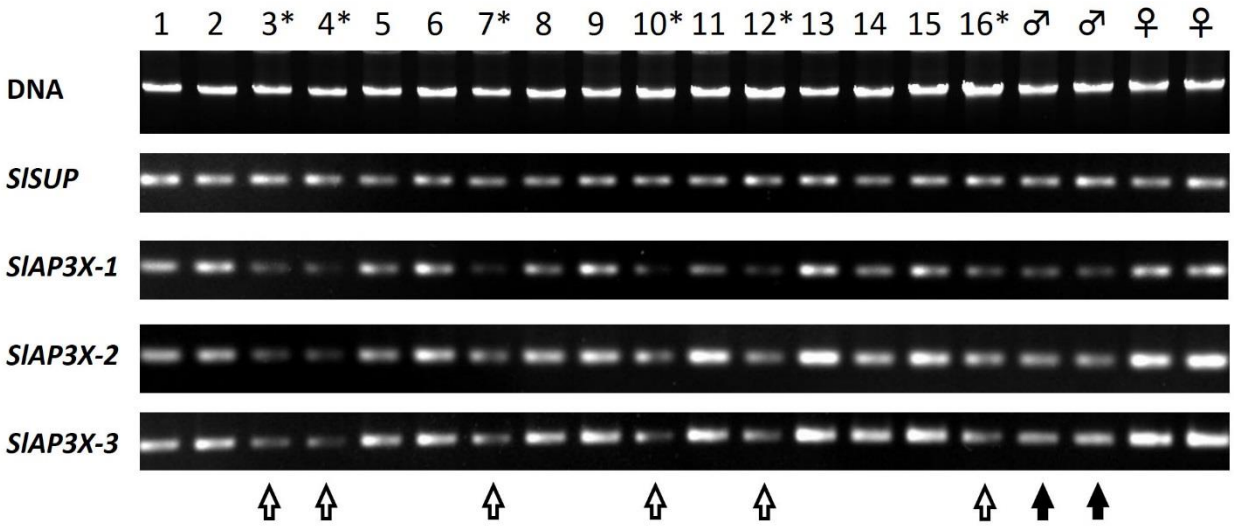

Fig. S3-3. Second PCR screening for *SlAP3X* hetero deletion mutants (*SlAP3X*, *ΔSlAP3X*). DNA was isolated from 16 prospective *SlAP3X* hetero deletion mutants, two WT males, and two WT females. All *SlAP3X-1, 2, and 3* bands in WT males were almost half as bright as those in WT females (solid arrows), because the WT males only had one allele. Similarly, all *SlAP3X-1*, *2*, and *3* bands in *SlAP3X* hetero deletion mutants were almost half as bright as those in WT females (open arrows, *).

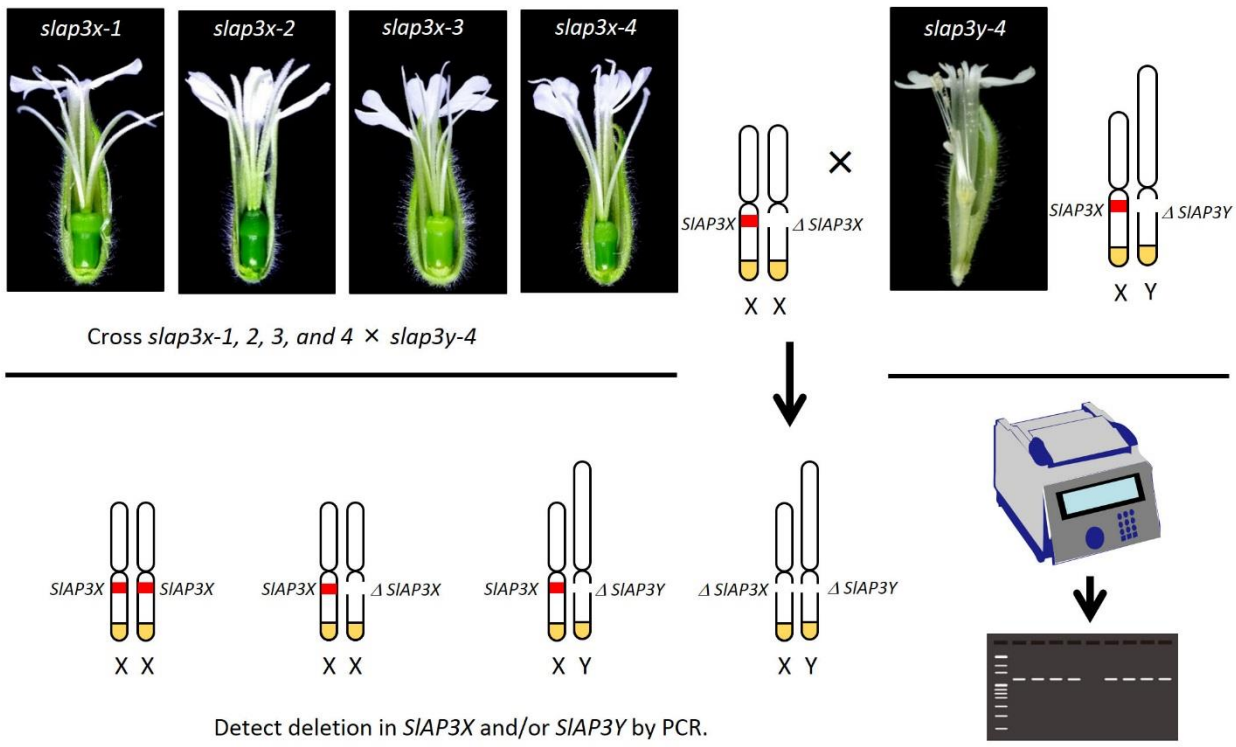

Fig. S3-4. The expected genetic segregation from the cross *slap3x* × *slap3y*. Seeds were obtained from the crosses *slap3x-1*, *2*, *3*, and *4* × *slap3y-4* and were sown to obtain progeny populations. Both *SlAP3X/Y* deletions and *SlAP3X* hetero deletions were screened by PCR.

CONCLUSIONS

In this study, I investigated three types of dioecism (mechanisms for maintaining distinct male and female plants in the dioecious plant *Silene latifolia*). The first mechanism was "synchronism of male and female anthesis," the second was "floral traits that appeared in hermaphroditic mutants," and the third was "gene complementarity for sex chromosome degeneration."

The first chapter reported the anthesis timing of male and female plants and maturation timing of stamens and pistils.

1. The corolla of both male and female flowers opened at sunset and closed at sunrise.
2. Male flowers had early- and late-maturing stamens with the highest pollen viability, germination rate, and pollen tube growth at midnight (24:00 h) at 1 DAA and 0000 h at 2 DAA, and female flowers maintained a germination rate of nearly 100% from 18:00 h at 1 DAA to 12:00 h at 3 DAA.
3. The results of both anthesis timing of male and female plants and maturation timing of stamens and pistils suggested that *S. latifolia* transferred the matured pollen grains from male flowers to female flowers at night.

The second chapter reported floral traits present in hermaphroditic mutants.

4. A trade-off relationship was revealed between pollen and ovules and between germinated pollen and seeds in the nine hermaphroditic mutants.
5. The hermaphroditic mutants could not effectively produce germinated pollen grains and seeds, and therefore the fitness of the WT male and WT female was higher than that of any of the hermaphroditic

mutants.

6. Herkogamy, which is a pattern opposite to that in *Silene viscosa*, was observed in five of nine hermaphroditic mutants because the pistil lengths were 2–10 mm longer than the stamens.

7. Two of nine hermaphroditic mutants showed signs of protogyny (dichogamy) as the maturation period of pistils began 12 h earlier than in WT females.

The third chapter reported gene complementarity for sex chromosome degeneration.

8. The *slap3y-4* mutant showed exactly the same phenotype as the WT male, and all *slap3x-1*, *2*, *3*, and *4* mutants showed exactly the same phenotype as the WT female.

9. The expression level of surviving *SlAP3X* increased in *SlAP3Y* deletion mutants and *SlAP3X* hetero mutants.

10. The complementary gene-expression pattern in these mutants suggested that the *SlAP3X/Y* functions were compensated by increasing the expression level of the surviving *SlAP3X* when *SlAP3Y* or *SlAP3X* was deleted in *S. latifolia*.

REFERENCES

Airoldi, Chiara A., and Brendan Davies. 2012. “Gene Duplication and the Evolution of Plant MADS-box Transcription Factors.” Journal of Genetics and Genomics **39**:157–65.

Aonuma, Wataru, Yuji Shimizu, Kotaro Ishii, Naoko Fujita, and Shigeyuki Kawano. 2013. “Maturation timing of stamens and pistils in the dioecious plant *Silene latifolia*.” Journal of Plant Research **126**:105–12.

Ashman, Tia-Lynn. 2003. “Constraints on the evolution of males and sexual dimorphism: field estimates of genetic architecture of reproductive traits in three populations of gynodioecious *Fragaria virginiana*.” Evolution: International Journal of Organic Evolution **57**:2012–25.

Atanassov, I. et al. 2001. “Analysis and evolution of two functional Y-linked loci in a plant sex chromosome system.” Molecular biology and evolution **18**:2162–68.

Bachtrog, Doris. 2006. “Expression profile of a degenerating neo-y chromosome in *Drosophila*.” Current biology : CB **16**:1694–99.

Barrett, Spencer C. H. 2003. “Mating strategies in flowering plants: the outcrossing-selfing paradigm and beyond.” Philosophical Transactions of the Royal Society of London - Series B: Biological Sciences **358**:991–1004.

Bergero, Roberta, and Deborah Charlesworth. 2011. “Preservation of the Y transcriptome in a 10-million-year-old plant sex chromosome system.” Current biology : CB **21(17)**:1470–74.

Bergero, Roberta, Alan Forrest, Esther Kamau, and Deborah Charlesworth. 2007. “Evolutionary strata on the X chromosomes of the dioecious plant *Silene latifolia*: evidence from new sex-linked genes.” Genetics **175**:1945–54.

Bergero, Roberta, Suo Qiu, Alan Forrest, Helen Borthwick, and Deborah Charlesworth. 2013. "Expansion of the Pseudo-autosomal Region and Ongoing Recombination Suppression in the *Silene latifolia* Sex Chromosomes." Genetics **194**:673–86.

Bertin, R. I., and C. M. Newman. 1993. "Dichogamy in angiosperms." Botanical Review **59**:112–52.

Buide, M. L. 2002. "Breeding System in the Dichogamous Hermaphrodite *Silene acutifolia* (Caryophyllaceae)." Annals of Botany **90**:691–99.

Bull, James J. 1983. Evolution of Sex Determining Mechanisms. Menlo Park, CA: The Benjamin/Cummings Publishing Company.

Burkhardt, Anne, Antonina Internicola, and Giorgina Bernasconi. 2009. "Effects of pollination timing on seed paternity and seed mass in *Silene latifolia* (Caryophyllaceae)." Annals of Botany **104**:767–73.

Campbell, Diane R. 2000. "Experimental tests of sex-allocation theory in plants." Trends in Ecology & Evolution **15**:227–32.

Cegan, Radim et al. 2010. "Structure and evolution of *Apetala3*, a sex-linked gene in *Silene latifolia*." BMC plant biology **10**:180.

Charlesworth, Brian, and Deborah Charlesworth. 1978. "A model for the evolution of dioecy and gynodioecy." The American Naturalist **112**:975–97.

Charlesworth, D., and B. Charlesworth. 1981. "Allocation of resources to male and female functions in hermaphrodites." Biological Journal of the Linnean Society **15**:57–74.

Charlesworth, Deborah. 2006. “Evolution of plant breeding systems.” Current Biology **16**:R726–R735.

Charlesworth, Deborah. 2008. “Sex chromosome origins and evolution. In Evolutionary Genomics and Proteomics.” Evolutionary Genomics and Proteomics 207–40.

Charnov, E. L. 1982. The theory of sex allocation.

Charter, A. O., and S. M. Walters. 1964. “*Silene L*. Flora Europeae.” Cambridge University press: Cambridge 158–81.

Chibalina, Margarita V, and Dmitry A. Filatov. 2011. “Plant Y chromosome degeneration is retarded by haploid purifying selection.” Current biology : CB **21(17)**:1475–79.

Comba, L. 1999. “Flowers, Nectar and Insect Visits: Evaluating British Plant Species for Pollinator-friendly Gardens.” Annals of Botany **83**:369–83.

Davis, Sandra L. 2002. “Allocation to floral structures in *Thalictrum pubescens* (Ranunculaceae), a cryptically dioecious species.” Annals of Botany **90**:119–26.

Davis, Sandra L., and Lynda F. Delph. 2005. “Prior selfing and gynomonoecy in *Silene noctiflora L* . (Caryophyllaceae): opportunities for enhanced outcrossing and reproductive assurance.” International Journal of Plant Sciences **166**:475–80.

Dawin, Charles. R. 1877. The different forms of flowers on plants of the same specie.

Delichère, C. et al. 1999. “*SlY1*, the first active gene cloned from a plant Y chromosome, encodes a WD-repeat protein.” The EMBO journal **18**:4169–79.

Delph, Lynda F., and Diana E. Wolf. 2005. “Evolutionary consequences of gender plasticity in genetically dimorphic breeding systems.” New Phytologist **166**:119–28.

Deng, Xinxian et al. 2011. “Evidence for compensatory upregulation of expressed X-linked genes in mammals, *Caenorhabditis elegans* and *Drosophila melanogaster*.” Nature Genetics **43**:1179–85.

Desfeux, C., S. Maurice, J. P. Henry, B. Lejeune, and P. H. Gouyon. 1996. “Evolution of reproductive systems in the genus *Silene*.” Proceedings of the Royal Society B: Biological Sciences **263**:409–14.

Deyhle, Florian, Ananda Kumar Sarkar, Elise J. Tucker, and Thomas Laux. 2007. “*WUSCHEL* regulates cell differentiation during anther development.” Developmental biology **302**:154–59.

Donnison, I. S., J. Siroky, B. Vyskot, H. Saedler, and S. R. Grant. 1996. “Isolation of Y chromosome-specific sequences from Silene latifolia and mapping of male sex-determining genes using representational difference analysis.” Genetics **144**:1893–1901.

Duan, Yuan-Wen, Amots Dafni, Qin-Zheng Hou, Ya-Ping He, and Jian-Quan Liu. 2010. “Delayed selfing in an alpine biennial *Gentianopsis paludosa* (Gentianaceae) in the Qinghai-Tibetan plateau.” Journal of Integrative Plant Biology **52**:593–99.

Fang, Xiangwen, Neil C. Turner, Guijun Yan, Fengmin Li, and Kadambot H. M. Siddique. 2010. “Flower numbers, pod production, pollen viability, and pistil function are reduced and flower and pod abortion increased in chickpea (*Cicer arietinum L.*) under terminal drought.” Journal of experimental botany **61(2)**:335–45.

Farbos, Isabelle, Margarida Oliveira, Ioan Negrutiu, and A. Mouras. 1997. "Sex organ determination and differentiation in the dioecious plant *Melandrium album* (*Silene latifolia*): a cytological and histological analysis." Sexual Plant Reproduction **10**:155–67.

Fenster, C. B., and S. D. A. Feb Marten-Rodriguez. 2007. "Reproductive assurance and the evolution of pollination specialization." International Journal of Plant Sciences **168**:215–28.

Filatov, Dmitry A. 2005. "Substitution rates in a new *Silene latifolia* sex-linked gene, *SlssX/Y*." Molecular biology and evolution **22**:402–8.

Friedrich, C. 1979. "Familie Caryophyllaceae. In Hegi, G. (Ed.), Illustrierte Flora von Mitteleuropa." Illustrierte Flora von Mitteleuropa **3**:763–1182.

Fujita, Naoko et al. 2012. "Narrowing Down the Mapping of Plant Sex-Determination Regions Using New Y-Chromosome-Specific Markers and Heavy-Ion Beam Irradiation-Induced Y-Deletion Mutants in *Silene latifolia*." G3; Genes|Genomes|Genetics **2**:271–78.

Fujita, Naoko, Kotaro Ishii, and Shigeyuki Kawano. 2008. "An STS Marker, Y202, Located on the *Silene latifolia* Y Chromosome between the Chromosomal Distal-end Satellite DNA and SlY1." CYTOLOGIA **73**:159–65.

Galen, C. 2000. "High and Dry: Drought Stress, Sex-Allocation Trade-offs, and Selection on Flower Size in the Alpine Wildflower *Polemonium viscosum* (Polemoniaceae)." The American naturalist **156**:72–83.

Galloway, L. F., T. Cirigliano, and K. Gremski. 2002. "The contribution of display size and dichogamy to potential geitonogamy in *Campanula americana*." International Journal of Plant Sciences **163**:133–39.

Grant, S., B. Hunkirchen, and H. Saedler. 1994. “Developmental Differences between Male and Female Flowers in the Dioecious Plant *Silene Latifolia*.” Plant Journal **6**:471–80.

Graves, Jennifer A. Marshall. 2006. “Sex chromosome specialization and degeneration in mammals.” Cell **124**:901–14.

Hardenack, S., D. Ye, H. Saedler, and S. Grant. 1994. “Comparison of MADS box gene expression in developing male and female flowers of the dioecious plant white campion.” The Plant cell **6**:1775–87.

Hobza, Roman et al. 2006. “MK17, a specific marker closely linked to the gynoecium suppression region on the Y chromosome in *Silene latifolia*.” Tag Theoretical And Applied Genetics Theoretische Und Angewandte Genetik **113**:280–87.

Ishii, Kotaro et al. 2008. “The Y chromosome-specific STS marker MS2 and its peripheral regions on the Y chromosome of the dioecious plant *Silene latifolia*.” Genome / National Research Council Canada = Genome / Conseil national de recherches Canada **51**:251–60.

Ishii, Kotaro et al. 2013. “Rapid Degeneration of Noncoding DNA Regions Surrounding *SlAP3X/Y* After Recombination Suppression in a Dioecious Plant, *Silene latifolia*.” G3; Genes|Genomes|Genetics Online First.

Jia, J., and D. Y. Tan. 2012. “Variation in style length and anther stigma distance in *Ixiolirion songaricum* (Amaryllidaceae).” South African Journal of Botany **81**:19–24.

Jolivet, C., and G. Bernasconi. 2007. “Within/between population crosses reveal genetic basis for siring success in *Silene latifolia* (Caryophyllaceae).” Journal of evolutionary biology **20**:1361–74.

Jürgens, A., T. Witt, and G. Gottsberger. 2002. “Pollen grain numbers, ovule numbers and pollen-ovule ratios in Caryophylloideae: correlation with breeding system, pollination, life form, style number, and sexual system.” Sexual Plant Reproduction **14**:279–89.

Kaiser, Vera B., Roberta Bergero, and Deborah Charlesworth. 2009. “*Slcyt*, a newly identified sex-linked gene, has recently moved onto the X chromosome in *Silene latifolia* (Caryophyllaceae).” Molecular biology and evolution **26**:2343–51.

Kazama, Y. et al. 2012. “SlWUS1; An X-linked Gene Having No Homologous Y-Linked Copy in *Silene latifolia*.” G3; Genes|Genomes|Genetics **2**:1269–78.

Kazama, Yusuke et al. 2003. “Organization of the KpnI family of chromosomal distal-end satellite DNAs in *Silene latifolia*.” Journal of plant research **116(4)**:317–26.

Kazama, Yusuke et al. 2009. “A *SUPERMAN*-like gene is exclusively expressed in female flowers of the dioecious plant *Silene latifolia*.” Plant & cell physiology **50**:1127–41.

Kejnovsky, E., R. Hobza, T. Cermak, Z. Kubat, and B. Vyskot. 2009. “The role of repetitive DNA in structure and evolution of sex chromosomes in plants.” Heredity **102**:533–41.

Kephart, S. R., E. Brown, and J. D. A. M. A. Y. Hall. 1999. “Inbreeding depression and partial selfing: evolutionary implications of mixed-mating in a coastal endemic, *Silene douglasii* var. oraria (Caryophyllaceae).” Heredity **82**:543–54.

Klinkhamer, P. G., T. J. de Jong, and H. Metz. 1997. “Sex and size in cosexual plants.” Trends in ecology & evolution (Personal edition) **12**:260–65.

Koizumi, Ayako et al. 2007. “Floral development of an asexual and female-like mutant carrying two deletions in gynoecium-suppressing and stamen-promoting functional regions on the Y chromosome of the dioecious plant *Silene latifolia*.” Plant cell physiology **48**:1450–61.

Koizumi, Ayako et al. 2010. “Two separate pathways including *SlCLV1*, *SlSTM* and *SlCUC* that control carpel development in a bisexual mutant of *Silene latifolia*.” Plant cell physiology **51**:282–93.

Kubat, Zdenek, Roman Hobza, Boris Vyskot, and Eduard Kejnovsky. 2008. “Microsatellite accumulation on the Y chromosome in *Silene latifolia*.” Genome / National Research Council Canada = Genome / Conseil national de recherches Canada **51**:350–56.

Laguerie, Patrick, Isabelle Olivieri, Anne Atlan, and Pierre-Henri Gouyon. 1991. “Analytic and simulation models predicting positive genetic correlations between traits linked by trade-offs.” Evolutionary Ecology **5**:361–69.

Lardon, A., S. Georgiev, A. Aghmir, G. Le Merrer, and I. Negrutiu. 1999. “Sexual dimorphism in white campion: complex control of carpel number is revealed by y chromosome deletions.” Genetics **151**:1173–85.

Laux, T., K. F. Mayer, J. Berger, and G. Jürgens. 1996. “The *WUSCHEL* gene is required for shoot and floral meristem integrity in *Arabidopsis*.” Development (Cambridge, England) **122**:87–96.

Lebel-Hardenack, Sabine, Elizabeth Hauser, Teresa F. Law, Jurg Schmid, and Sarah R. Grant. 2002. “Mapping of sex determination loci on the white campion (*Silene latifolia*) Y chromosome using amplified fragment length polymorphism.” Genetics **160**:717–25.

Lemaitre, Claire et al. 2009. “Footprints of inversions at present and past pseudoautosomal boundaries in human sex chromosomes.” Genome biology and evolution **1**:56–66.

Lloyd, D. G., and D. J. D. A. S. E. P. Schoen. 1992. “SELF-FERTILIZATION AND CROSS-FERTILIZATION IN PLANTS .1. FUNCTIONAL DIMENSIONS.” International Journal of Plant Sciences **153**:358–369 ST – SELF–FERTILIZATION AND CROSS–FERTILI.

Lloyd, David G., and C. J. Webb. 1986. “The avoidance of interference between the presentation of pollen and stigmas in angiosperms I . Dichogamy.pdf.” New Zealand Journal of Botany **24**:135–62.

Luo, Yonghai, and Alex Widmer. 2013. “Herkogamy and Its Effects on Mating Patterns in *Arabidopsis thaliana*.” PLoS One **8**:e57902.

Mandaokar, Ajin, and John Browse. 2009. “*MYB108* acts together with *MYB24* to regulate jasmonate-mediated stamen maturation in *Arabidopsis*.” Plant physiology **149(2)**:851–62.

Mank, Judith E. 2013. “Sex chromosome dosage compensation: definitely not for everyone.” Trends in genetics : TIG 1–7.

Marais, Gabriel A. B. et al. 2011. “Multiple nuclear gene phylogenetic analysis of the evolution of dioecy and sex chromosomes in the genus *Silene*.” PLoS ONE **6**:e21915.

De Martino, Gemma, Irvin Pan, Eyal Emmanuel, Avraham Levy, and Vivian F. Irish. 2006. “Functional analyses of two tomato *APETALA3* genes demonstrate diversification in their roles in regulating floral development.” The Plant cell **18**:1833–45.

Matsunaga, S., and S. Kawano. 2001. “Sex determination by sex chromosomes in dioecious plants.” Plant biology **3**:481–88.

Matsunaga, Sachihiro et al. 2003. "Duplicative transfer of a MADS box gene to a plant Y chromosome." Molecular biology and evolution **20**:1062–69.

Matsunaga, Sachihiro, Shigeyuki Kawano, Takeshi Michimoto, Tetsuya Higashiyama, and Sbunsuke Nakao. 1999. "Semi-Automatic Laser Beam Micro dissection of the Y Chromosome and Analysis of Y Chromosome DNA in a Dioecious Plant , *Silene latifolia*." Plant Cell Physiology **40**:60–68.

Miller, Paige M., and Richard V Kesseli. 2011. "A sex-chromosome mutation in *Silene latifolia*." Sexual Plant Reproduction **24**:211–17.

Ming, Ray, Abdelhafid Bendahmane, and Susanne S. Renner. 2011. "Sex chromosomes in land plants." Annual review of plant biology **62**:485–514.

Muyle, Aline et al. 2012. "Rapid De Novo Evolution of X Chromosome Dosage Compensation in *Silene latifolia*, a Plant with Young Sex Chromosomes." PLoS Biology **10**:e1001308.

Narbona, Eduardo, Pedro L. Ortiz, and Montserrat Arista. 2011. "Linking self-incompatibility, dichogamy, and flowering synchrony in two Euphorbia species: alternative mechanisms for avoiding self-fertilization?" PloS one **6**:e20668.

Negrutiu, Ioan, Boris Vyskot, Nicolae Barbacar, Sevdalin Georgiev, and Francoise Moneger. 2001. "Dioecious Plants. A Key to the Early Events of Sex Chromosome Evolution" Plant physiology **127**:1418–24.

Nicolas, Michael et al. 2005. "A Gradual Process of Recombination Restriction in the Evolutionary History of the Sex Chromosomes in Dioecious Plants." Plos Biology **3**:47–56.

Nishiyama, Rie et al. 2010. “Sex chromosome evolution revealed by physical mapping of SlAP3X/Y in the dioecious plant *Silene latifolia*.” Cytologia **75(3)**:319–25.

Obara, Mari, Sachihiro Matsunaga, Shunsuke Nakao, and Shigeyuki Kawano. 2002. “A plant Y chromosome-STS marker encoding a degenerate retrotransposon.” Genes & genetic systems **77**:393–98.

Renner, Susanne S., and Robert E. Ricklefs. 1995. “DIOECY AND ITS CORRELATES IN THE FLOWERING PLANTS.” American Journal of Botany **82**:596–606.

Renner, Susanne S., and Robert E. Ricklefs. 1995. “Dioecy and Its Correlates in the Flowering Plants.” American Journal of Botany **82**:596.

Rijpkema, Anneke S. et al. 2006. “Analysis of the Petunia *TM6* MADS box gene reveals functional divergence within the *DEF/AP3* lineage.” The Plant cell **18**:1819–32.

Rosas, F., and C. A. Domínguez. 2009. “Male sterility, fitness gain curves and the evolution of gender specialization from distyly in *Erythroxylum havanense*.” Journal of Evolutionary Biology **22**:50–59.

Routley, Matthew B., Robert I. Bertin, and Brian C. Husband. 2004. “Correlated Evolution of Dichogamy and Self‐Incompatibility: A Phylogenetic Perspective.” International Journal of Plant Sciences **165**:983–93.

Ruan, Cheng-Jiang, and Jaime A. Teixeira da Silva. 2012. “Evolutionary Assurance vs. Mixed Mating” Critical Reviews in Plant Sciences **31**:290–302.

Schärer, Lukas. 2009. “Tests of sex allocation theory in simultaneously hermaphroditic animals.” Evolution; international journal of organic evolution **63**:1377–1405.

Smyth, D. R., J. L. Bowman, and E. M. Meyerowitz. 1990. “Early flower development in *Arabidopsis*.” The Plant cell **2**:755–67.

Steinacher, Gerlinde, and Johanna Wagner. 2010. “Flower longevity and duration of pistil receptivity in high mountain plants.” Flora - Morphology, Distribution, Functional Ecology of Plants **205**:376–87.

Vicoso, Beatriz, and Doris Bachtrog. 2009. “Progress and prospects toward our understanding of the evolution of dosage compensation.” Chromosome Research **17**:585–602.

Vos, Jurriaan M. de, Barbara Keller, Samuel T. Isham, Sylvia Kelso, and Elena Conti. 2012. “Reproductive implications of herkogamy in *homostylous primroses* variation during anthesis and reproductive assurance in alpine environments.” Functional Ecology **26**:854–65.

Vyskot, Boris, and Roman Hobza. 2004. “Gender in plants: sex chromosomes are emerging from the fog.” Trends in genetics : TIG **20**:432–38.

Webb, C. J., and David G. Lloyd. 1986. “The avoidance of interference between the presentation of pollen and stigmas in angiosperms II . Herkogamy.” New Zealand Journal of Botany **24**:37–41.

Westergaard, M. 1958. “The mechanism of sex determination in dioecious flowering plants.” Advances in genetics **9**:217–81.

Wilson, Melissa A., and Kateryna D. Makova. 2009. “Evolution and survival on eutherian sex chromosomes.” PLoS genetics **5**:e1000568.

Witt, T., Andreas Jürgens, R. Geyer, and G. Gottsberger. 1999. “Nectar dynamics and sugar composition in flowers of *Silene* and *Saponaria* species (Caryophyllaceae).” Plant Biology **1**:334–45.

Wyckoff, Gerald J., Joyce Li, and Chung-I. Wu. 2002. “Molecular evolution of functional genes on the mammalian Y chromosome.” MOLECULAR BIOLOGY AND EVOLUTION **19(9)**:1633–36.

Young, Helen J. 2002. “Diurnal and nocturnal pollination of *Silene alba* (Caryophyllaceae).” American journal of botany **89**:433–40.

Young, Helen J., and Lauren Gravitz. 2002. “The effects of stigma age on receptivity in *Silene alba* (Caryophyllaceae).” American journal of botany **89**:1237–41.

Zhang, Y. Hi et al. 1998. “Y chromosome specific markers and the evolution of dioecy in the genus *Silene*.” Genome **41**:141–47.

Zluvova, J. et al. 2005. “The inter-specific hybrid *Silene latifolia* x *S-viscosa* reveals early events of sex chromosome evolution.” Evolution & Development **7**:327–36.

Zluvova, Jitka, Jiri Zak, Bohuslav Janousek, and Boris Vyskot. 2010. “Dioecious *Silene latifolia* plants show sexual dimorphism in the vegetative stage.” BMC plant biology **10**:208.

PERSPECTIVE

The goal of this study was to characterize dioecism (maintenance mechanism of male and female reproductive organs borne on separate individuals of the same species) in *Silene latifolia*. The evolution from hermaphroditism to dioecy results in every offspring being obtained by cross-pollination and can be considered an "outcrossing mechanism." Outcrossing mechanisms include dichogamy, herkogamy, and self-incompatibility (Barrett 2003; Bertin and Newman 1993; Lloyd and Webb 1986; Webb and Lloyd 1986). In most flowering plants, the commonly held belief is that one species would not simultaneously show synchronous dichogamy and self-incompatibility because they are redundant mechanisms to reduce selfing (Narbona, Ortiz, and Arista 2011; Routley, Bertin, and Husband 2004). My analysis of dichogamy in the dioecious plant *S. latifolia* showed that both stamens and pistils mature simultaneously at night, and suggested that one species would not simultaneously show synchronous dichogamy and dioecism. In addition, hermaphroditic mutants isolated by mutagenesis showed herkogamy and signs of dichogamy to compensate for the absence of dioecism. Perhaps the outcrossing species selected one outcrossing mechanism and avoided self-pollination. Future studies are required to consider dioecism as an outcrossing mechanism and to explore pollination and mating systems in flowering plants.

Screening for hermaphroditic mutants yielded byproduct mutants, such as asexual mutants, anther defect mutants, and pollen defect mutants. Previous studies have constructed Y chromosome deletion maps using 10 hermaphroditic mutants, 3 asexual mutants, 5 stamen defect mutants, and 1 pollen defect mutant obtained from M_1 plants (Fujita et al. 2012). My study expanded on the Y deletion map to 13 hermaphroditic

mutants, 10 asexual mutants, 9 stamen defect mutants, and 5 pollen defect mutants. I also isolated an XY female mutant containing a deletion in both GSF and SPF. Currently, a joint research project with Dr. Yusuke Kazama, Dr. Kotaro Ishii, and Dr. Tomoko Abe of RIKEN is constructing a more detailed Y-chromosome deletion map using the newly isolated 100 STS markers and an algorithm to address the traveling-salesman problem (Kazama et al. unpublished data). My mutants can contribute to identifying the STS marker most proximal to the sex-determining gene in *S. latifolia*. In addition, next-generation RNA sequencing can be applied to these mutants to identify the sex-determining genes based on genes that are not expressed in mutants.

The sex chromosomes of *S. latifolia* have been irreversibly degenerated since they evolved from a pair of autosomes 5–10 million years ago (Charlesworth 2008). Although NGS revealed that Y-linked genes show more rapid accumulation of amino-acid replacements and loss of expression (Bergero and Charlesworth 2011; Chibalina and Filatov 2011) compared to X-linked genes, little is known about the detailed structure of genome and sex-linked genes in *S. latifolia*. Newly isolated *SlAP3Y* deletion mutants and *SlAP3X* hetero-deletion mutants increase our understanding regarding the influence of sex chromosome degeneration in *S. latifolia*. The increased expression levels of X-linked genes in Y-linked gene deletion mutants were suggestive of a dosage compensation mechanism in *S. latifolia*, similar to that in *Drosophila* (upregulation of X in males). Recent genome-wide studies showed species with global dosage compensation that equalize all sex-linked gene expression between the sexes, such as *Drosophila*, mammals, and *Caenorhabditis elegans* (Vicoso and Bachtrog 2009). Other species have been reported to show partial

dosage compensation, which equalize a part of the sex-linked gene expression between the sexes such as birds, including chickens and zebra finches (reviewed in (Mank 2013)). The mechanism of dosage compensation *S. latifolia* remains unclear, and whether *S. latifolia* equalizes all sex-linked gene expression between the sexes requires further study. Further investigation into the mechanism of dosage compensation in *S. latifolia* requires the isolation of Y-linked gene deletion mutants and the analysis of gene expression in these mutants (other than *SlAP3X/Y*). Plant sex chromosome evolution was described in six stages; *S. latifolia* was stage 4 because the male-specific region expanded in size and degenerated in gene content via accumulation of transposable element insertions and intrachromosomal rearrangements, and the X and Y chromosomes became heteromorphic (Ming, Bendahmane, and Renner 2011). Analysis of gene expression between the sexes in the species (including six stages) will increase our understanding of dosage compensation in plants. Although studies on dosage compensation are limited in animals, further studies on the evolution of young sex-chromosomes in plant species are ongoing.